NISTIR 8280

Face Recognition Vendor Test (FRVT)
Part 3: Demographic Effects

Patrick Grother
Mei Ngan
Kayee Hanaoka

This publication is available free of charge from:
https://doi.org/10.6028/NIST.IR.8280

National Institute of
Standards and Technology
U.S. Department of Commerce

NISTIR 8280

Face Recognition Vendor Test (FRVT)
Part 3: Demographic Effects

Patrick Grother
Mei Ngan
Kayee Hanaoka
Information Access Division
Information Technology Laboratory

This publication is available free of charge from:
https://doi.org/10.6028/NIST.IR.8280

December 2019

U.S. Department of Commerce
Wilbur L. Ross, Jr., Secretary

National Institute of Standards and Technology
Walter Copan, NIST Director and Undersecretary of Commerce for Standards and Technology

Certain commercial entities, equipment, or materials may be identified in this document in order to describe an experimental procedure or concept adequately. Such identification is not intended to imply recommendation or endorsement by the National Institute of Standards and Technology, nor is it intended to imply that the entities, materials, or equipment are necessarily the best available for the purpose.

National Institute of Standards and Technology Interagency or Internal Report 8280
Natl. Inst. Stand. Technol. Interag. Intern. Rep. 8280, 81 pages (December 2019)

This publication is available free of charge from:
https://doi.org/10.6028/NIST.IR.8280

EXECUTIVE SUMMARY

OVERVIEW

This is the third in a series of reports on ongoing face recognition vendor tests (FRVT) executed by the National Institute of Standards and Technology (NIST). The first two reports cover, respectively, the performance of one-to-one face recognition algorithms used for verification of asserted identities, and performance of one-to-many face recognition algorithms used for identification of individuals in photo data bases. This document extends those evaluations to document accuracy variations across demographic groups.

MOTIVATION

The recent expansion in the availability, capability, and use of face recognition has been accompanied by assertions that demographic dependencies could lead to accuracy variations and potential bias. A report from Georgetown University [14] work noted that prior studies [22], articulated sources of bias, described the potential impacts particularly in a policing context, and discussed policy and regulatory implications. Additionally, this work is motivated by studies of demographic effects in more recent face recognition [9,16,23] and gender estimation algorithms [5,36].

AIMS AND SCOPE

NIST has conducted tests to quantify demographic differences in contemporary face recognition algorithms. This report provides details about the recognition process, notes where demographic effects could occur, details specific performance metrics and analyses, gives empirical results, and recommends research into the mitigation of performance deficiencies.

NIST intends this report to inform discussion and decisions about the accuracy, utility, and limitations of face recognition technologies. Its intended audience includes policy makers, face recognition algorithm developers, systems integrators, and managers of face recognition systems concerned with mitigation of risks implied by demographic differentials.

WHAT WE DID

The NIST Information Technology Laboratory (ITL) quantified the accuracy of face recognition algorithms for demographic groups defined by sex, age, and race or country of birth.

We used both one-to-one verification algorithms and one-to-many identification search algorithms. These were submitted to the FRVT by corporate research and development laboratories and a few universities. As prototypes, these algorithms were not necessarily available as mature integrable products. Their performance is detailed in FRVT reports [16,17].

We used these algorithms with four large datasets of photographs collected in U.S. governmental applications that are currently in operation:

- **Domestic mugshots** collected in the United States.
- **Application photographs** from a global population of applicants for immigration benefits.
- **Visa photographs** submitted in support of visa applicants.
- **Border crossing photographs** of travelers entering the United States.

All four datasets were collected for authorized travel, immigration or law enforcement processes. The first three sets have good compliance with image capture standards. The last set does not, given constraints on capture duration and environment. Together these datasets allowed us to process a total of 18.27 million images of 8.49 million people through 189 mostly commercial algorithms from 99 developers.

The datasets were accompanied by sex and age metadata for the photographed individuals. The mugshots have metadata for race, but the other sets only have country-of-birth information. We restrict the analysis to 24 countries in 7 distinct global regions that have seen lower levels of long-distance immigration. While country-of-birth information may be a reasonable proxy for race in these countries, it stands as a meaningful factor in its own right particularly for travel-related applications of face recognition.

The tests aimed to determine whether, and to what degree, face recognition algorithms differed when they processed photographs of individuals from various demographics. We assessed accuracy by demographic group and report on false negative and false positive effects. False negatives are the failure to associate one person in two images; they occur when the similarity between two photos is low, reflecting either some change in the person's appearance or in the image properties. False positives are the erroneous association of samples of two persons; they occur when the digitized faces of two people are similar.

In background material that follows we give examples of how algorithms are used, and we elaborate on the consequences of errors noting that the impacts of demographic differentials can be advantageous or disadvantageous depending on the application.

WHAT WE FOUND

The accuracy of algorithms used in this report has been documented in recent FRVT evaluation reports [16, 17]. These show a wide range in accuracy across developers, with the most accurate algorithms producing many fewer errors. These algorithms can therefore be expected to have smaller demographic differentials.

Contemporary face recognition algorithms exhibit demographic differentials of various magnitudes. Our main result is that false positive differentials are much larger than those related to false negatives and exist broadly, across many, but not all, algorithms tested. Across demographics, false positives rates often vary by factors of 10 to beyond 100 times. False negatives tend to be more algorithm-specific, and vary often by factors below 3.

- ▷ **False positives:** Using the higher quality Application photos, false positive rates are highest in West and East African and East Asian people, and lowest in Eastern European individuals. This effect is generally large, with a factor of 100 more false positives between countries. However, with a number of algorithms developed in China this effect is reversed, with low false positive rates on East Asian faces. With domestic law enforcement images, the highest false positives are in American Indians, with elevated rates in African American and Asian populations; the relative ordering depends on sex and varies with algorithm.

  We found false positives to be higher in women than men, and this is consistent across algorithms and datasets. This effect is smaller than that due to race.

  We found elevated false positives in the elderly and in children; the effects were larger in the oldest and youngest, and smallest in middle-aged adults.

- **False negatives:** With domestic mugshots, false negatives are higher in Asian and American Indian individuals, with error rates above those in white and African American faces (which yield the lowest false negative rates). However, with lower-quality border crossing images, false negatives are generally higher in people born in Africa and the Caribbean, the effect being stronger in older individuals. These differing results relate to image quality: The mugshots were collected with a photographic setup specifically standardized to produce high-quality images across races; the border crossing images deviate from face image quality standards.

  In cooperative access control applications, false negatives can be remedied by users making second attempts.

The presence of an enrollment database affords one-to-many identification algorithms a resource for mitigation of demographic effects that purely one-to-one verification systems do not have. Nevertheless, demographic differentials present in one-to-one verification algorithms are usually, but not always, present in one-to-many search algorithms. One important exception is that some developers supplied highly accurate identification algorithms for which false positive differentials are undetectable.

More detailed results are introduced in the Technical Summary.

IMPLICATIONS OF THESE TESTS

Operational implementations usually employ a single face recognition algorithm. Given algorithm-specific variation, it is incumbent upon the system owner to know their algorithm. While publicly available test data from NIST and elsewhere can inform owners, it will usually be informative to specifically measure accuracy of the operational algorithm on the operational image data, perhaps employing a biometrics testing laboratory to assist.

Since different algorithms perform better or worse in processing images of individuals in various demographics, policy makers, face recognition system developers, and end users should be aware of these differences and use them to make decisions and to improve future performance. We supplement this report with more than 1200 pages of charts contained in seventeen annexes that include exhaustive reporting of results for each algorithm. These are intended to show the breadth of the effects, and to inform the algorithm developers.

There are a variety of techniques that might mitigate performance limitations of face recognition systems performance issues overall and specifically those that relate to demographics. This report includes recommendations for research in developing and evaluating the value, costs, and benefits of potential mitigation techniques - see sections 8 and 9.

Reporting of demographic effects often has been incomplete in academic papers and in media coverage. In particular, accuracy is discussed without stating the quantity of interest be it false negatives, false positives or failure to enroll. As most systems are configured with a fixed threshold, it is necessary to report both false negative and false positive rates for each demographic group at that threshold. This is rarely done - most reports are concerned only with false negatives. We make suggestions for augmenting reporting with respect to demographic difference and effects.

BACKGROUND: ALGORITHMS, ERRORS, IMPACTS

FACE ANALYSIS: CLASSIFICATION, ESTIMATION, RECOGNITION

Before presenting results in the Technical Summary we describe what face recognition is, contrasting it with other applications that analyze faces, and then detail the errors that are possible in face verification and identification and their impacts.

Much of the discussion of face recognition bias in recent years cites two studies [5,36] showing poor accuracy of face gender classification algorithms on black women. Those studies did not evaluate face recognition algorithms, yet the results have been widely cited to indict their accuracy. Our work was undertaken to quantify analogous effects in face recognition algorithms. We strongly recommend that reporting of bias should include information about the class of algorithm evaluated. We use the term **face analysis** as an umbrella for any algorithm that consumes face images and produces some output. Within that are **estimation** algorithms that output some continuous quantity (e.g., age or degree of fatigue). There are **classification** algorithms that aim to determine some categorical quantity such as the sex of a person or their emotional state. Face classification algorithms are built with inherent knowledge of the classes they aim to produce (e.g., happy, sad). Face **recognition** algorithms, however, have no built-in notion of a particular person. They are not built to identify particular people; instead they include a face detector followed by a feature extraction algorithm that converts one or more images of a person into a vector of values that relate to the identity of the person. The extractor typically consists of a neural network that has been trained on ID-labeled images available to the developer. In operations, they act as generic extractors of identity-related information from photos of persons they have usually never seen before. Recognition proceeds as a differential operator: Algorithms compare two feature vectors and emit a similarity score. This is a vendor-defined numeric value expressing how similar the parent faces are. It is compared to a threshold value to decide whether *two* samples are from, or represent, the same person or not. Thus, recognition is mediated by persistent identity information stored in a feature vector (or "template"). Classification and estimation, on the other hand, are single-shot operations from *one* sample alone, employing machinery that is different from that used for face recognition.

VERIFICATION

Errors: A comparison of images from the same person yields a genuine or "mate" score. A comparison of images from different people yields an imposter or "nonmate" score. Ideally, nonmate scores should be low and mate scores should be high. In practice, some imposter scores are above a numeric threshold giving false positives, and some genuine comparisons yield scores below threshold giving false negatives.

Applications: One-to-one verification is used in applications including logical access to a phone or physical access through a security check point. It also supports non-repudiation e.g. to authorize the dispensing of a prescription drug. Two photos are involved: one in the database that is compared with one taken of the person seeking access to answer the question: ”Is this the same person or not?”

Impact of errors: Errors have different implications for the system owner and for the individual whose photograph is being used, depending upon the application. In verification applications, false negatives cause inconvenience for the user. For example, an individual may not be able to get into their phone or they are delayed entering a facility or crossing a border. These errors can usually be remediated with a second attempt. False positives, on the other hand, present a security concern to the system owner, as they allow access to imposters.

IDENTIFICATION

Identification algorithms, referred to commonly as one-to-many or "1-to-N" search algorithms, notionally compare features extracted from a search "probe" image with all feature vectors previously enrolled from "gallery" images. The algorithms return either a fixed number of the most similar candidates, or only those that are above a preset threshold. A candidate is an index and a similarity score. Some algorithms execute an exhaustive search of all N enrollments and a sort operation to yield the most similar. Other algorithms implement "fast-search" techniques [2,19,21,26] that avoid many of the N comparisons and are therefore highly economical [17].

Identification applications: There are two broad uses of identification algorithms. First, they can be used to facilitate positive access like in one-to-one verification but without presentation of an identity claim. For example, a subject is given access to a building solely on the basis of presentation a photograph that matches *any* enrolled identity with a score above threshold. Second, they can be used for so-called negative identification where the system operator claims implicitly that searched individuals are not enrolled - for example, checking databases of gamblers previously banned from a casino.

Impacts: As with verification, the impact of a demographic differential will depend on the application. In one-to-many searches, false positives primarily occur when a search of a subject who is not present in the database yields a candidate identity for human review. This type of "one to many" search is often employed to check for a person who might be applying for a visa or driver's license under a name different than their own. False positives may also occur when a search of someone who is enrolled produces the wrong identity with, or instead of, the correct identity. Identification algorithms produce such outcomes when the search yields a comparison score above a chosen threshold.

In identification applications such as visa or passport fraud detection, or surveillance, a false positive match to another individual could lead to a false accusation, detention or deportation. Higher false negatives would be an advantage to an enrollee in such a system, as their fraud would go undetected, and a disadvantage to the system owner whose security goals will be undermined.

Investigation: This is a special-case application of identification algorithms where the threshold is set to zero so that all searches will produce a fixed number of candidates. In such cases, the false positive identification rate is 100% because any search of someone not in the database will still yield candidates. Algorithms used in this way are part of a hybrid *machine-human system*: The algorithm offers up candidates for human adjudication, for which labor must be available. In such cases, false positive differentials from the algorithm are immaterial - the machine returns say 50 candidates regardless. What matters then is the human response, and the evidence there is for both poor [10, 42] and varied human capability, even without time constraints [34], and sex and race performance differentials, particularly an interaction between the reviewer's demographics with those of the photographs under review [7]. The interaction of machine and human is beyond the scope of this report, as is human efficacy.

TECHNICAL SUMMARY

This section summarizes the results of the study. This is preceded by an introduction to terminology and discussion of a vital aspect in reporting demographic effects, namely that it is necessary to report both false negative and false positive error rates.

ACCURACY DIFFERENTIALS When similarity scores are computed over a collection of images from demographic A (say elderly Asian men) they may be higher than from demographic B (say young Asian women). We adopt terminology from a Department of Homeland Security Science and Technology Directorate article [20] and define **differential performance** as a "difference in the genuine or imposter [score] distributions". Such differentials are inconsequential unless they prompt a **differential outcome**. An outcome occurs when a score is compared with an operator-defined threshold. A genuine score below threshold yields a false negative outcome, and an imposter score at or above threshold, a false positive outcome. The subject of this report is to quantify differential outcomes between demographics. The term demographic differential is inherited from an ISO technical report [6] now under development.

FIXED THRESHOLD OPERATION A crucial point in reasoning about differentials is that the vast majority of biometric systems are configured with a fixed threshold against which all comparisons are made (i.e., the threshold is not tailored to cameras, environmental conditions or, particularly, demographics). Most academic studies ignore this point (even in demographics e.g., [13]) by reporting false negative rates at fixed false positive rates rather than at fixed thresholds, thereby hiding excursions in false positive rates and misstating false negative rates. This report includes documentation of demographic differentials about typical operating thresholds.

We report false positive and false negative rates separately because the consequences of each type of error are of importance to different communities. For example, in a one-to-one access control, false negatives inconvenience legitimate users; false positives undermine a system owners security goals. On the other hand, in a one-to-many deportee detection application, a false negative would present a security problem, and a false positive would flag legitimate visitors. The prior probability of imposters in each case is important. For example, in some access control cases, imposters almost never attempt access and the only germane error rate is the false negative rate.

RESULTS OVERVIEW We found empirical evidence for the existence of demographic differentials in the majority of contemporary face recognition algorithms that we evaluated. The false positive differentials are much larger than those related to false negatives. False positive rates often vary by one or two orders of magnitude (i.e., 10x, 100x). False negative effects vary by factors usually much less than 3. The false positive differentials exist broadly, across many, but not all, algorithms. The false negatives tend to be more algorithm-specific. Research toward mitigation of differentials is discussed in sections 9 and 8.

The accuracy of algorithms used in this report has been documented in recent FRVT evaluation reports [16, 17]. These show a wide range in accuracy across algorithm developers, with the most accurate algorithms producing many fewer errors than lower-performing variants. More accurate algorithms produce fewer errors, and will be expected therefore to have smaller demographic differentials.

FALSE NEGATIVES

With regard to false negative demographic differentials we make the observations below. Note that in real-time cooperative applications, false negatives can often be remedied by making second attempts.

▷ False negative error rates vary strongly by algorithm, from below 0.5% to above 10%. For the more accurate algorithms, false negative rates are usually low with average demographic differentials being, necessarily, smaller still. This is an important result: use of inaccurate algorithms will increase the magnitude of false negative differentials. See Figure 22 and Annex 12 .

▷ In domestic mugshots, false negatives are higher in Asian and American Indian individuals, with error rates above those in white and black faces. The lowest false negative rates occur in black faces. This result might not be related to race - it could arise due to differences in the time elapsed between photographs because ageing is highly influential on face recognition false negatives. We will report on that analysis going forward. See Figure 17.

▷ False negative error rates are often higher in women and in younger individuals, particularly in the mugshot images. There are many exceptions to this, so universal statements pertaining to algorithms false negative rates across sex and age are not supported.

▷ When comparing high-quality application photos, error rates are very low and measurement of false negative differentials across demographics is difficult. This implies that better image quality reduces false negative rates and differentials. See Figure 22.

▷ When comparing high-quality application images with lower-quality border crossing images, false negative rates are higher than when comparing the application photos. False negative rates are often higher in recognition of women, but the differentials are smaller and not consistent. See Figure 21.

▷ In the border crossing images, false negatives are generally higher in individuals born in Africa and the Caribbean, the effect being stronger in older individuals. See Figure 18.

FALSE POSITIVES

Verification Algorithms: With regard to false positive demographic differentials we make the following observations.

▷ We found false positives to be between 2 and 5 times higher in women than men, the multiple varying with algorithm, country of origin and age. This increase is present for most algorithms and datasets. See Figure 6.

▷ With respect to race, false positive rates are highest in West and East African and East Asian people (but with exceptions noted next). False positive rates are also elevated but slightly less so in South Asian and Central American people. The lowest false positive rates generally occur with East European individuals. See Figure 5.

▷ A number of algorithms developed in China give low false positive rates on East Asian faces, and sometimes these are lower than those with Caucasian faces. This observation - that the location of the developer as a proxy for the race demographics of the data they used in training - matters was noted in 2011 [33], and is potentially important to the reduction of demographic differentials due to race and national origin.

- ▷ We found elevated false positives in the elderly and in children; the effects were larger in the oldest adults and youngest children, and smallest in middle aged adults. The effects are consistent across country-of-birth, datasets and algorithms but vary in magnitude. See Figure 14 and Figure 15.

- ▷ With mugshot images, the highest false positives are in American Indians, with elevated rates in African American and Asian populations; the relative ordering depends on sex and varies with algorithm. See Figure 12 and Figure 13.

Identification Algorithms: The presence of an enrollment database affords one-to-many algorithms a resource for mitigation of demographic effects that purely one-to-one verification systems do not have. We note that demographic differentials present in one-to-one verification algorithms are usually, but not always, present in one-to-many search algorithms. See Section 7.

One important exception is that some developers supplied identification algorithms for which false positive differentials are undetectable. Among those is Idemia, who publicly described how this was achieved [15]. A further algorithm, NEC-3, is on many measures, the most accurate we have evaluated. Other developers producing algorithms with stable false positive rates are Aware, Toshiba, Tevian and Real Networks. These algorithms also give false positive identification rates that are approximately independent of the size of enrollment database. See Figure 27.

PRIOR WORK

This report is the first to describe demographic differentials for identification algorithms. There are, however, recent prior tests of verification algorithms whose results comport with ours regarding demographic differentials between races.

- ▷ Using four verification algorithms applied to domestic mugshots, the Florida Institute of Technology and its collaborators showed [23] simultaneously elevated false positives and reduced false negatives in African Americans vs. Caucasians.

- ▷ Cavazos et al. [8] applied four verification algorithms to GBU challenge images [32] to show order-of-magnitude higher false positives in Asians vs. Caucasians. The paper articulates five lessons related to measurement of demographic effects.

- ▷ In addition, a recent Department of Homeland Security (DHS) Science and Technology / SAIC study [20] using a leading commercial algorithm showed that pairing of imposters by age, sex and race gives false positive rates that are two orders of magnitude higher than by pairing individuals randomly.

- ▷ On an approximately monthly schedule starting in 2017, NIST has reported [16] on demographic effects in one-to-one verification algorithms submitted to the FRVT process. Those tests employed smaller sets of mugshot and visa photographs than are used here.

WHAT WE DID NOT DO

This report establishes context, gives results and impacts, and discusses additional research that can support mitigation of observed deficiencies. It does not address the following:

▷ **Training of algorithms**: We did not train algorithms. The prototype algorithms submitted to NIST are fixed and were not refined or adapted. This reflects the usual operational situation in which face recognition systems are not adapted on customers local data. We did not attempt, or invite developers to attempt, mitigation of demographic differentials by retraining the algorithms on image sets maintained at NIST. We simply ran the tests using algorithms as submitted.

▷ **Analyze cause and effect:** We did not make efforts to explain the technical reasons for the observed results, nor to build an inferential model of them. Specifically, we have not tried to relate recognition errors to skin tone or any other phenotypes evident in faces in our image sets. We think it likely that modeling will need richer sets of covariates than are available. In particular, efforts to estimate skin tone and other phenotypes will involve an algorithm that itself may exhibit demographic differentials.

We did not yet pursue regression approaches due to the volume of data, the number of algorithms tested, and the need to model each recognition algorithms separately, as they are built and trained independently. Due to their ability to handle imbalanced data, we note, however, the utiltity of mixed effects models [3, 4, 9] previously developed for explaining recognition failure. Such approaches can use subject-specific variables (age, sex, race, etc.) and image-specific variables (contrast, brightness, blur, uniformity, etc.). Models are often useful, even though it is inevitable that germane quantities will be unavailable to the analysis.

▷ **Consider the effect of cameras:** The possible role of the camera, and the subject-camera interaction, has been detailed recently [9]. This is particularly important when standards-compliant photography is not possible, or not intended, for example, in high throughput access control. Without access to human-camera interaction data, we do not report on quantities like satisfaction, difficulty of use, and failure to enroll. Along these lines, it has been suggested [41] that NISTs tests using standards-compliant images “don’t translate to everyday scenarios”.

In fact, we note demographic effects *even* in high-quality images, notably elevated false positives. Additionally, we quantify false negatives on a border crossing dataset which is collected at a different point in the trade space between quality and speed than are our other three mostly high-quality portrait datasets.

Finally, some governmental organizations dedicated resources to advancing standards so that the “real-world” images in their applications are high-quality portraits. For example, the main criminal justice application is supported by the FBI and others being proactive in the 1990s in establishing portrait capture standards, and then promulgating them.

▷ **Use wild images:** We did not use image data from the Internet nor from video surveillance. This report does not capture demographic differentials that may occur in such photographs.

RESEARCH RECOMMENDATIONS

We now discuss research germane to the quantification, handling and mitigation of demographic differentials.

Testing: Since 2017 NIST has provided demographic differential data to developers of one-to-one verification algorithms. Our goal has been to encourage developers to remediate the effects. While that may have happened in some cases, a prime incentive for a developer when participating in NIST evaluations is to reduce false negatives rates globally. Going forward, we plan to start reporting accuracy that pushes developers to produce approximately equal false positive rates across all demographics.

Mitigation of false positive differentials: With adequate research and development, the following may prove effective at mitigating demographic differentials with respect to false positives: Threshold elevation, refined training, more diverse training data, discovery of features with greater discriminative power - particularly techniques capable of distinguishing between twins - and use of face and iris as a combined modality. These are discussed in section 9. We also discuss, and discount, the idea of user-specific thresholds.

Mitigation of false negative differentials: False negative error rates, and demographic differentials therein, are reduced in standards-compliant images. This motivates the suggestions of further research into image quality analysis, face-aware cameras and improved standards-compliance discussed in section 8.

Policy research: The degree to which demographic differentials could be tolerated has never been formally specified in any biometric application. Any standard directed toward limiting allowable differentials in the automated processing of digitized biological characteristics might weigh the actual consequences of differentials which are strongly application dependent.

REPORTING OF DEMOGRAPHIC EFFECTS

Reporting of demographic effects has been incomplete, in both academic papers and in media coverage. In particular, accuracy is discussed without specifying, particularly, false positives or false negatives. We therefore suggest that reports covering demographic differentials should describe:

- The purpose of the system - initial enrollment of individuals into a system, identity verification or identification:
- The stage at which the differential occurred - at the camera, during quality assessment, in the detection and feature extraction phase, or during recognition;
- The relevant metric: false positive or false negative occurrences during recognition, failures to enroll, failed detections by the camera, for example;
- Any differentials in duration of processes or difficulty in using the system;
- Any known information on recognition threshold value, whether the threshold is fixed, and what the target false positive rate is;
- Which demographic group has the elevated failure rates - for example by age, sex, race, height, or in some intersection thereof; and
- Consequences of any error, if known, and procedures for error remediation.

ACKNOWLEDGMENTS

The authors are grateful to Yevgeniy Sirotin and John Howard of SAIC at the Maryland Test Facility, Arun Vemury of DHS S&T, Michael King of Florida Institute of Technology, and John Campbell of Bion Biometrics for detailed discussions of their work in this area.

The authors are grateful to staff in the NIST Biometrics Research Laboratory for infrastructure supporting rapid evaluation of algorithms.

DISCLAIMER

Specific hardware and software products identified in this report were used in order to perform the evaluations described in this document. In no case does identification of any commercial product, trade name, or vendor, imply recommendation or endorsement by the National Institute of Standards and Technology, nor does it imply that the products and equipment identified are necessarily the best available for the purpose. Developers participating in FRVT grant NIST permission to publish evaluation results.

ANNEXES

We supplement this report with more than 1200 pages of charts contained in 17 Annexes which include exhaustive reporting of results for each algorithm. These are intended to show the breadth of the effects and to inform the algorithms' developers. We do not take averages over algorithms, for example the average increase of false match rate in women, because averages of samples from different distributions are seldom meaningful (by analogy, taking the average of temperatures in Montreal and Miami). Applications typically employ just one algorithm, so averages and indeed any statements purporting to summarize the entirety of face recognition will not always be correct.

The annexes to this report are listed in Table 1. The first four detail the datasets used in this report. The remaining annexes contain more than 1200 pages of automatically generated graphs, usually one for each algorithm evaluated. These are intended to show the breadth of the effects, and to inform the algorithms' developers.

#	CATEGORY		DATASET	CONTENT
Annex 1	Datasets		Mugshot	Description and examples of images and metadata: Mugshots
Annex 2	Datasets		Application	Description and examples of images and metadata: Application portraits
Annex 3	Datasets		Visa	Description and examples of images and metadata: Visa portraits
Annex 4	Datasets		Border crossing	Description and examples of images and metadata: Border crossing photos
Annex 5	Results	1:1	Application	False match rates for demographically matched impostors
Annex 6	Results	1:1	Mugshot	Cross-race and sex false match rates in United States mugshot images
Annex 7	Results	1:1	Application	Cross-race and sex false match rates in worldwide application images
Annex 8	Results	1:1	Application	False match rates with matched demographics using application images
Annex 9	Results	1:1	Application	Cross-age false match rates with application photos
Annex 10	Results	1:1	Visa	Cross age false match rates with visa photos
Annex 11	Results	1:1	Mugshot	Cross age and country with application photos
Annex 12	Results	1:1	Mugshot	Error tradeoff characteristics with United States mugshots
Annex 13	Results	1:1	Mugshot	False negative rates in United States mugshot images by sex and race
Annex 14	Results	1:1	Mugshot	False negative rates by country for global application and border crossing photos
Annex 15	Results	1:1	Mugshot	Genuine and impostor score distributions for United States mugshots
Annex 16	Results	1:N	Mugshot	Identification error characteristics by race and sex
Annex 17	Results	1:N	Mugshot	Candidate list score magnitudes by sex and race

Table 1: **Annexes and their content.**

TERMS AND DEFINITIONS

The following table defines common terms appearing in this document. A more complete, consistent biometrics vocabulary is available as ISO/IEC 2382 Part 37.

DATA TYPES	Feature vector	A vector of real numbers that encodes the identity of a person
	Sample	One or more images of the face of a person
	Similarity score	Degree of similarity of two faces in two samples, as rendered by a recognition algorithm
	Template	Data produced by face recognition algorithm that includes a feature vector
	Threshold	Any real number, against which similarity scores are compared to produce a verification decision
ALGORITHM COMPONENTS	Face detector	Component that finds faces in an image
	Comparator	Component that compares two templates and produces a similarity score
	Searcher	Component that searches a database of templates to produce a list of candidates
	Template generator	Component of a face recognition algorithm that converts a sample into a template; this component implicitly embeds a face detector
ONE-TO-ONE VERIFICATION	Imposter comparison	Comparison of samples from different persons
	Genuine comparison	Comparison of samples from the same person
	False match	Incorrect association of two samples from different persons, declared because similarity score is at or above a threshold
	False match rate	Proportion of imposter comparisons producing false matches
	False non-match	Failure to associate two samples from one person, declared because similarity score is below a threshold
	False non-match rate	Proportion of genuine comparisons producing false non-matches
	Verification	The process of comparing two samples to determine if they belong to the same person or not
ONE-TO-MANY IDENTIFICATION	Gallery	A set of templates, each tagged with an identity label
	Consolidated gallery	A gallery for which all samples of a person are enrolled under one identifier, whence $N = N_G$
	Unconsolidated gallery	A gallery for which samples of a person are enrolled under different identifiers, when $N < N_G$
	Identity label	Some index or pointer to an identifier for an individual
	Identification	The process of searching a probe into gallery
	Identification decision	The assignment either of an identity label or a declaration that a person is not in the gallery
SYMBOLS	FMR	Verification false match rate (measured over comparison of samples)
	FNMR	Verification false non-match rate (measured over comparison of samples)
	FPIR	Identification false match rate (measured over comparison of samples)
	FNIR	Identification false non-match rate (measured over comparison of samples)
	N	The number of subjects whose faces are enrolled into a gallery
	N_G	The number of samples enrolled into a gallery, $N_G \geq N$.
	N_{NM}	The number of non-mated searches conducted
	N_M	The number of mated searches conducted

Contents

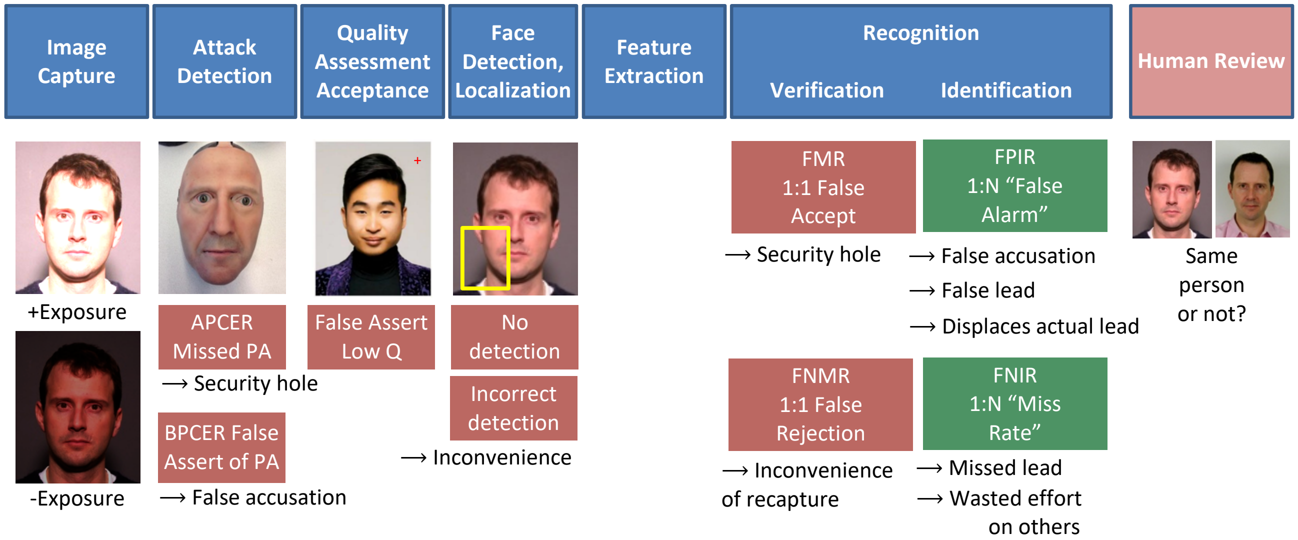

+ Source: http://www.telegraph.co.uk/technology/2016/12/07/robot-passport-checker-rejects-asian-mans-photo-having-eyes/

Figure 1: The figure is intended to show possible stages in a face recognition pipeline at which demographic differentials could, in principle, arise. Note that none of these stages necessarily includes algorithms that may be labelled artificial intelligence, though typically the detection and feature extraction modules are AI-based now.

1 Introduction

Over the last two years there has been expanded coverage of face recognition in the popular press. In some part this is due to the expanded capability of the algorithms, a larger number of applications, lowered barriers to algorithm development[1], and, not least, reports that the technology is somehow biased. This latter aspect is based on Georgetown [14] and two reports by MIT [5, 36]. The Georgetown work noted prior studies [22] articulated sources of bias, and described the potential impacts particularly in a policing context, and discussed policy and regulatory implications. The MIT work did not study face recognition, instead it looked at how well publicly accessible cloud-based *estimation* algorithms can determine gender from a single image. The studies have widely cited as evidence that face *recognition* is biased.

This stems from a confusion in terminology: Face classification algorithms, of the kind MIT reported on, accept one face image sample and produce an estimate of age, or sex, or some other property of the subject. Face recognition algorithms, on the other hand, operate as differential operators: They compare identity information in features vectors extract from two face image samples and produce a measure of similarity between the two, which can be used to answer the "question same person or not?". Face algorithms, both one-to-one identity verification and one-to-many search algorithms, are built on this differential comparison. The salient point, in the demographic context, is that one or two people are involved in a comparison and, as we will see, the age,

[1] Gains in face recognition performance stem from well-capitalized AI research in industry and academic leading to the development of convolutional neural networks, and open-source implementations thereof (Caffe, Tensorflow etc.). For face recognition the availability of large numbers of identity-labeled images (from the web, and in the form of web-curated datasets [VGG2, IJB-C]), and the availability of ever more powerful GPUs has supported training those networks.

sex, race and other demographic properties of both will be material to the recognition outcome.

The MIT reports nevertheless serve as a cautionary tale in two respects. First, that demographic group membership can have a sizeable effect on algorithms that process face photographs; second, that algorithm capability varies considerably by developer.

1.1 Potential sources of bias in face recognition systems

Lost in the discussion of bias is specificity on exactly what component of the process is at fault. Accordingly, we introduce Figure 1 to show that a face recognition system is composed of several parts. The figure shows a notional face recognition pipeline consisting of a capture subsystem, primarily a camera, followed by a presentation attack detection (PAD) module intended to detect impersonation attempts, a quality acceptance (QA) step aimed at checking portrait standard compliance, then the recognition components of feature extraction and 1:1 or 1:N comparison, the output of which may prompt human involvement. The order of the components may be different in some systems, for example the QA component may be coupled to the capture process and would precede PAD. Some components may not exist in some systems, particularly the QA and PAD functions may not be necessary.

The Figure shows performance metrics, any of which could notionally have a demographic differential. Errors at one stage will generally have downstream consequences. In a system where subjects make cooperative presentation to the camera, a person could be rejected in the early stages before recognition itself. For example, a camera equipped with optics that have too narrow a field of view could produce an image of a tall individual in which in which the top part of the head was cropped. This could cause rejection at almost any stage and a system owner would need to determine the origin of errors.

1.2 The role of image quality

Recent research [9] has shown that cameras can have an effect on a generic downstream recognition engine. A poor image can undermine detection or recognition, and it is possible that certain demographics yield photographs ill-suited to face recognition e.g. young children [28], or very tall individuals. As pointed out above there is potential for demographic differentials to appear at the capture stage, that is when only a single image is being collected before any comparison with other images. Demographic differentials that occur during collection could arise from (at least) inadequacies of the camera, from the environment or "stage", and from client-side detection or quality assessment algorithms. Note that manifestly poor (and unrecognizable) images can be collected from mis-configured cameras, without any algorithmic or AI culpability. Indeed, after publication of the MIT studies [5,36] on bias in gender-estimation algorithms, suspicion fell upon the presence of poor photographs, due to under-exposure of dark-skinned individuals in that dataset. An IBM gender estimation algorithm had been faulted in the MIT study; in response, and previously, IBM has been active in addressing AI bias. Relevant here is that it produced a better algorithm[2], and examined whether skin tone itself drove gender classification accuracy [30, 31] - in short, "skin type *by itself* has a minimal effect on the classification decision".

False negatives occur in biometric systems when samples from one individual yield a comparison score below a threshold. This will occur when the features extracted from two input photographs are insufficiently similar. Recall that face recognition is implemented as a differential operator: two samples are analyzed and compared. So a false negative occurs when two from the same face appear different to the algorithm.

It is very common to attribute false negatives to factors such as pose, illumination and expression so much so that dedicated databases have been built up to support development of algorithms with immunity to such[3]. Invariance to such "nuisance" factors has been the focus of the bulk of face recognition research for more two decades. Indeed over the last five years there have been great advances in this respect due to the adoption of deep convolutional neural networks which demonstrate remarkable tolerance to very sub-standard photographs i.e. those that deviate from formal portrait standards most prominently ISO/IEC 39794-5 and its law-enforcement equivalent ANSI/NIST ITL 1-2017.

However, here we need to distinguish between factors that are expected to affect one photo in a mated pair - due to poor photography (e.g. mis-focus), poor illumination (e.g. too dark), and poor presentation (e.g. head down) - and those that would affect both photographs over time, potentially including properties related to demographics.

1.3 Photographic Standards

In the late 1990s the FBI asked NIST to establish photographic best-practices for mugshot collection[4]. This was done to guide primarily state and local police departments in the capture of photographs that would support forensic (i.e. human) review. It occurred more than a decade before the FBI deployed automated face recognition. That standardization work was conducted in anticipation of digital cameras[5] being available to replace film cameras that had been used for almost a century. The standardization work included consideration of cameras, lights and geometry[6]. There was explicit consideration of the need to capture images of both dark and light skinned individuals, it being understood that it is relatively easy to produce photographs for which

[2] See Mitigating Bias in AI Models.

[3] The famous PIE databases, for example.

[4] Early documents, such as Best Practice Recommendation for the Capture of Mugshots, 1999, seeded later formal standardization of ISO/IEC 19794-5.

[5] See NIST Interagency Report 6322, 1999.

[6] See this overview.

large areas of dark or bright pixels can render detection of anatomical features impossible.

Face recognition proceeds as a differential operation on features extracted from two photographs. Accuracy can be undermined by poor photography/illumination/presentation and by differences in those i.e. any change in the digital facial appearance. Of course an egregiously underexposed photograph will have insufficient information content, but two photographs taken with even moderately poor exposure can match, and leading contemporary algorithms are highly tolerant of quality degradations.

1.4 Age and ageing

Ageing will change appearance over decades and will ultimately undermine automated face recognition[7]. In the current study, we don't consider ageing to be a demographic factor because it is a slow, more-or-less graceful, process that happens to all of us. However, there is at least one demographic group that ages more quickly than others - children - who are disadvantaged in many automated border control systems either by being excluded by policy, or by encountering higher false negatives. Age itself is a demographic factor as accuracy in the elderly and the young differ for face recognition (usually) and also for fingerprint authentication. This applies even without significant time lapse between two photographs.

Clearly injury or disease can change appearance on very short timescales, so such factors should be excluded, when possible, from studies dedicated to detection of broad demographic effects. Development of equipment and algorithms, and studies thereof, that are dedicated to the inclusive use of biometrics are valuable of course - for example recognition of photosensitive subjects wearing sunglasses, or finger amputees presenting fingerprints.

[7] See recent results for verification algorithms in the FRVT reports, and for identification algorithms in NIST Interagency Report 8271 [17]. For a formal longitudinal analysis of ageing, using mixed-effects models, see Best-Rowden [3].

#	SOURCE	IMAGE	NUMBER OF		DISCUSSION
			SUBJECTS	IMAGES	
1	Cavazos et al. [8] at UT Dallas	Notre Dame GBU [32] portraits	389	<1085	The study showed order-of-magnitude elevations in false positive rates in university volunteer Asian vs. Caucasian faces. The study reported FMR(T). As the study showed neither FNMR(T) nor linked error tradeoff characteristics the false negative differential is not apparent. It discusses the effect of "yoking" i.e the pairing of imposters by sex and race. It deprecates area-under-the-curve (AUC). The study used two related algorithms from the University of Maryland, one open-source algorithm [38], and one older inaccurate pre-DCNN algorithm.
2	Krishnapriya et al. [23] at Florida Inst. Tech	Operational mugshots: Morph db [37]	10 350 African Am. + 2 769 Caucasians	42 620 African Am. + 10 611 Caucasians	The study reported: order-of-magnitude elevated false positives in African Americans vs. Caucasians; lower false negative rates in African Americans; and reduced differentials in higher quality images [23,24]. That study used three open-source algorithms, and one commercial algorithm. Two of the open-source algorithms are quite inaccurate and not representative of commercial deployment. Importantly, the study also noted the inadequacies of error tradeoff characteristics for documenting fixed-threshold demographic differentials.
3	Howard et al. [20] at SAIC/MdTF with DHS S&T	Lab collected, adult volunteers [9]	363	-	The study establish useful definitions for "differential performance" and "differential outcome" and for broad and narrow heterogeneity of imposter distributions. It showed order-of-magnitude variation in false positive rates with age, sex and race, establishing an information gain approach to formally ordering their effect. The study employed images from 11 capture devices, and applied one leading commercial verification algorithm.

Table 2: Prior studies.

2 Prior work

All prior work relates to one-to-one verification algorithms. This report, in contrast, includes results for many recent, mostly commercial, algorithms implementing both verification and identification.

Except as detailed below, this report is the first to properly report and distinguish between false positive and false negative effects, something that is often missing in other reports.

The broad effects given in this report concerning age and sex have been known as far back as 2003 [35]. Since 2017, our ongoing FRVT report [16] has reported large false positive differential across sex, age and race.

Tables 2 and 3 summarize recent work in demographic effects in automated face recognition.

#	SOURCE	IMAGE	NUMBER OF		DISCUSSION
			SUBJECTS	IMAGES	
4	Cook et al. [9] at SAIC/MdTF with DHS S&T	Lab collected, adult volunteers	525		The study deployed mixed-effects regression models to examine dependence of genuine similarity scores on sex, age, height, eyewear, skin reflectance and on capture device. The report displayed markedly different images of the same people from different capture devices, showing potential for the camera to induce demographic differential performance. The study found lower similarity scores in those identifying as Black or African American, comporting with [22] but contrary to the best ageing study [3]. The study also showed that comparison of samples collected on the same day have different demographic differentials than those collected up to four years apart, in particular that women give lower genuine scores than men with time separation. Same-day biometrics are useful for short-term recognition applications like transit through an airport.
5	El Khiyari et al. [13]	Operational mugshots: Morph db [37]	724 adult, balanced on race + sex	2896 = 1448 each African Am. + Caucasians, balanced on sex	The paper used a subset of the MORPH database with two algorithms([38], modified and one COTS) to show better verification error rates in the men, the elderly, and in whites. The study should be discounted for two reasons: First the algorithms give high error rates at very modest false match rates: the best FNMR = 0.06 at FMR = 0.01. Second the paper reports FNMR at fixed FMR, not at fixed thresholds thereby burying FMR differentials. Moreover, the paper does not disclose how imposters were paired e.g. randomly or, say, with same age, race, and sex.

Table 3: Prior studies (continued).

3 Performance metrics

Both verification and identification systems generally commit two kinds of errors, the so-called Type I error where an individual is incorrectly associated with another, and Type II where the individual is incorrectly not associated with themselves.

The ISO/IEC 19795-1 performance testing and reporting standard requires different metrics to be reported for identification and verification implementations. Accordingly the following subsections define the formal metrics used throughout this document.

3.1 Verification metrics

Verification accuracy is estimated by forming two sets of scores: Genuine scores are produced from mated pairs; imposter scores are produced from non-mated pairs. These comparisons should be done in random order so that the algorithm under test cannot infer that a comparison is mated or not.

From a vector of N genuine scores, u, the false non-match rate (FNMR) is computed as the proportion below some threshold, T:

$$\text{FNMR}(T) = 1 - \frac{1}{N}\sum_{i=1}^{N} H(u_i - T) \tag{1}$$

where $H(x)$ is the unit step function, and $H(0)$ taken to be 1.

Similarly, given a vector of M imposter scores, v, the false match rate (FMR) is computed as the proportion above T:

$$\text{FMR}(T) = \frac{1}{M}\sum_{i=1}^{M} H(v_i - T) \tag{2}$$

The threshold, T, can take on any value. We typically generate a set of thresholds from quantiles of the observed imposter scores, v, as follows. Given some interesting false match rate range, $[\text{FMR}_L, \text{FMR}_U]$, we form a vector of K thresholds corresponding to FMR measurements evenly spaced on a logarithmic scale. This supports plotting of FMR on a logarithmic axis. This is done because typical operations target false match rates spanning several decades 10^{-6} to as high as 10^{-2}.

$$T_k = Q_v(1 - \text{FMR}_k) \tag{3}$$

where Q_v is the quantile function, and FMR_k comes from

$$\log_{10}\text{FMR}_k = \log_{10}\text{FMR}_L + \frac{k}{K}\,\left[\log_{10}\text{FMR}_U - \log_{10}\text{FMR}_L\right] \tag{4}$$

Error tradeoff characteristics are plots of FNMR(T) vs. FMR(T). These are plotted with $\text{FMR}_U \rightarrow 1$ and FMR_L as low as is sustained by the number of imposter comparisons, M. This should be somewhat higher than the "rule of three" limit $3/N$ because samples are generally not independent due to the use of the same image in multiple comparisons.

3.2 Identification metrics

Identification accuracy is estimated from two sets of candidate lists: First, a set of candidate lists obtained from mated-searches; second, a set from non-mated searches. These searches should not be conducted by randomly ordering mated and non-mated searches so that the algorithm under test cannot infer that a search has a mate or not. Tests of open-set biometric identification algorithms must quantify frequency of two error conditions:

- ▷ **False positives**: Type I errors occur when search data from a person who has never been seen before is incorrectly associated with one or more enrollees' data.
- ▷ **Misses**: Type II errors arise when a search of an enrolled person's biometric does not return the correct identity.

Many practitioners prefer to talk about "hit rates" instead of "miss rates" - the first is simply one minus the other as detailed below. Sections 3.2.1 and 3.2.2 define metrics for the Type I and Type II performance variables.

Additionally, because recognition algorithms sometimes fail to produce a template from an image, or fail to execute a one-to-many search, the occurrence of such events must be recorded. Further because algorithms might elect to not produce a template from, for example, a poor quality image, these failure rates must be combined with the recognition error rates to support algorithm comparison. This is addressed in section 3.4.

3.2.1 Quantifying false positives

It is typical for a search to be conducted into an enrolled population of N identities, and for the algorithm to be configured to return the closest L candidate identities. These candidates are ranked by their score, in descending order, with all scores required to be greater than or equal to zero. A human analyst might examine either all L candidates, or just the top $R \leq L$ identities, or only those with score greater than threshold, T.

From the candidate lists, we compute **false positive identification rate** as the proportion of non-mate searches that erroneously return candidates:

$$\text{FPIR}(N,T) = \frac{\text{Num. non-mate searches with one or more candidates returned with score at or above threshold}}{\text{Num. non-mate searches attempted.}} \tag{5}$$

Under this definition, FPIR can be computed from the highest non-mate candidate produced in a search - it is not necessary to consider candidates at rank 2 and above. An alternative quantity, selectivity, accounts for multiple candidates above threshold - see [17].

3.2.2 Quantifying hits and misses

If L candidates are returned in a search, a shorter candidate list can be prepared by taking the top $R \leq L$ candidates for which the score is above some threshold, $T \geq 0$. This reduction of the candidate list is done because thresholds may be applied, and only short lists might be reviewed (according to policy or labor availability, for example). It is useful then to state accuracy in terms of R and T, so we define a "miss rate" with the general name **false negative identification rate** (FNIR), as follows:

$$\text{FNIR}(N, R, T) = \frac{\text{Num. mate searches with enrolled mate found outside top R ranks or score below threshold}}{\text{Num. mate searches attempted.}} \tag{6}$$

This formulation is simple for evaluation in that it does not distinguish between causes of misses. Thus a mate that is not reported on a candidate list is treated the same as a miss arising from face finding failure, algorithm intolerance of poor quality, or software crashes. Thus if the algorithm fails to produce a candidate list, either because the search failed, or because a search template was not made, the result is regarded as a miss, adding to FNIR.

Hit rates, and true positive identification rates: While FNIR states the "miss rate" as how often the correct candidate is either not above threshold or not at good rank, many communities prefer to talk of "hit rates". This is simply the **true positive identification rate**(TPIR) which is the complement of FNIR giving a positive statement of how often mated searches are successful:

$$\text{TPIR}(N, R, T) = 1 - \text{FNIR}(N, R, T) \tag{7}$$

This report does not report true positive "hit" rates, preferring false negative miss rates for two reasons. First, costs rise linearly with error rates. For example, if we double FNIR in an access control system, then we double user inconvenience and delay. If we express that as decrease of TPIR from, say 98.5% to 97%, then we mentally have to invert the scale to see a doubling in costs. More subtly, readers don't perceive differences in numbers near 100% well, becoming inured to the "high nineties" effect where numbers close to 100 are perceived indifferently.

Reliability is a corresponding term, typically being identical to TPIR, and often cited in automated (fingerprint) identification system (AFIS) evaluations.

An important special case is the **cumulative match characteristic**(CMC) which summarizes accuracy of mated-searches only. It ignores similarity scores by relaxing the threshold requirement, and just reports the fraction of mated searches returning the mate at rank R or better.

$$\text{CMC}(N, R) = 1 - \text{FNIR}(N, R, 0) \tag{8}$$

We primarily cite the complement of this quantity, FNIR$(N, R, 0)$, the fraction of mates *not* in the top R ranks.

The **rank one hit rate** is the fraction of mated searches yielding the correct candidate at best rank, i.e. CMC(N, 1). While this quantity is the most common summary indicator of an algorithm's efficacy, it is not dependent on similarity scores, so it does not distinguish between strong (high scoring) and weak hits. It also ignores that an adjudicating reviewer is often willing to look at many candidates.

3.3 DET interpretation

In biometrics, a false negative occurs when an algorithm fails to match two samples of one person − a Type II error. Correspondingly, a false positive occurs when samples from two persons are improperly associated − a Type I error.

Matches are declared by a biometric system when the native comparison score from the recognition algorithm meets some threshold. Comparison scores can be either similarity scores, in which case higher values indicate that the samples are more likely to come from the same person, or dissimilarity scores, in which case higher values indicate different people. Similarity scores are traditionally computed by fingerprint and face recognition algorithms, while dissimilarities are used in iris recognition. In some cases, the dissimilarity score is a distance possessing metric properties. In any case, scores can be either mate scores, coming from a comparison of one person's samples, or nonmate scores, coming from comparison of different persons samples.

The words "genuine" or "authentic" are synonyms for mate, and the word "imposters"" is used as a synonym for nonmate. The words "mate" and "nonmate" are traditionally used in identification applications (such as law enforcement search, or background checks) while genuine and imposter are used in verification applications (such as access control).

An error tradeoff characteristic represents the tradeoff between Type II and Type I classification errors. For identification this plots false negative vs. false positive identification rates i.e. FNIR vs. FPIR parametrically with T. Such plots are often called detection error tradeoff (DET) characteristics or receiver operating characteristic (ROC). These serve the same function − to show error tradeoff − but differ, for example, in plotting the complement of an error rate (e.g. TPIR = 1 − FNIR) and in transforming the axes, most commonly using logarithms, to show multiple decades of FPIR.

3.4 Failure to extract features

During enrollment some algorithms fail to convert a face image to a template. The proportion of failures is the failure-to-enroll rate, denoted by FTE. Similarly, some search images are not converted to templates. The corresponding proportion is termed failure-to-extract, denoted by FTX. We do not report FTX because we assume that the same underlying algorithm is used for template generation for enrollment and search.

In verification, we do not need to explicitly include failure to extract rates into the FNMR and FMR accuracy statements, because we regard any comparison that involves an image for which a failure-to-extract occurred as producing a zero similarity score. This increases FNMR and decreases FMR. Gaming opportunities that theoretically arise from this treatment of FMR are generally not of concern because the algorithm under test does not know whether any given image will be used in genuine comparisons, imposter comparisons or both.

For identification, we similarly incorporate failure-to-extract events into FNIR and FPIR measurements as follows.

- **Enrollment templates**: Any failed enrollment is regarded as producing a zero length template. Algorithms are required by the API [18] to transparently process zero length templates. The effect of template generation failure on search accuracy depends on whether subsequent searches are mated, or non-mated: Mated searches will fail giving elevated FNIR; non-mated searches will not produce false positives so, to first order, FPIR will be reduced by a factor of 1−FTE.

- **Search templates and 1:N search**: In cases where the algorithm fails to produce a search template from input imagery, the result is taken to be a candidate list whose entries have no hypothesized identities and zero score. The effect of template generation failure on search accuracy depends on whether searches are mated, or non-mated: Mated searches will fail giving elevated FNIR; Non-mated searches will not produce false positives, so FPIR will be reduced.

This approach is the correct treatment for positive-identification applications such as access control where cooperative users are enrolled and make attempts at recognition. This approach is not appropriate to negative identification applications, such as visa fraud detection, in which hostile individuals may attempt to evade detection by submitting poor quality samples. In those cases, template generation failures should be investigated as though a false alarm had occurred.

	Developer	Verification algorithms	Identification algorithms
1	3Divi	3divi-003 3divi-004	3divi-0 3divi-3
2	Adera Global PTE Ltd	adera-001	
3	Alchera Inc	alchera-000 alchera-001	alchera-0
4	Alivia / Innovation Sys	isystems-001 isystems-002	isystems-0 isystems-3
5	AllGoVision	allgovision-000	allgovision-000
6	AlphaSSTG	alphaface-001	
7	Amplified Group	amplifiedgroup-001	
8	Anke Investments	anke-004	anke-0 anke-002
9	AnyVision	anyvision-002 anyvision-004	
10	Aware	aware-003 aware-004	aware-0 aware-3
11	Awidit Systems	awiros-001	
12	Ayonix	ayonix-000	ayonix-0
13	Beijing Vion Technology Inc	vion-000	
14	Bitmain	bm-001	
15	CSA IntelliCloud Technology	intellicloudai-001	
16	CTBC Bank Co Ltd	ctbcbank-000	
17	Camvi Technologies	camvi-002 camvi-004	camvi-1 camvi-3 camvi-4
18	China Electronics Import-Export Corp	ceiec-001 ceiec-002	
19	China University of Petroleum	upc-001	
20	Chunghwa Telecom Co. Ltd	chtface-001	
21	Cognitec Systems GmbH	cognitec-000 cognitec-001	cognitec-0 cognitec-2
22	Cyberextruder	cyberextruder-001 cyberextruder-002	
23	Cyberlink Corp	cyberlink-002 cyberlink-003	
24	DSK	dsk-000	
25	Dahua Technology Co Ltd	dahua-002 dahua-003	dahua-0 dahua-1 dahua-002
26	Deepglint	deepglint-001	deepglint-001
27	Dermalog	dermalog-005 dermalog-006	dermalog-0 dermalog-5 dermalog-6
28	DiDi ChuXing Technology Co	didiglobalface-001	
29	Digital Barriers	digitalbarriers-002	
30	Eyedea Recognition		eyedea-0 eyedea-3
31	FaceSoft Ltd	facesoft-000	
32	FarBar Inc	f8-001	f8-001
33	Gemalto Cogent	cogent-003 cogent-004	
34	Glory Ltd	glory-001	glory-0
35	Gorilla Technology	gorilla-003	gorilla-0
36	Guangzhou Pixel Solutions Co Ltd	pixelall-002	pixelall-002
37	Hengrui AI Technology Ltd	hr-001 hr-002	
38	Hikvision Research Institute	hik-001	hik-0 hik-5
39	ID3 Technology	id3-003 id3-004	
40	ITMO University	itmo-005 itmo-006	
41	Idemia	idemia-004 idemia-005	idemia-0 idemia-4 idemia-5
42	Imagus Technology Pty Ltd	imagus-000	imagus-0
43	Imperial College London	imperial-000 imperial-002	imperial-000
44	Incode Technologies Inc	incode-004	incode-0 incode-004

Table 4: Algorithms evaluated in this report.

	Developer	Verification algorithms	Identification algorithms
45	Innovatrics	innovatrics-004 innovatrics-006	innovatrics-0
46	Institute of Information Technologies	iit-001	
47	Intel Research Group	intelresearch-000	
48	Intellivision	intellivision-001 intellivision-002	
49	Is It You	isityou-000	
50	Kakao Corp	kakao-001 kakao-002	
51	Kedacom International Pte	kedacom-000	kedacom-001
52	Kneron Inc	kneron-003	
53	Lomonosov Moscow State University	intsysmsu-000	intsysmsu-000
54	Lookman Electroplast Industries	lookman-002 lookman-004	
55	Megvii/Face++	megvii-001 megvii-002	megvii-0 megvii-1
56	MicroFocus	microfocus-002 microfocus-001	microfocus-0
57	Microsoft		microsoft-0 microsoft-5
58	Momentum Digital Co Ltd	sertis-000	
59	Moontime Smart Technology	mt-000	
60	N-Tech Lab	ntechlab-006 ntechlab-007	ntechlab-0 ntechlab-6 ntechlab-007
61	NEC		nec-2 nec-3
62	Neurotechnology	neurotechnology-005 neurotechnology-006	neurotechnology-0 neurotechnology-5 neurotechnology-007
63	Nodeflux	nodeflux-001 nodeflux-002	
64	NotionTag Technologies Private Limited	notiontag-000	
65	Panasonic R+D Center Singapore	psl-002 psl-003	
66	Paravision (EverAI)	everai-paravision-003 paravision-004	everai-0 everai-3 everai-paravision-004
67	Rank One Computing	rankone-007	rankone-0 rankone-5 rankone-006 rankone-007
68	Realnetworks Inc	realnetworks-002 realnetworks-003	realnetworks-0 realnetworks-2 realnetworks-003
69	Remark Holdings	remarkai-001	remarkai-0 remarkai-000
70	Rokid Corporation Ltd	rokid-000	
71	Saffe Ltd	saffe-001 saffe-002	
72	Sensetime Group Ltd	sensetime-002	sensetime-0 sensetime-1 sensetime-002
73	Shaman Software	shaman-000 shaman-001	shaman-0
74	Shanghai Jiao Tong University	sjtu-001	
75	Shanghai Ulucu Electronics Technology Co. Ltd	uluface-002	
76	Shanghai Universiy - Shanghai Film Academy	shu-001	
77	Shanghai Yitu Technology	yitu-003	yitu-0 yitu-4 yitu-5
78	Shenzhen EI Networks Limited	einetworks-000	
79	Shenzhen Inst Adv Integrated Tech CAS	siat-004 siat-002	siat-0
80	Shenzhen Intellifusion Technologies Co Ltd	intellifusion-001	
81	Smilart	smilart-002 smilart-003	smilart-0
82	Star Hybrid Limited	starhybrid-001	
83	Synesis	synesis-005	synesis-0
84	Tech5 SA	tech5-002 tech5-003	tech5-001
85	Tencent Deepsea Lab	deepsea-001	deepsea-001
86	Tevian	tevian-004 tevian-005	tevian-0 tevian-4
87	Thales		cogent-0 cogent-3
88	TigerIT Americas LLC	tiger-002 tiger-003	tiger-0

Table 5: Algorithms evaluated in this report.

	Developer	Verification algorithms	Identification algorithms
89	TongYi Transportation Technology	tongyi-005	
90	Toshiba	toshiba-002 toshiba-003	toshiba-0 toshiba-1
91	Trueface.ai	trueface-000	
92	ULSee Inc	ulsee-001	
93	Veridas Digital Authentication Solutions S.L.	veridas-002	
94	Via Technologies Inc.	via-000	
95	Videonetics Technology Pvt Ltd	videonetics-001	
96	Vigilant Solutions	vigilantsolutions-006 vigilantsolutions-007	vigilantsolutions-0
97	Visidon	vd-001	vd-0
98	Vision-Box	visionbox-000 visionbox-001	
99	VisionLabs	visionlabs-006 visionlabs-007	visionlabs-7 visionlabs-008
100	Vocord	vocord-006 vocord-007	vocord-0 vocord-3
101	Winsense Co Ltd	winsense-000	
102	X-Laboratory	x-laboratory-000	
103	Xiamen Meiya Pico Information Co. Ltd	meiya-001	
104	Zhuhai Yisheng Electronics Technology	yisheng-004	yisheng-0
105	iQIYI Inc	iqface-000	
106	iSAP Solution Corporation	isap-001	

Table 6: Algorithms evaluated in this report.

4 False positive differentials in verification

False positives occur in biometric systems when samples from two individuals yield a comparison score at or above a set threshold. Most systems are configured with a threshold that is fixed for all users. False positives present a security hazard to one-to-one verification applications. They have similarly serious consequences in one-to-many identification applications. For example, in applications where subjects apply for some benefit more than once under different biographic identities e.g. visa-shopping, driving license issuance, benefits fraud, an otherwise undetected false positive might lead to various downstream consequences such a financial loss. In a surveillance application a false positive may lead to a false accusation.

This section gives empirical quantification of the variation in verification false match rates across demographics. We present results for one-to-many identification later in section 7.

We conduct several experiments with images drawn from both domestic United States and worldwide populations.

1. One-to-one application photo cross comparison, by age, sex, country-of-birth.
2. One-to-one mugshot cross comparison by age, sex, and race.
3. One-to-one visa photo cross comparison by age.

4.1 Metrics

The metrics appropriate to verification have been detailed in section 3.1. These are related to particular applications in Figure 2. The discussion in subsequent sections centers on false match rates at particular thresholds, i.e. FMR(T).

4.2 False match rates under demographic pairing

It is necessary in many biometric tests to estimate false match rates. This is done by executing imposter comparisons, and measuring false positive outcomes at some threshold(s). Historically biometric evaluations generated imposter comparisons by randomly pairing individuals, or by exhaustively comparing all individuals. As we will show in this section, this practice is inappropriate for evaluation of face recognition algorithms as it underestimates false match rates that would occur in practice. The random pairing of imposters is sometimes referred to as zero-effort pairing, mean that no effort is expended by an imposter to look like the target of the recognition attempt.

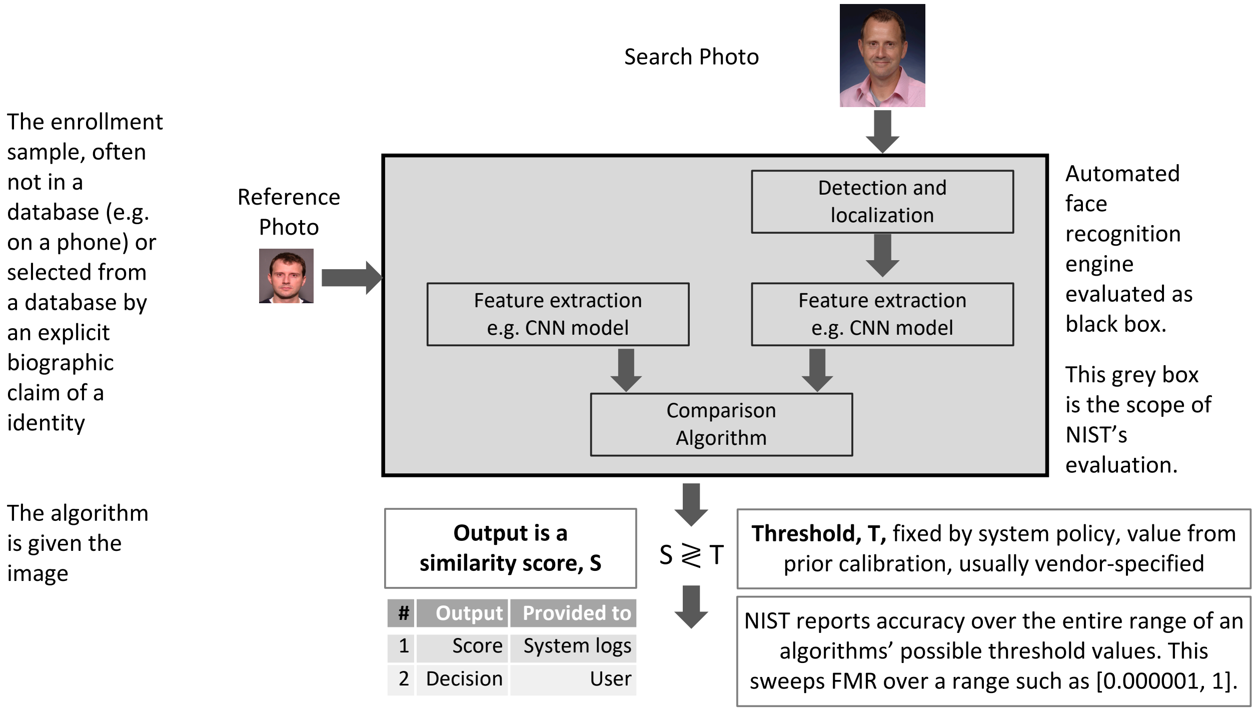
Search Photo
The enrollment sample, often not in a database (e.g. on a phone) or selected from a database by an explicit biographic claim of a identity
Reference Photo
Detection and localization
Feature extraction e.g. CNN model
Feature extraction e.g. CNN model
Comparison Algorithm
Automated face recognition engine evaluated as black box.
This grey box is the scope of NIST's evaluation.
The algorithm is given the image
Output is a similarity score, S
S ≷ T
Threshold, T, fixed by system policy, value from prior calibration, usually vendor-specified
NIST reports accuracy over the entire range of an algorithms' possible threshold values. This sweeps FMR over a range such as [0.000001, 1].

#	Output	Provided to
1	Score	System logs
2	Decision	User

	Access Control	**Non-repudiation**
Role	Afford access of a person to a physical or logical resource.	Record the presence of a specific individual
Example	Door unlock. Phone unlock.	Refutation of a claim by a pharmacist that they did not dispense a particular drug, or an employer that an employee did not arrive for work.
Claim of identity	Explicit claim with an identity token such as a phone, passport or ID card.	Claim with a prior login to a system.
Threshold	High, to limit false positives	Moderate, to prevent confederates using system
Result	Acceptance decision Y/N.	Logged verification decision
Human role	Adjudicate failed rejections, to determine a false rejection, or detect an actual impostor attempt	Retrieve records to resolve a dispute
Intended human involvement frequency	Rare – approx. the false rejection rate identification rate plus prior probability of an actual mate	Rare – approx. the fraud rate multiplied by the false positive rate
Performance metric of interest	**FNMR at low FMR. See sec. 3.1, 3.2 and Tables 10, 19**	**FNMR at moderate FMR.**

Figure 2: Verification applications and relevant metrics.

reports/11/figures/dhs_obim/cross_country/impostors/fmr_same_same_same/imperial_002.pdf

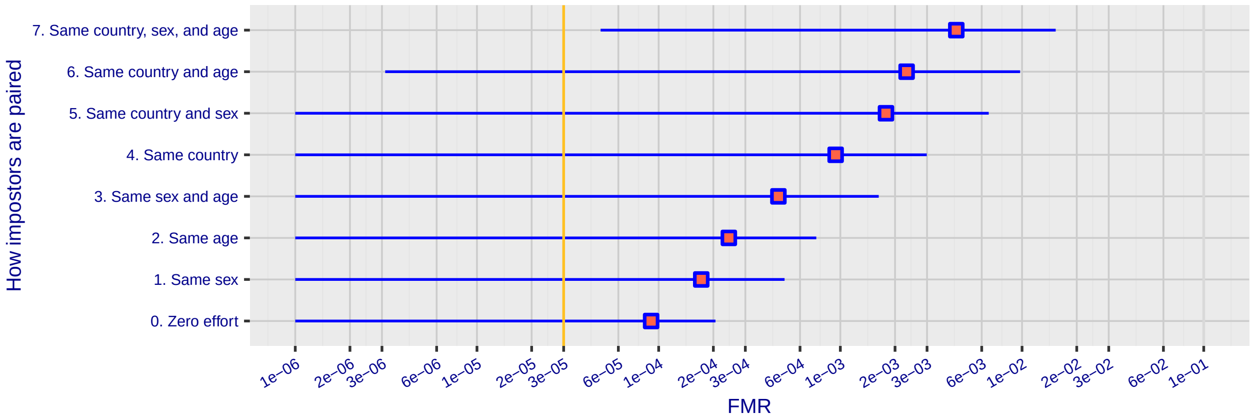

Figure 3: For application photos, the figure shows growth in one-to-one verification false match rates as the imposter demographic pairings are made more similar. At each level the point shows the mean FMR over all countries, age groups, and sexes. For example, in the second row "6. Same country and age" the mean is taken over 24 within-country times 5 within age-group times 4 within and cross sex FMR estimates, i.e. 480 FMR values. The blue line spans the 5-th to 95-th percentiles of the FMR estimates. The vertical line shows a nominal FMR value of 0.00003 obtained by setting the threshold on randomly associated i.e. zero-effort pairs of mugshot images.

Method: We used each verification algorithm to compare 442 019 application images with a disjoint set of 441 517 other application images. The two sets are subject-disjoint. The subjects were born in 24 countries. This produced 195 billion imposter scores. The images are described in Annex 2 .

The red point in the plot shows the mean of false match rates over particular sets of demographic groups.

- **Row 7**: The uppermost point corresponds to the mean over 240 FMR estimates, namely those comparing each of two sexes with each other, in each of five age-groups, and within each of 24 countries (2 x 5 x 24 = 240).
- **Row 6**: As row 7, but the average is over 480 FMR estimates that now includes different sex FMR estimates also.
- **Row 5**: As row 7, but now the average is over 1200 FMR estimates that additionally includes all cross-age group imposter scores.
- **Row 4**: As row 7, but now the average is over 2400 FMR estimates that additionally includes all cross-age and cross-sex imposter scores.
- **Row 3**: The average is over 5760 FMR estimates that includes 24^2 cross-country comparisons within each sex and age group.
- **Row 2**: The average is over 11520 FMR estimates now including different sex FMR estimates also.

- ▷ **Row 1**: The average is over 28880 FMR estimates now including five different within-age FMR estimates also.

- ▷ **Row 0**: The average is over 57600 FMR estimates reflecting within- and between-group estimates for 24 countries, 5 age groups and 2 sexes $(24^2.5^2.2^2)$.

The ordering of these rows is hand-crafted. Evaluators at DHS' Maryland Test Facility developed [20] a formal approach to showing the most influential pairing factor by quantifying information gained about FMR by having knowledge of the demographic factors, age, sex and race.

The figure shows how false match rates increase when imposters are drawn from increasingly similar demographics. This shows that fully zero-effort imposter pairings understate false match rates relative to the situation of a slightly more active imposters who would chose to present (stolen) credentials from subjects of the same sex, age and ethnicity. The practice of using zero-effort imposter pairings in tests, we think, stems from tests of fingerprint algorithm that use where friction ridge structure, particularly minutiae point arrangements, that are thought to be a developmental trait without clear genetic influence[8]

Note that our analysis has not so far documented whether particular demographic groups give higher false match rates. To address this question we introduce Figure 4 which shows results similar to those above but now for each specific country of birth.

We make the following observations:

- ▷ **Restricted pairing increases FMR**: Within each country, there is a more than order of magnitude increase in FMR between the zero-effort pair anyone-with-anyone setting, and the same-age, same-sex, same-country pairing. This re-iterates the results of the previous section, and shows it applies globally.

- ▷ **Country-of-birth matters**: For many of the different levels of demographic pairing there is between one and two orders of magnitude between the 24 countries represented in this dataset. For example when imposters are from the same sex and country but of any age, the algorithm gives FMR of 0.000046 on Polish faces and 0.0024 on Vietnamese, a fifty fold increase.

- ▷ **Regions with highest and lowest FMR**: Across algorithms often the lowest FMR is observed in Eastern European populations and the highest in East Asian populations. However there are important exceptions: Some algorithms developed in East Asia tend to give lower FMR in photos of subjects born in East Asian countries[9]. This observation and the topic of demographic differentials associated with na-

[8] Genetic influence on friction ridge structure is known: The absence of the SMARCAD1 gene leads to absence of fingerprints at birth. Further, the distance between friction ridges is smaller, on average in women than in men, and this may well be under genetic influence. The distance itself is likely not used as a biometric feature, at least not explicitly. Fingerprint pattern classes (arch, whorl etc.), however, have been shown to have regional (geographic) variations, and these were, at least historically, used in one-to-many multi-finger search strategies.

[9] See, for example, the figure in Annex 8 for algorithms from HIK, Dahua, Yitu, Alphaface, Deepsea Tencent, Toshiba.

tional origin are covered more completely in the next section which includes results for comparison of individuals within and across national boundaries.

Discussion: The results above show that false match rates for imposter pairings in likely real-world scenarios are much higher than those from measured when imposters are paired with zero-effort. For this reason NIST has been reporting "matched-covariate" accuracy results in its FRVT evaluation of face verification algorithms [16]. Along similar lines the Australian Department of Foreign Affairs and Trade in tests it sponsors only uses same-sex imposter pairings. The effect of this is to raise thresholds, and thereby raise false non-march rates also. Thresholds increase because they are determined from non-mate scores, s, via the quantile function Q, as that value, T, which gives a proportion, FMR, at or above threshold:

$$T = Q(s, 1 - \text{FMR}) \tag{9}$$

and the set of demographically matched scores is smaller than if all possible comparisons is used.

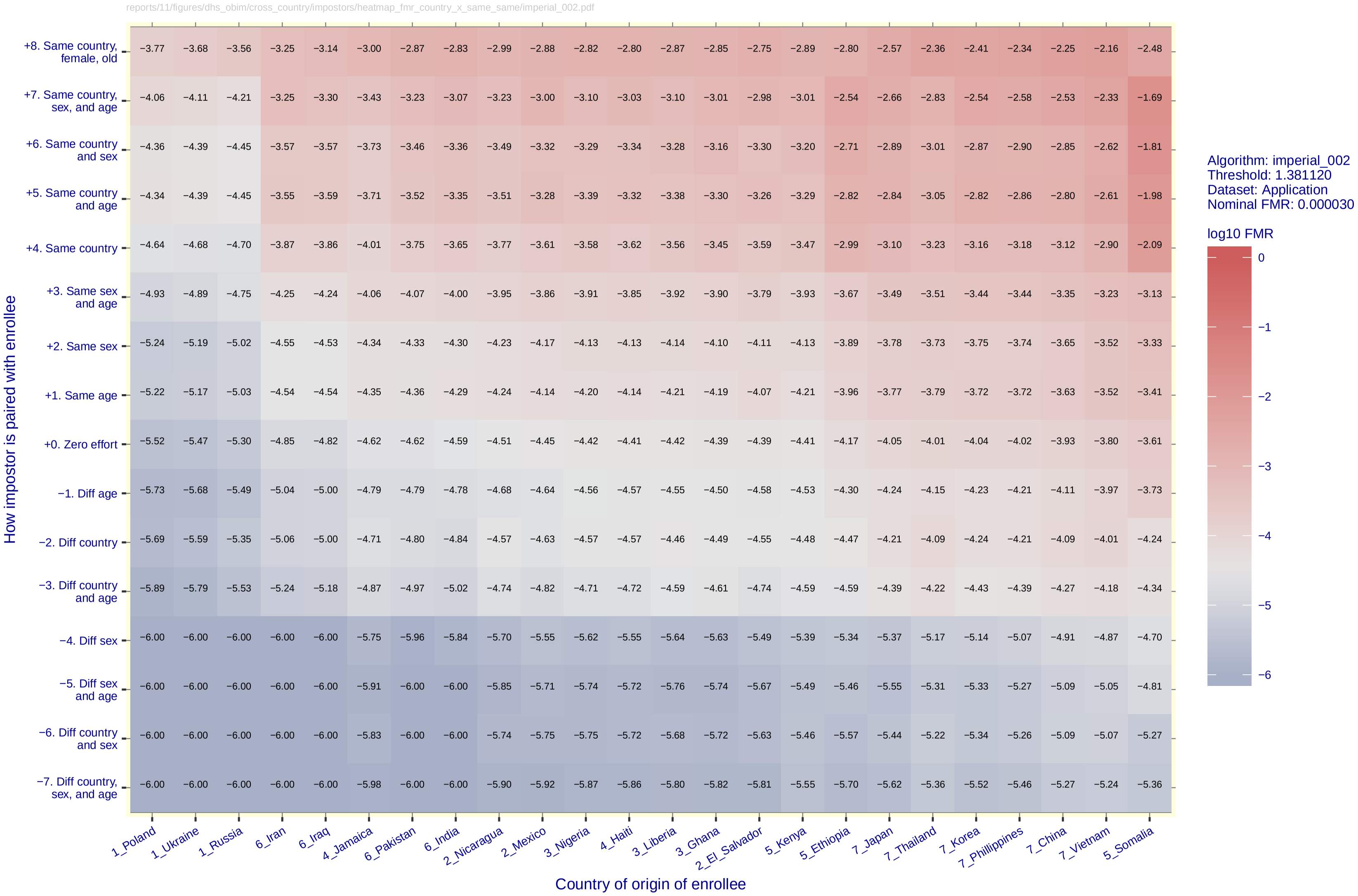

Figure 4: The heatmap shows FMR for each country-of-birth, when the imposter comparisons are drawn from increasingly demographically-matched individuals. Each cell depicts FMR on a logarithmic scale. The text value is $\log_{10}(\text{FMR})$ *with large negative values encoding superior false match rates. The center row ("0. Zero effort") row compares individuals without regard to demographics. Rows above that pair imposters more closely until, in the second row, the imposters are of the same sex, age and country of origin. The top row corresponds to one particular demographic often associated with the highest FMR values. The rows below center pair for increasingly unlikely imposter pairings. For example "-5. Diff sex and age" shows FMR for imposters of different sex and age group. The countries appear in order of increasing mean FMR. Values below -6 are pinned to -6. Annex 8 contains the corresponding figure for all algorithms.*

4.3 False match rates within and across countries

Method: Using high quality application portraits drawn from the corpus described in Annex 2 , we compared 442 019 images from 24 countries with 441 517 images of different individuals from the same countries, yielding 195.2 billion imposter comparisons. We executed this set of comparisons with 126 verification algorithms submitted to the FRVT Verification track. These are listed in Table 4-6. We compared scores with a set of 10 thresholds to produce FMR estimates at each of those thresholds. The thresholds were computed over a set of 93 070 400 imposter comparisons made using a different set of images, namely the law enforcement mugshots detailed in Annex 1 . Each threshold was selected as the lowest value that gave FMR at or below a target FMR. The target FMR value was 0.00003.

Each photograph was assigned to the age groups defined by the intervals $(00-20]$, $(20-35]$, $(35-50]$, $(50-65]$, and $(65-99]$.

We excluded small numbers of photographs for which country of birth was not available, or for which sex was not listed as male or female.

Each comparison is accompanied by sex, country of birth and age group metadata for the two individuals represented in the photographs. Given many comparisons with the same demographic pairing, we can produce a measurement of FMR when comparing individuals from two demographic groups, for example Polish men over the age of 65 with Mexican women between 20 and 35.

Analysis: To address the issue addressed in the title of this section we produced figures depicting cross-country false match rates. Figure 5 is an example. We restricted the demographics to just men in the largest age group, $(35-50]$, and then repeated that for women. We remove sex and age from the discussion for two reasons: First, to isolate the country-of-origin effect, and, second, to reflect what real-world imposters would do: procure identity credentials from persons of the same age and sex.

Figure 5 shows cross-country FMR for one of the more accurate algorithms. Annex 7 contains corresponding figures for all algorithms, for both men and women. The annex therefore extends to more than 250 pages. We could repeat this visualization for other age groups - the results are similar. We discuss the effect of age itself later. Likewise, we could repeat the visualization for other recognition thresholds. The one adopted corresponds to a FMR = 0.00003. The trends are very similar at any threshold.

The Figure shows FMR as a heatmap. It uses a logarithmic scale, so that a FMR of 0.0001 is represented by a color and a text value of -4, i.e. log to the base 10. Low FMR values are shown in blue. High FMR values are shown in red. A grey color connotes the target FMR value ($\log_{10} 0.00003 = -4.5$). High FMR values present a security concern in verification applications.

Discussion: From the Figure and those in the annexes, we make a number of observations. First by assigning

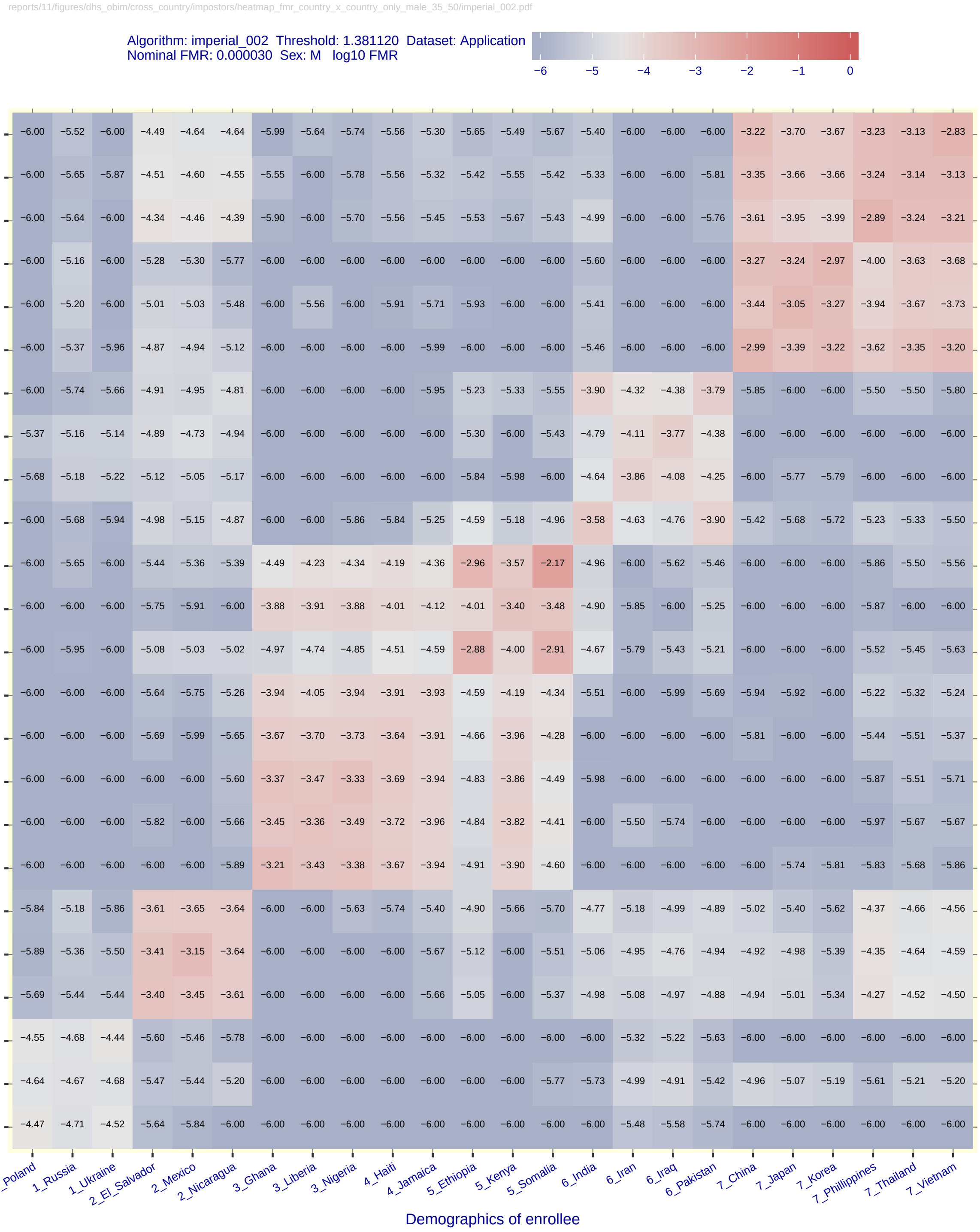

	1_Poland	1_Russia	1_Ukraine	2_El_Salvador	2_Mexico	2_Nicaragua	3_Ghana	3_Liberia	3_Nigeria	4_Haiti	4_Jamaica	5_Ethiopia	5_Kenya	5_Somalia	6_India	6_Iran	6_Iraq	6_Pakistan	7_China	7_Japan	7_Korea	7_Phillippines	7_Thailand	7_Vietnam
7_Vietnam	−6.00	−5.52	−6.00	−4.49	−4.64	−4.64	−5.99	−5.64	−5.74	−5.56	−5.30	−5.65	−5.49	−5.67	−5.40	−6.00	−6.00	−6.00	−3.22	−3.70	−3.67	−3.23	−3.13	−2.83
7_Thailand	−6.00	−5.65	−5.87	−4.51	−4.60	−4.55	−5.55	−6.00	−5.78	−5.56	−5.32	−5.42	−5.55	−5.42	−5.33	−6.00	−6.00	−5.81	−3.35	−3.66	−3.66	−3.24	−3.14	−3.13
7_Phillippines	−6.00	−5.64	−6.00	−4.34	−4.46	−4.39	−5.90	−6.00	−5.70	−5.56	−5.45	−5.53	−5.67	−5.43	−4.99	−6.00	−6.00	−5.76	−3.61	−3.95	−3.99	−2.89	−3.24	−3.21
7_Korea	−6.00	−5.16	−6.00	−5.28	−5.30	−5.77	−6.00	−6.00	−6.00	−6.00	−6.00	−6.00	−6.00	−6.00	−5.60	−6.00	−6.00	−6.00	−3.27	−3.24	−2.97	−4.00	−3.63	−3.68
7_Japan	−6.00	−5.20	−6.00	−5.01	−5.03	−5.48	−6.00	−5.56	−6.00	−5.91	−5.71	−5.93	−6.00	−6.00	−5.41	−6.00	−6.00	−6.00	−3.44	−3.05	−3.27	−3.94	−3.67	−3.73
7_China	−6.00	−5.37	−5.96	−4.87	−4.94	−5.12	−6.00	−6.00	−6.00	−6.00	−5.99	−6.00	−6.00	−6.00	−5.46	−6.00	−6.00	−6.00	−2.99	−3.39	−3.22	−3.62	−3.35	−3.20
6_Pakistan	−6.00	−5.74	−5.66	−4.91	−4.95	−4.81	−6.00	−6.00	−6.00	−6.00	−5.95	−5.23	−5.33	−5.55	−3.90	−4.32	−4.38	−3.79	−5.85	−6.00	−6.00	−5.50	−5.50	−5.80
6_Iraq	−5.37	−5.16	−5.14	−4.89	−4.73	−4.94	−6.00	−6.00	−6.00	−6.00	−6.00	−5.30	−6.00	−5.43	−4.79	−4.11	−3.77	−4.38	−6.00	−6.00	−6.00	−6.00	−6.00	−6.00
6_Iran	−5.68	−5.18	−5.22	−5.12	−5.05	−5.17	−6.00	−6.00	−6.00	−6.00	−6.00	−5.84	−5.98	−6.00	−4.64	−3.86	−4.08	−4.25	−6.00	−5.77	−5.79	−6.00	−6.00	−6.00
6_India	−6.00	−5.68	−5.94	−4.98	−5.15	−4.87	−6.00	−6.00	−5.86	−5.84	−5.25	−4.59	−5.18	−4.96	−3.58	−4.63	−4.76	−3.90	−5.42	−5.68	−5.72	−5.23	−5.33	−5.50
5_Somalia	−6.00	−5.65	−6.00	−5.44	−5.36	−5.39	−4.49	−4.23	−4.34	−4.19	−4.36	−2.96	−3.57	−2.17	−4.96	−6.00	−5.62	−5.46	−6.00	−6.00	−6.00	−5.86	−5.50	−5.56
5_Kenya	−6.00	−6.00	−6.00	−5.75	−5.91	−6.00	−3.88	−3.91	−3.88	−4.01	−4.12	−4.01	−3.40	−3.48	−4.90	−5.85	−6.00	−5.25	−6.00	−6.00	−6.00	−5.87	−6.00	−6.00
5_Ethiopia	−6.00	−5.95	−6.00	−5.08	−5.03	−5.02	−4.97	−4.74	−4.85	−4.51	−4.59	−2.88	−4.00	−2.91	−4.67	−5.79	−5.43	−5.21	−6.00	−6.00	−6.00	−5.52	−5.45	−5.63
4_Jamaica	−6.00	−6.00	−6.00	−5.64	−5.75	−5.26	−3.94	−4.05	−3.94	−3.91	−3.93	−4.59	−4.19	−4.34	−5.51	−6.00	−5.99	−5.69	−5.94	−5.92	−6.00	−5.22	−5.32	−5.24
4_Haiti	−6.00	−6.00	−6.00	−5.69	−5.99	−5.65	−3.67	−3.70	−3.73	−3.64	−3.91	−4.66	−3.96	−4.28	−6.00	−6.00	−6.00	−6.00	−5.81	−6.00	−6.00	−5.44	−5.51	−5.37
3_Nigeria	−6.00	−6.00	−6.00	−6.00	−6.00	−5.60	−3.37	−3.47	−3.33	−3.69	−3.94	−4.83	−3.86	−4.49	−5.98	−6.00	−6.00	−6.00	−6.00	−6.00	−6.00	−5.87	−5.51	−5.71
3_Liberia	−6.00	−6.00	−6.00	−5.82	−6.00	−5.66	−3.45	−3.36	−3.49	−3.72	−3.96	−4.84	−3.82	−4.41	−6.00	−5.50	−5.74	−6.00	−6.00	−6.00	−6.00	−5.97	−5.67	−5.67
3_Ghana	−6.00	−6.00	−6.00	−6.00	−6.00	−5.89	−3.21	−3.43	−3.38	−3.67	−3.94	−4.91	−3.90	−4.60	−6.00	−6.00	−6.00	−6.00	−6.00	−5.74	−5.81	−5.83	−5.68	−5.86
2_Nicaragua	−5.84	−5.18	−5.86	−3.61	−3.65	−3.64	−6.00	−6.00	−5.63	−5.74	−5.40	−4.90	−5.66	−5.70	−4.77	−5.18	−4.99	−4.89	−5.02	−5.40	−5.62	−4.37	−4.66	−4.56
2_Mexico	−5.89	−5.36	−5.50	−3.41	−3.15	−3.64	−6.00	−6.00	−6.00	−6.00	−5.67	−5.12	−6.00	−5.51	−5.06	−4.95	−4.76	−4.94	−4.92	−4.98	−5.39	−4.35	−4.64	−4.59
2_El_Salvador	−5.69	−5.44	−5.44	−3.40	−3.45	−3.61	−6.00	−6.00	−6.00	−6.00	−5.66	−5.05	−6.00	−5.37	−4.98	−5.08	−4.97	−4.88	−4.94	−5.01	−5.34	−4.27	−4.52	−4.50
1_Ukraine	−4.55	−4.68	−4.44	−5.60	−5.46	−5.78	−6.00	−6.00	−6.00	−6.00	−6.00	−6.00	−6.00	−6.00	−6.00	−5.32	−5.22	−5.63	−6.00	−6.00	−6.00	−6.00	−6.00	−6.00
1_Russia	−4.64	−4.67	−4.68	−5.47	−5.44	−5.20	−6.00	−6.00	−6.00	−6.00	−6.00	−6.00	−6.00	−5.77	−5.73	−4.99	−4.91	−5.42	−4.96	−5.07	−5.19	−5.61	−5.21	−5.20
1_Poland	−4.47	−4.71	−4.52	−5.64	−5.84	−6.00	−6.00	−6.00	−6.00	−6.00	−6.00	−6.00	−6.00	−6.00	−6.00	−5.48	−5.58	−5.74	−6.00	−6.00	−6.00	−6.00	−6.00	−6.00

Figure 5: For 24 countries in seven regions the figure shows false positive rates when the reference algorithm is used to compare single photos of mid-aged male subjects from the countries identified in the respective columns. The threshold is to a preset fixed value everywhere. Each cell depicts FMR on a logarithmic scale. The text value is $\log_{10}(\text{FMR})$ *with large negative values encoding superior false match rates. Annex 7 contains the corresponding figure for all algorithms.*

reports/11/figures/dhs_obim/cross_country/impostors/heatmap_fmr_country_x_country_only_female_35_50/imperial_002.pdf

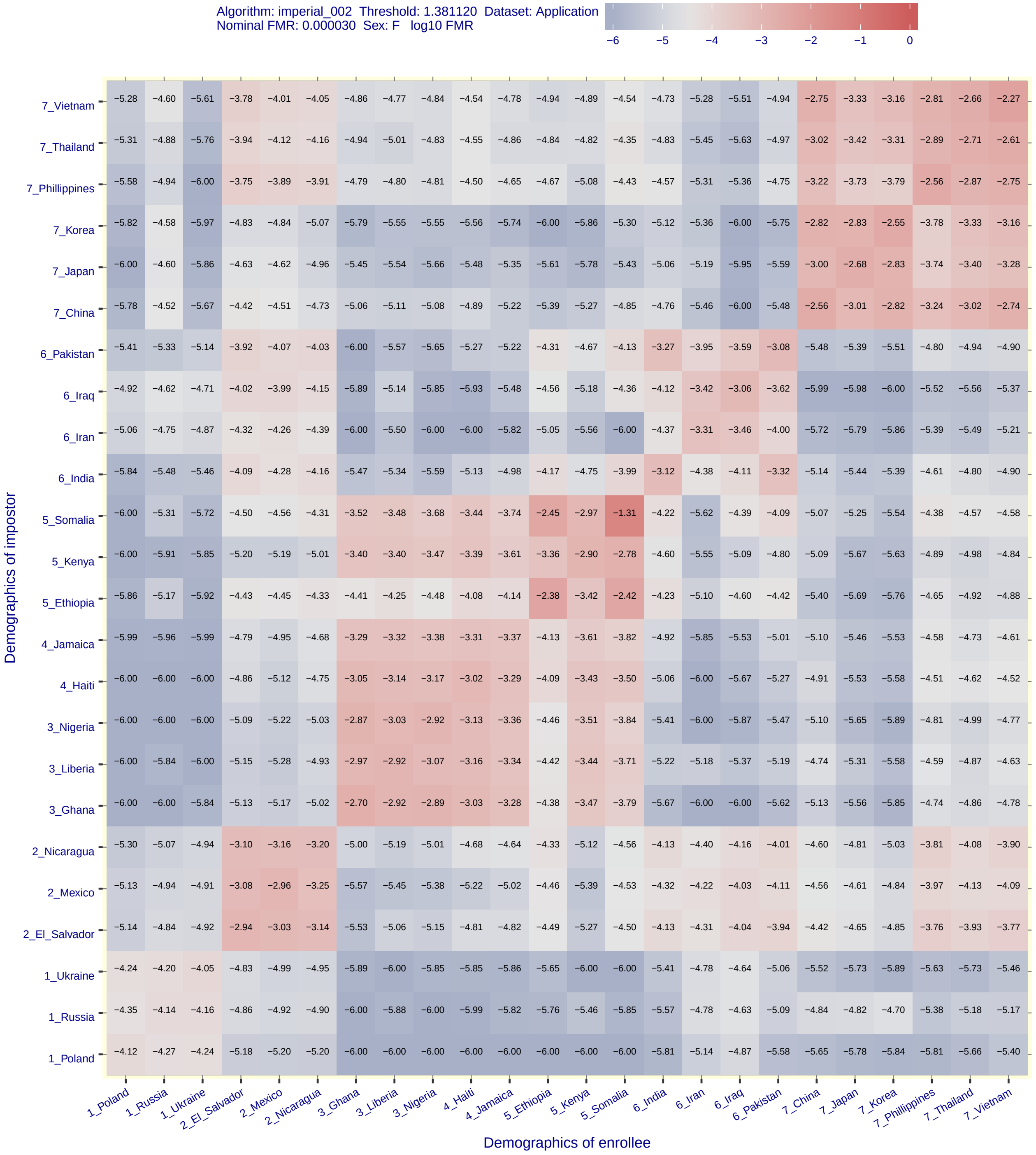

	1_Poland	1_Russia	1_Ukraine	2_El_Salvador	2_Mexico	2_Nicaragua	3_Ghana	3_Liberia	3_Nigeria	4_Haiti	4_Jamaica	5_Ethiopia	5_Kenya	5_Somalia	6_India	6_Iran	6_Iraq	6_Pakistan	7_China	7_Japan	7_Korea	7_Phillippines	7_Thailand	7_Vietnam
7_Vietnam	−5.28	−4.60	−5.61	−3.78	−4.01	−4.05	−4.86	−4.77	−4.84	−4.54	−4.78	−4.94	−4.89	−4.54	−4.73	−5.28	−5.51	−4.94	−2.75	−3.33	−3.16	−2.81	−2.66	−2.27
7_Thailand	−5.31	−4.88	−5.76	−3.94	−4.12	−4.16	−4.94	−5.01	−4.83	−4.55	−4.86	−4.84	−4.82	−4.35	−4.83	−5.45	−5.63	−4.97	−3.02	−3.42	−3.31	−2.89	−2.71	−2.61
7_Phillippines	−5.58	−4.94	−6.00	−3.75	−3.89	−3.91	−4.79	−4.80	−4.81	−4.50	−4.65	−4.67	−5.08	−4.43	−4.57	−5.31	−5.36	−4.75	−3.22	−3.73	−3.79	−2.56	−2.87	−2.75
7_Korea	−5.82	−4.58	−5.97	−4.83	−4.84	−5.07	−5.79	−5.55	−5.55	−5.56	−5.74	−6.00	−5.86	−5.30	−5.12	−5.36	−6.00	−5.75	−2.82	−2.83	−2.55	−3.78	−3.33	−3.16
7_Japan	−6.00	−4.60	−5.86	−4.63	−4.62	−4.96	−5.45	−5.54	−5.66	−5.48	−5.35	−5.61	−5.78	−5.43	−5.06	−5.19	−5.95	−5.59	−3.00	−2.68	−2.83	−3.74	−3.40	−3.28
7_China	−5.78	−4.52	−5.67	−4.42	−4.51	−4.73	−5.06	−5.11	−5.08	−4.89	−5.22	−5.39	−5.27	−4.85	−4.76	−5.46	−6.00	−5.48	−2.56	−3.01	−2.82	−3.24	−3.02	−2.74
6_Pakistan	−5.41	−5.33	−5.14	−3.92	−4.07	−4.03	−6.00	−5.57	−5.65	−5.27	−5.22	−4.31	−4.67	−4.13	−3.27	−3.95	−3.59	−3.08	−5.48	−5.39	−5.51	−4.80	−4.94	−4.90
6_Iraq	−4.92	−4.62	−4.71	−4.02	−3.99	−4.15	−5.89	−5.14	−5.85	−5.93	−5.48	−4.56	−5.18	−4.36	−4.12	−3.42	−3.06	−3.62	−5.99	−5.98	−6.00	−5.52	−5.56	−5.37
6_Iran	−5.06	−4.75	−4.87	−4.32	−4.26	−4.39	−6.00	−5.50	−6.00	−6.00	−5.82	−5.05	−5.56	−6.00	−4.37	−3.31	−3.46	−4.00	−5.72	−5.79	−5.86	−5.39	−5.49	−5.21
6_India	−5.84	−5.48	−5.46	−4.09	−4.28	−4.16	−5.47	−5.34	−5.59	−5.13	−4.98	−4.17	−4.75	−3.99	−3.12	−4.38	−4.11	−3.32	−5.14	−5.44	−5.39	−4.61	−4.80	−4.90
5_Somalia	−6.00	−5.31	−5.72	−4.50	−4.56	−4.31	−3.52	−3.48	−3.68	−3.44	−3.74	−2.45	−2.97	−1.31	−4.22	−5.62	−4.39	−4.09	−5.07	−5.25	−5.54	−4.38	−4.57	−4.58
5_Kenya	−6.00	−5.91	−5.85	−5.20	−5.19	−5.01	−3.40	−3.40	−3.47	−3.39	−3.61	−3.36	−2.90	−2.78	−4.60	−5.55	−5.09	−4.80	−5.09	−5.67	−5.63	−4.89	−4.98	−4.84
5_Ethiopia	−5.86	−5.17	−5.92	−4.43	−4.45	−4.33	−4.41	−4.25	−4.48	−4.08	−4.14	−2.38	−3.42	−2.42	−4.23	−5.10	−4.60	−4.42	−5.40	−5.69	−5.76	−4.65	−4.92	−4.88
4_Jamaica	−5.99	−5.96	−5.99	−4.79	−4.95	−4.68	−3.29	−3.32	−3.38	−3.31	−3.37	−4.13	−3.61	−3.82	−4.92	−5.85	−5.53	−5.01	−5.10	−5.46	−5.53	−4.58	−4.73	−4.61
4_Haiti	−6.00	−6.00	−6.00	−4.86	−5.12	−4.75	−3.05	−3.14	−3.17	−3.02	−3.29	−4.09	−3.43	−3.50	−5.06	−6.00	−5.67	−5.27	−4.91	−5.53	−5.58	−4.51	−4.62	−4.52
3_Nigeria	−6.00	−6.00	−6.00	−5.09	−5.22	−5.03	−2.87	−3.03	−2.92	−3.13	−3.36	−4.46	−3.51	−3.84	−5.41	−6.00	−5.87	−5.47	−5.10	−5.65	−5.89	−4.81	−4.99	−4.77
3_Liberia	−6.00	−5.84	−6.00	−5.15	−5.28	−4.93	−2.97	−2.92	−3.07	−3.16	−3.34	−4.42	−3.44	−3.71	−5.22	−5.18	−5.37	−5.19	−4.74	−5.31	−5.58	−4.59	−4.87	−4.63
3_Ghana	−6.00	−6.00	−5.84	−5.13	−5.17	−5.02	−2.70	−2.92	−2.89	−3.03	−3.28	−4.38	−3.47	−3.79	−5.67	−6.00	−6.00	−5.62	−5.13	−5.56	−5.85	−4.74	−4.86	−4.78
2_Nicaragua	−5.30	−5.07	−4.94	−3.10	−3.16	−3.20	−5.00	−5.19	−5.01	−4.68	−4.64	−4.33	−5.12	−4.56	−4.13	−4.40	−4.16	−4.01	−4.60	−4.81	−5.03	−3.81	−4.08	−3.90
2_Mexico	−5.13	−4.94	−4.91	−3.08	−2.96	−3.25	−5.57	−5.45	−5.38	−5.22	−5.02	−4.46	−5.39	−4.53	−4.32	−4.22	−4.03	−4.11	−4.56	−4.61	−4.84	−3.97	−4.13	−4.09
2_El_Salvador	−5.14	−4.84	−4.92	−2.94	−3.03	−3.14	−5.53	−5.06	−5.15	−4.81	−4.82	−4.49	−5.27	−4.50	−4.13	−4.31	−4.04	−3.94	−4.42	−4.65	−4.85	−3.76	−3.93	−3.77
1_Ukraine	−4.24	−4.20	−4.05	−4.83	−4.99	−4.95	−5.89	−6.00	−5.85	−5.85	−5.86	−5.65	−6.00	−6.00	−5.41	−4.78	−4.64	−5.06	−5.52	−5.73	−5.89	−5.63	−5.73	−5.46
1_Russia	−4.35	−4.14	−4.16	−4.86	−4.92	−4.90	−6.00	−5.88	−6.00	−5.99	−5.82	−5.76	−5.46	−5.85	−5.57	−4.78	−4.63	−5.09	−4.84	−4.82	−4.70	−5.38	−5.18	−5.17
1_Poland	−4.12	−4.27	−4.24	−5.18	−5.20	−5.20	−6.00	−6.00	−6.00	−6.00	−6.00	−6.00	−6.00	−6.00	−5.81	−5.14	−4.87	−5.58	−5.65	−5.78	−5.84	−5.81	−5.66	−5.40

Figure 6: For 24 countries in seven regions the figure shows false positive rates when the reference algorithm is used to compare single photos of mid-aged female subjects from the countries identified in the respective columns. The threshold is to a preset fixed value everywhere. Each cell depicts FMR on a logarithmic scale. The text value is $\log_{10}(\mathrm{FMR})$ *with large negative values encoding superior false match rates. Annex 7 contains the corresponding figure for all algorithms.*

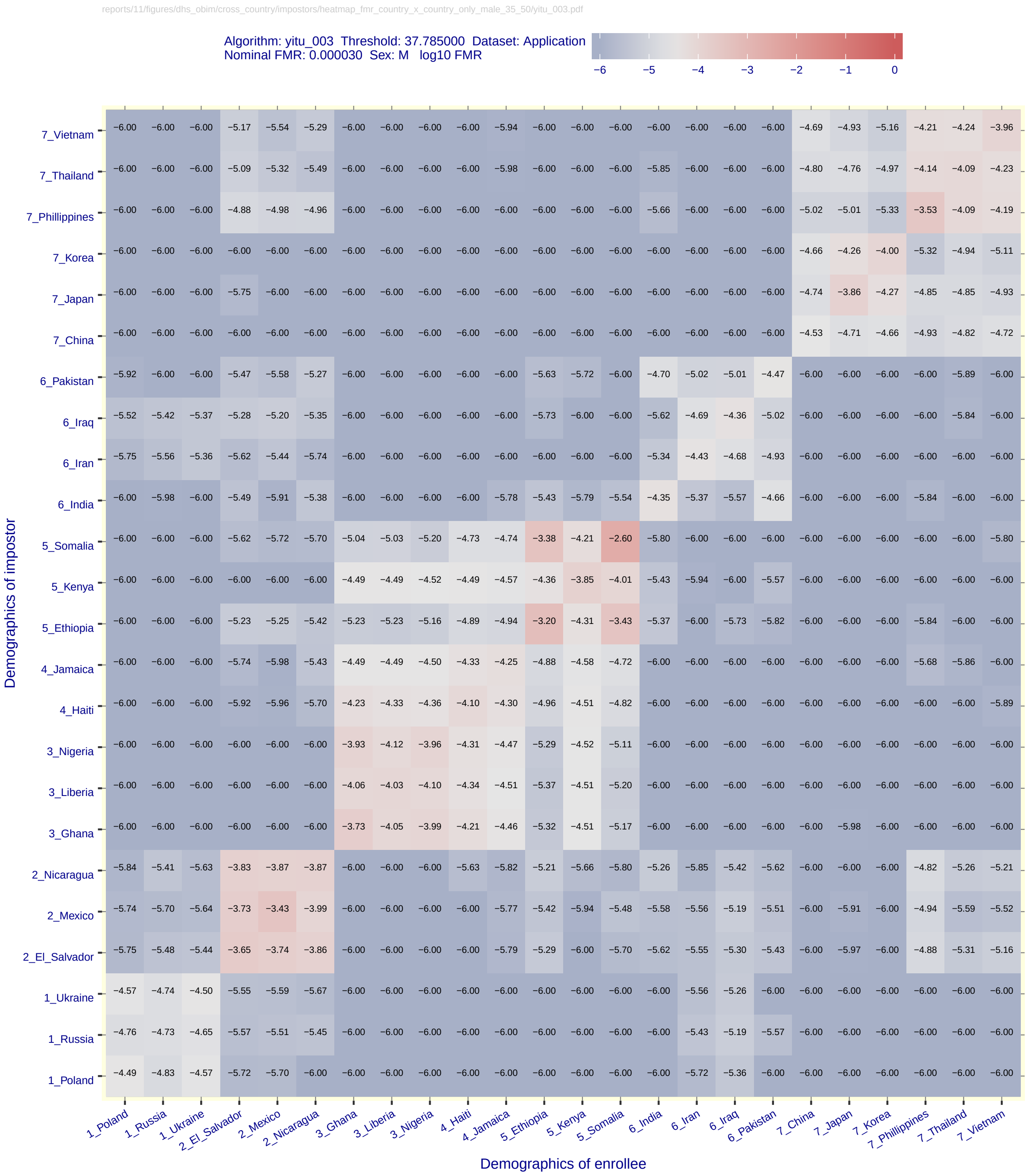

	1_Poland	1_Russia	1_Ukraine	2_El_Salvador	2_Mexico	2_Nicaragua	3_Ghana	3_Liberia	3_Nigeria	4_Haiti	4_Jamaica	5_Ethiopia	5_Kenya	5_Somalia	6_India	6_Iran	6_Iraq	6_Pakistan	7_China	7_Japan	7_Korea	7_Phillippines	7_Thailand	7_Vietnam
7_Vietnam	−6.00	−6.00	−6.00	−5.17	−5.54	−5.29	−6.00	−6.00	−6.00	−6.00	−5.94	−6.00	−6.00	−6.00	−6.00	−6.00	−6.00	−6.00	−4.69	−4.93	−5.16	−4.21	−4.24	−3.96
7_Thailand	−6.00	−6.00	−6.00	−5.09	−5.32	−5.49	−6.00	−6.00	−6.00	−6.00	−5.98	−6.00	−6.00	−6.00	−5.85	−6.00	−6.00	−6.00	−4.80	−4.76	−4.97	−4.14	−4.09	−4.23
7_Phillippines	−6.00	−6.00	−6.00	−4.88	−4.98	−4.96	−6.00	−6.00	−6.00	−6.00	−6.00	−6.00	−6.00	−6.00	−5.66	−6.00	−6.00	−6.00	−5.02	−5.01	−5.33	−3.53	−4.09	−4.19
7_Korea	−6.00	−6.00	−6.00	−6.00	−6.00	−6.00	−6.00	−6.00	−6.00	−6.00	−6.00	−6.00	−6.00	−6.00	−6.00	−6.00	−6.00	−6.00	−4.66	−4.26	−4.00	−5.32	−4.94	−5.11
7_Japan	−6.00	−6.00	−6.00	−5.75	−6.00	−6.00	−6.00	−6.00	−6.00	−6.00	−6.00	−6.00	−6.00	−6.00	−6.00	−6.00	−6.00	−6.00	−4.74	−3.86	−4.27	−4.85	−4.85	−4.93
7_China	−6.00	−6.00	−6.00	−6.00	−6.00	−6.00	−6.00	−6.00	−6.00	−6.00	−6.00	−6.00	−6.00	−6.00	−6.00	−6.00	−6.00	−6.00	−4.53	−4.71	−4.66	−4.93	−4.82	−4.72
6_Pakistan	−5.92	−6.00	−6.00	−5.47	−5.58	−5.27	−6.00	−6.00	−6.00	−6.00	−6.00	−5.63	−5.72	−6.00	−4.70	−5.02	−5.01	−4.47	−6.00	−6.00	−6.00	−6.00	−5.89	−6.00
6_Iraq	−5.52	−5.42	−5.37	−5.28	−5.20	−5.35	−6.00	−6.00	−6.00	−6.00	−6.00	−5.73	−6.00	−6.00	−5.62	−4.69	−4.36	−5.02	−6.00	−6.00	−6.00	−6.00	−5.84	−6.00
6_Iran	−5.75	−5.56	−5.36	−5.62	−5.44	−5.74	−6.00	−6.00	−6.00	−6.00	−6.00	−6.00	−6.00	−6.00	−5.34	−4.43	−4.68	−4.93	−6.00	−6.00	−6.00	−6.00	−6.00	−6.00
6_India	−6.00	−5.98	−6.00	−5.49	−5.91	−5.38	−6.00	−6.00	−6.00	−6.00	−5.78	−5.43	−5.79	−5.54	−4.35	−5.37	−5.57	−4.66	−6.00	−6.00	−6.00	−5.84	−6.00	−6.00
5_Somalia	−6.00	−6.00	−6.00	−5.62	−5.72	−5.70	−5.04	−5.03	−5.20	−4.73	−4.74	−3.38	−4.21	−2.60	−5.80	−6.00	−6.00	−6.00	−6.00	−6.00	−6.00	−6.00	−6.00	−5.80
5_Kenya	−6.00	−6.00	−6.00	−6.00	−6.00	−6.00	−4.49	−4.49	−4.52	−4.49	−4.57	−4.36	−3.85	−4.01	−5.43	−5.94	−6.00	−5.57	−6.00	−6.00	−6.00	−6.00	−6.00	−6.00
5_Ethiopia	−6.00	−6.00	−6.00	−5.23	−5.25	−5.42	−5.23	−5.23	−5.16	−4.89	−4.94	−3.20	−4.31	−3.43	−5.37	−6.00	−5.73	−5.82	−6.00	−6.00	−6.00	−5.84	−6.00	−6.00
4_Jamaica	−6.00	−6.00	−6.00	−5.74	−5.98	−5.43	−4.49	−4.49	−4.50	−4.33	−4.25	−4.88	−4.58	−4.72	−6.00	−6.00	−6.00	−6.00	−6.00	−6.00	−6.00	−5.68	−5.86	−6.00
4_Haiti	−6.00	−6.00	−6.00	−5.92	−5.96	−5.70	−4.23	−4.33	−4.36	−4.10	−4.30	−4.96	−4.51	−4.82	−6.00	−6.00	−6.00	−6.00	−6.00	−6.00	−6.00	−6.00	−6.00	−5.89
3_Nigeria	−6.00	−6.00	−6.00	−6.00	−6.00	−6.00	−3.93	−4.12	−3.96	−4.31	−4.47	−5.29	−4.52	−5.11	−6.00	−6.00	−6.00	−6.00	−6.00	−6.00	−6.00	−6.00	−6.00	−6.00
3_Liberia	−6.00	−6.00	−6.00	−6.00	−6.00	−6.00	−4.06	−4.03	−4.10	−4.34	−4.51	−5.37	−4.51	−5.20	−6.00	−6.00	−6.00	−6.00	−6.00	−6.00	−6.00	−6.00	−6.00	−6.00
3_Ghana	−6.00	−6.00	−6.00	−6.00	−6.00	−6.00	−3.73	−4.05	−3.99	−4.21	−4.46	−5.32	−4.51	−5.17	−6.00	−6.00	−6.00	−6.00	−6.00	−5.98	−6.00	−6.00	−6.00	−6.00
2_Nicaragua	−5.84	−5.41	−5.63	−3.83	−3.87	−3.87	−6.00	−6.00	−6.00	−5.63	−5.82	−5.21	−5.66	−5.80	−5.26	−5.85	−5.42	−5.62	−6.00	−6.00	−6.00	−4.82	−5.26	−5.21
2_Mexico	−5.74	−5.70	−5.64	−3.73	−3.43	−3.99	−6.00	−6.00	−6.00	−6.00	−5.77	−5.42	−5.94	−5.48	−5.58	−5.56	−5.19	−5.51	−6.00	−5.91	−6.00	−4.94	−5.59	−5.52
2_El_Salvador	−5.75	−5.48	−5.44	−3.65	−3.74	−3.86	−6.00	−6.00	−6.00	−6.00	−5.79	−5.29	−6.00	−5.70	−5.62	−5.55	−5.30	−5.43	−6.00	−5.97	−6.00	−4.88	−5.31	−5.16
1_Ukraine	−4.57	−4.74	−4.50	−5.55	−5.59	−5.67	−6.00	−6.00	−6.00	−6.00	−6.00	−6.00	−6.00	−6.00	−6.00	−5.56	−5.26	−6.00	−6.00	−6.00	−6.00	−6.00	−6.00	−6.00
1_Russia	−4.76	−4.73	−4.65	−5.57	−5.51	−5.45	−6.00	−6.00	−6.00	−6.00	−6.00	−6.00	−6.00	−6.00	−6.00	−5.43	−5.19	−5.57	−6.00	−6.00	−6.00	−6.00	−6.00	−6.00
1_Poland	−4.49	−4.83	−4.57	−5.72	−5.70	−6.00	−6.00	−6.00	−6.00	−6.00	−6.00	−6.00	−6.00	−6.00	−6.00	−5.72	−5.36	−6.00	−6.00	−6.00	−6.00	−6.00	−6.00	−6.00

Figure 7: For 24 countries in seven regions the figure shows false positive rates when the **Chinese-developed** *algorithm is used to compare single photos of mid-aged male subjects from the countries identified in the respective columns. The threshold is to a preset fixed value everywhere. Each cell depicts FMR on a logarithmic scale. The text value is* $\log_{10}(\text{FMR})$ *with large negative values encoding superior false match rates. Annex 7 contains the corresponding figure for all algorithms.*

countries into the following regions

- 1: Eastern Europe - Russia, Poland and Ukraine
- 2: Central America - Mexico, Honduras, El Salvador, Nicaragua
- 3: West Africa - Ghana, Liberia, Nigeria
- 4: The Caribbean - Haiti, Jamaica
- 5: East Africa - Ethiopia, Kenya, Somalia
- 6: South Asia - India, Iran, Iraq, Pakistan
- 7: East Asia - China, Japan, Korea, Philippines, Thailand, Vietnam

we see a block structure, in particular a block-diagonal structure indicative of strongly correlated false match rates within region. For example it is true that when comparing photos of individuals from East Africa with those from Eastern Europe, most algorithms give very low FMR. The more interesting results are within-region, around the diagonal, and between regions along the diagonal. We now note the following common trends, and then some notable exceptions. We then conclude with some comments on what the ideal situation would be, and on the meaning. Each Annex includes a "contact sheet" which shows all heatmaps on a single page as thumbnails. The idea is to show macroscopic behavior across all algorithms. When viewed on a computer the figure has very high resolution and zooming in reveals full detail; when printed it will likely just show coarse trends.

- Nominal FMR in Eastern Europe: For many algorithms, FMR within Eastern Europe is close to the nominal target false match rate i.e. a grey color, $-5 \leq \log_{10}$ FMR ≤ -4. There are few exceptions to this, even for algorithms developed in China, Western Europe and the USA.
- Higher FMR in East Africa: For almost all algorithms the highest FMR is for comparison of Somali faces. We suspected this could be due to mislabeled data or statistical (in)significance but rejected those possibilities[10]. Further the FMR is high within Ethiopia and between Ethiopia and Somalia. Similarly Kenya-Kenya comparisons give high FMR, although somewhat reduced. In a substantial majority of photos of Somalian women, the subject is wearing full head dress that typically covers the hair and ears leaving only the face exposed. While this might produce false positives, headwear is almost always absent in photographs of men. Further work is needed to explain the observation in more detail.

[10] We discount that this result is anomalous as follows: 1. The sample size may be small for this study, but not absolutely small: The Somalia-Somalia FMR measurement is obtained from 1 733 116 comparisons involving 2632 images of 1974 males. 2. The effect persists when comparing Somalian and Ethiopian faces, and we'd suspect that ground-truth labelling errors - instances of one person being present two IDs - would not persist across national boundaries. 3. In addition to high FMR, which is a count of high imposter scores, the mean similarity score is also very high, an observation that again applies to all algorithms.

- ▷ Higher FMR in West Africa too: The countries with the second highest FMR tend to be in West Africa, i.e. Ghana, Liberia and Nigeria. These countries do not share any borders. The high FMR values occur almost equally within and between countries.

- ▷ Higher FMR between West Africa and the Caribbean: Elevated FMR occurs when comparing faces of individuals from countries in West Africa with those in the Caribbean.

- ▷ Higher FMR between West and East Africa: Elevated FMR occurs when comparing faces of individuals from countries in West Africa and Kenya. The effect is often lower than within either region alone. However, the high FMR does not extend to comparisons of West African and Ethiopian or Somali faces.

- ▷ Higher FMR in East Asia: It is very common for algorithms to give high FMR within East Asian countries and between them. For the algorithm shown, Vietnamese faces strongly match other Vietnamese, and with all the other countries in the region. The East Asian block often divides into northern and southern blocks with reduced, but still high, FMR when individuals are compared between those blocks (e.g. Korea and Vietnam).

- ▷ Some Chinese algorithms give nominal FMR when comparing Chinese: As shown in Annex 7 some algorithms developed in China exhibit much reduced FMR on the East Asian population - for example, see Figure 7. These algorithms are from Megvii, Meiya, Hik Vision, Dahua, X-Laboratory, Yitu and SHU (Shanghai University Film Academy). For Deepsea Tencent the same applies, but less prominently in South East Asia. In some cases the effect is only apparent for comparisons involving images of Chinese, e.g. Star Hybrid. Other Chinese algorithms, however, exhibit the more common trend of producing elevated FMR across East Asia. These include developers of more accurate algorithm such as Alphaface, Deepglint and Sensetime. Thus it is not sufficient for an algorithm to be developed in China for it to mitigate the FMR increase on images from the local population.

- ▷ One of the most accurate algorithms produces more uniform FMR: The corresponding Figure for the Yitu-003 algorithm - Figure 7) - shows that the demographic differentials in FMR are attenuated. As noted the FMR values for comparisons within East Asia are near the nominal value. Notably, however, this applies to West Africa also. This appears to be an important result, as it is a proof that some algorithms do not exhibit higher FMR in those populations. Yitu reported in a meeting in London in October 2017 that its training data included on order of 10^9 photographs of an unspecified (lower) number of Chinese nationals. Whether that is the entirety of their training data is not known.

- ▷ Developer dependency does not apply to South Asia: Neither Lookman nor Tiger IT's algorithm produce nominal FMR on the S. Asian imposter comparisons.

- ▷ Magnitudes are large: The East African FMR values are often two orders of magnitude higher than the nominal value and those recorded within Eastern Europe. That is, the $\log_{10}$ FMR values are $+2$ higher corresponding to FMR that is of order 100 times larger than the de-facto baseline. From a security perspective this is analogous to using a two-digit PIN instead of the common four digits. For West Africa, the FMR values are between one and two orders of magnitude above baseline. A shift of 1.4 on the logarithmic scale corresponds to a factor of 25 increase, for example.

- ▷ Anomalies in the figures: The cross-country heatmaps for the SIAT-004, Panasonic PSL-001, and Sensetime-002 algorithms are mostly red, indicating high false match rates for all comparisons. This may arise because the threshold used was computed over comparisons of a different kind of images - mugshots not application portraits. The algorithms are told what kind of image they are being given at the time features are extracted from the image. The consequence is that the imposter distribution for mugshots looks different to that for the application images, and thus thresholds are not portable. This would present an operational issue to any end-user not informed to set the threshold accordingly. In any case, while the heatmaps are mostly red, they still exhibit the same kind of FMR variations seen for many other algorithms.

Discussion: The heatmap figures of Annex 7 show a widespread elevation of false match rates in African faces relative to those in Eastern Europe. The reasons for these shifts are unknown. We did not make any attempts to explain the effects. To summarize the effect we include the scatter plots of Figures 10 - 9. Each point corresponds to one algorithm. Its coordinates show false match rates within West Africa against those within Eastern Europe. The degree to which the point is above the diagonal line shows the extent that FMR in the African countries exceeds that in the Eastern European ones.

We note several outcomes of this visualization.

- ▷ **Worst case** In the scatter plot for African women Figure 9 there is a cluster of algorithms located near $x = 0.00012$ and $y = 0.003$. Compared to the target FMR value of 0.00003 (the vertical line) there is a near four-fold increase in FMR of women over men. Much more significantly there is a more than 100-fold vertical excursion from white men to African women.

- ▷ **Dispersion** Some algorithms, most notably those from Sensetime give FMR much different to the target value. The threshold was set using Annex 1 mugshots but the Figure reflects FMR measured over comparison of Annex 2 application photos. Both sets of photos are well illuminated portraits, so this instability across datasets would be unwelcome, especially if an algorithm were to be fielded on imagery qualitatively different. Many algorithms do give the expected FMR for white men FMR = 0.00003 as seen in Figure 8.

Figures 10 and 11 repeat the scatterplot summaries for the East Asian demographic too. The picture there is more interesting. While the same pattern is present, it is clear that some algorithms developed in China do not give elevated false match rates relative to Eastern Europeans. The absence of the effect is important in that it implies high FMR in that population is not inevitable. We did not see a corresponding improvement for South Asian faces for the few algorithms we understand were submitted by developers there (in India and Bangladesh).

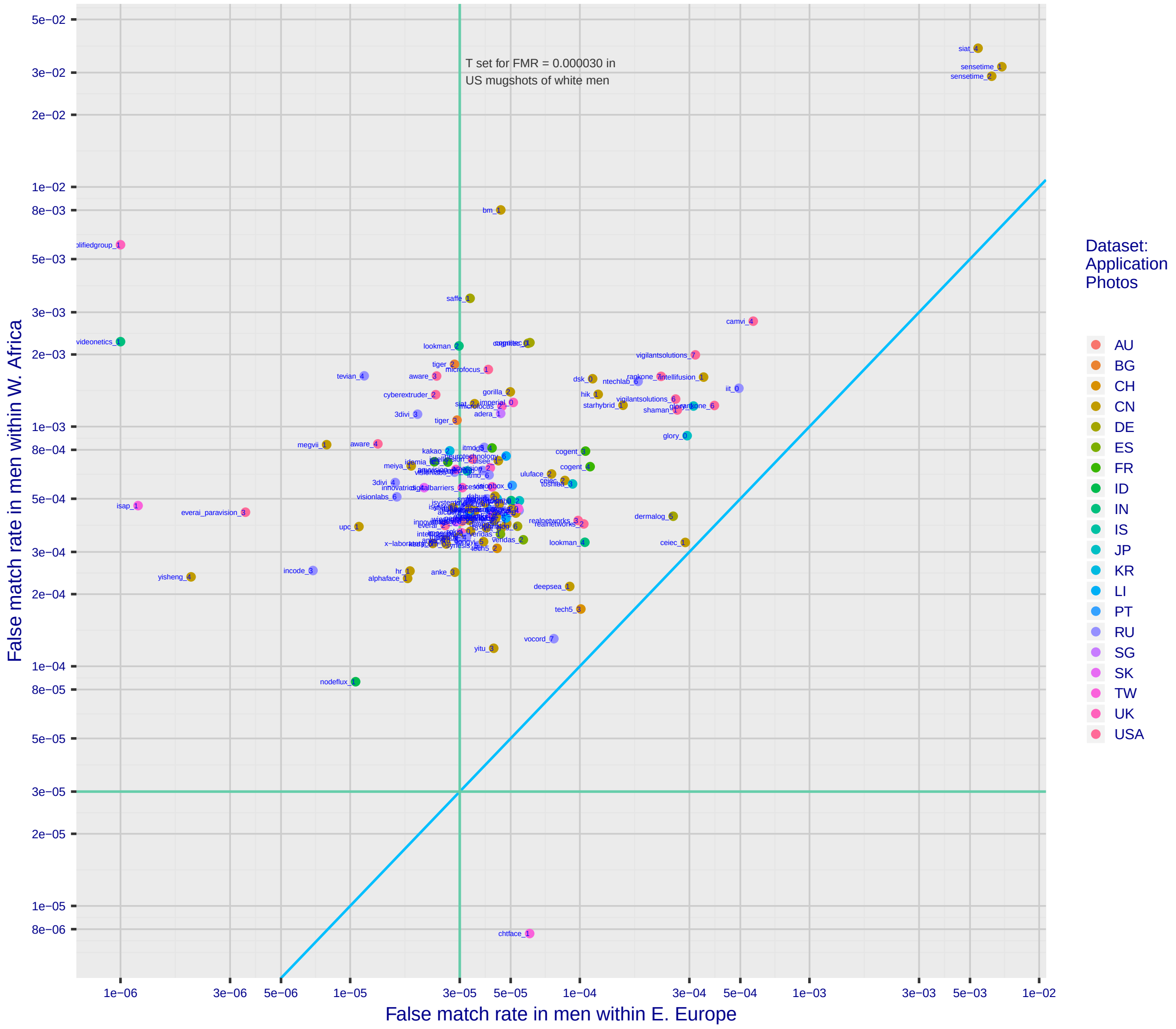

Figure 8: The scatter plot shows FMR when comparing same-age **men** within and across three Eastern European countries (Russia, Ukraine, Poland), against FMR obtained comparing men within and across three West African countries (Ghana, Liberia, Nigeria). The threshold is fixed for each algorithm to give the FMR noted in the annotation over white men in the U.S. mugshot database. This is indicated by the vertical and horizontal green lines. The blue diagonal line $y = x$ is included to show "over/under". The color code identifies the domicile of the developer - some multinationals conduct research elsewhere. Training data likewise may originate elsewhere.

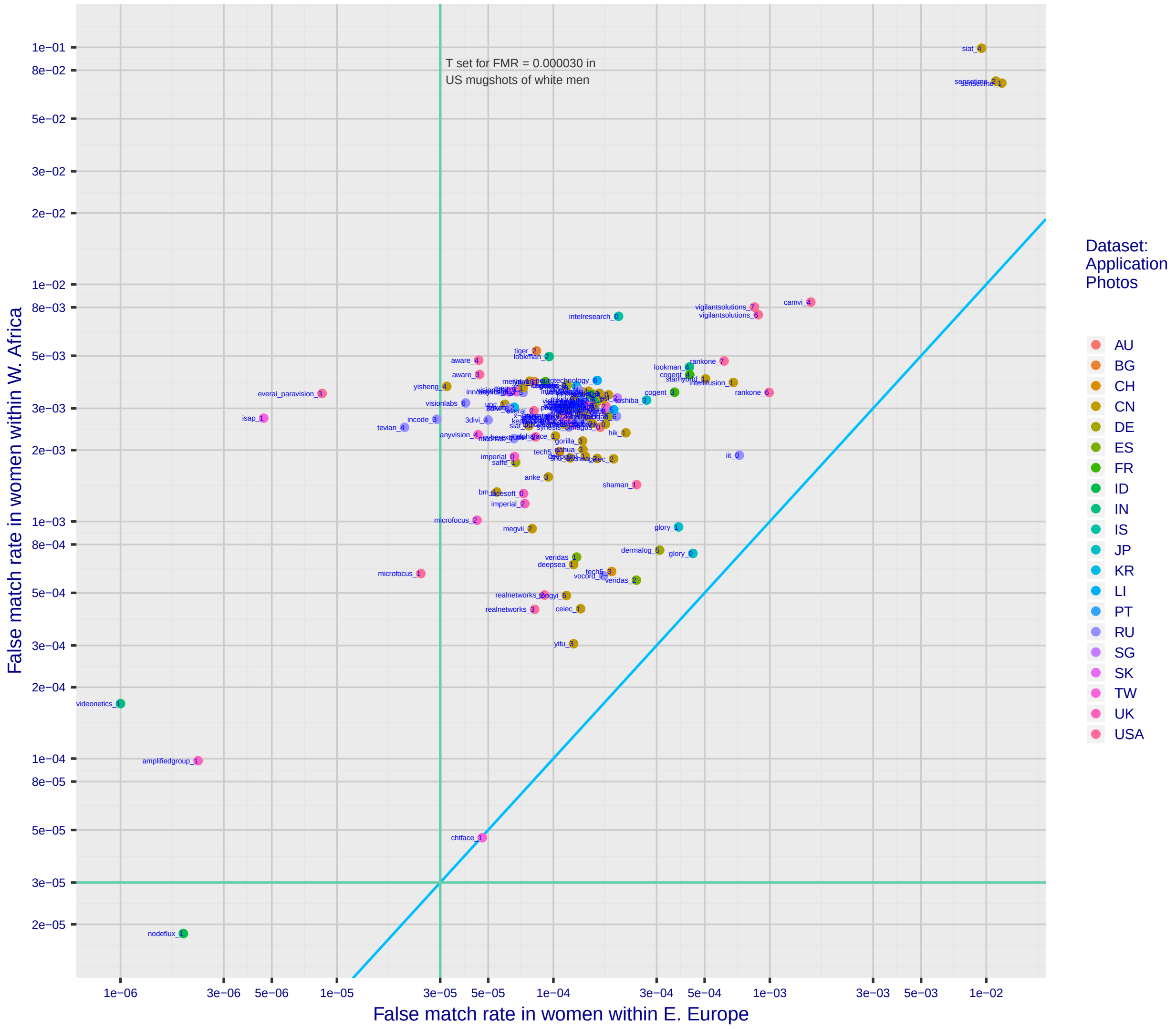

Figure 9: The scatter plot shows FMR when comparing same-age **women** *within and across three Eastern European countries (Russia, Ukraine, Poland), against FMR obtained comparing women within and across three West African countries (Ghana, Liberia, Nigeria). The threshold is fixed for each algorithm to give the FMR noted in the annotation over white men in the U.S. mugshot database. This is indicated by the vertical and horizontal green lines. The blue diagonal line $y = x$ is included to show "over/under". The color code identifies the domicile of the developer - some multinationals conduct research elsewhere. Training data likewise may originate elsewhere.*

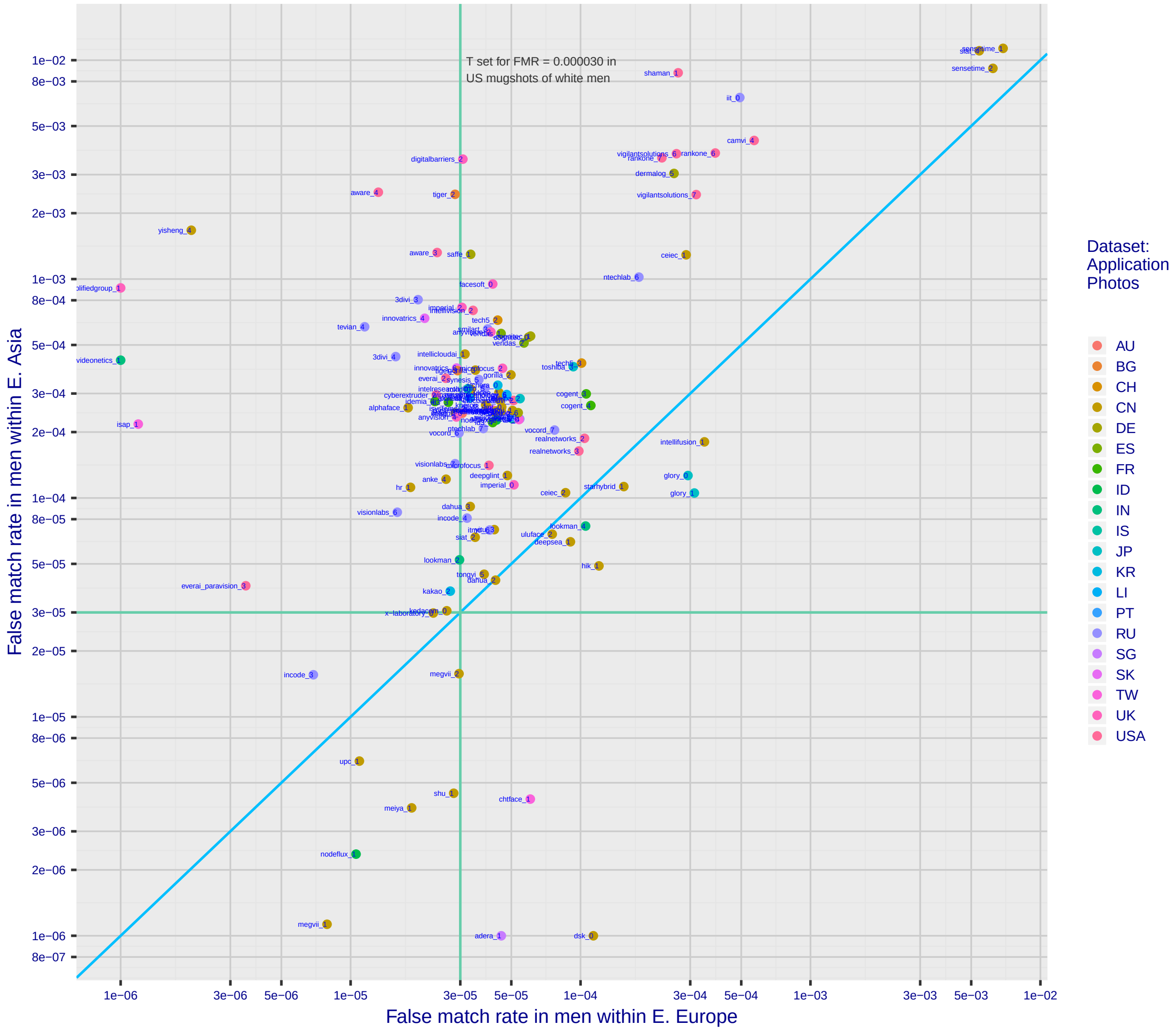

Figure 10: The scatter plot shows FMR when comparing same-age **men** *within and across three Eastern European countries (Poland, Russia, Ukraine), against FMR obtained comparing men within and across six East Asian countries (China, Japan, Korea, Philippines, Thailand and Vietnam). The threshold is fixed for each algorithm to give the FMR noted in the annotation over white men in the U.S. mugshot database. This is indicated by the vertical and horizontal green lines. The blue diagonal line $y = x$ is included to show "over/under". The color code identifies the domicile of the developer - some multinationals conduct research elsewhere. Training data likewise may originate elsewhere.*

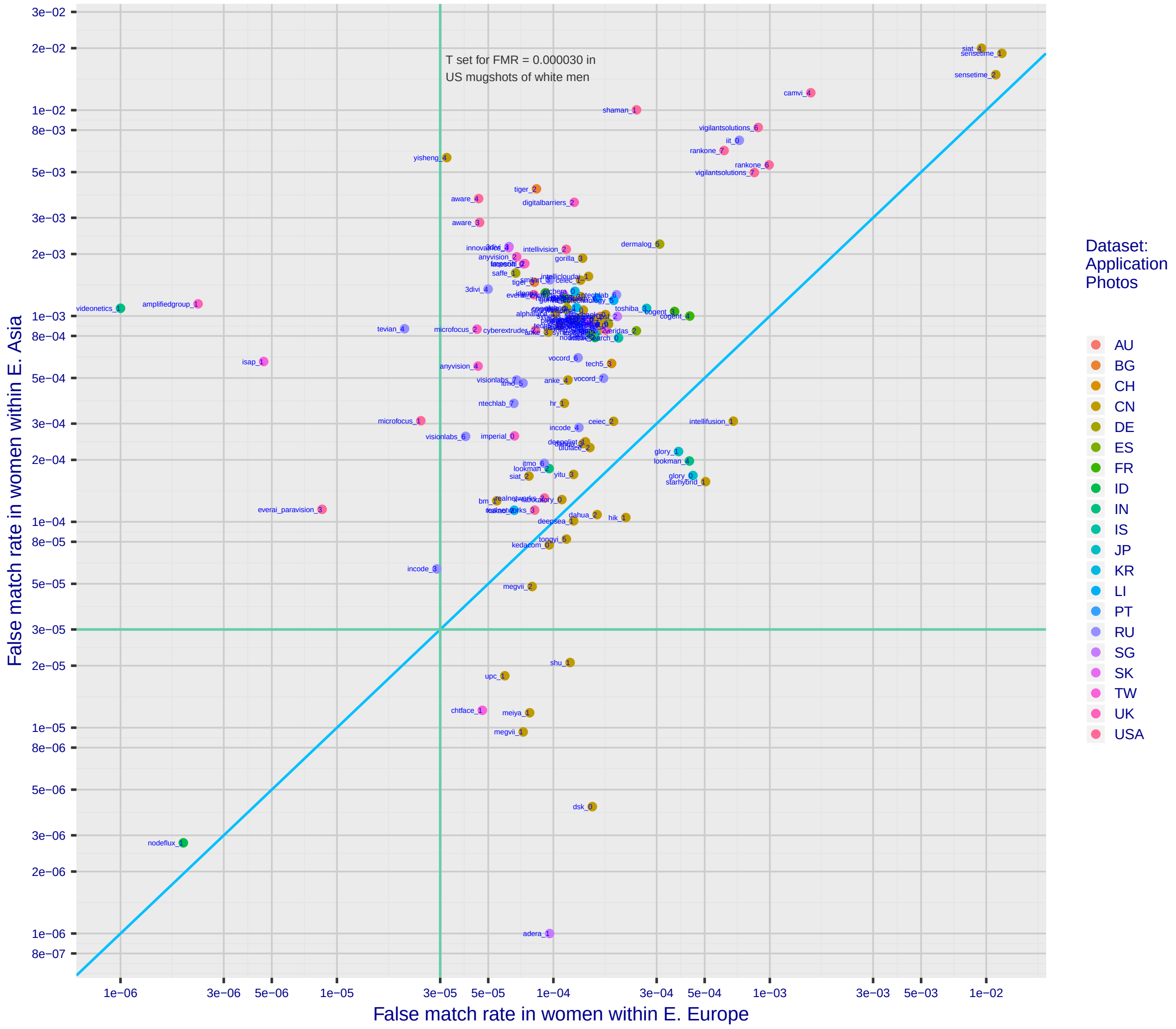

Figure 11: The scatter plot shows FMR when comparing same-age **women** *within and across three Eastern European countries (Poland, Russia, Ukraine), against FMR obtained comparing women within and across six East Asian countries (China, Japan, Korea, Philippines, Thailand and Vietnam). The threshold is fixed for each algorithm to give the FMR noted in the annotation over white men in the U.S. mugshot database. This is indicated by the vertical and horizontal green lines. The blue diagonal line $y = x$ is included to show "over/under". The color code identifies the domicile of the developer - some multinationals conduct research elsewhere. Training data likewise may originate elsewhere.*

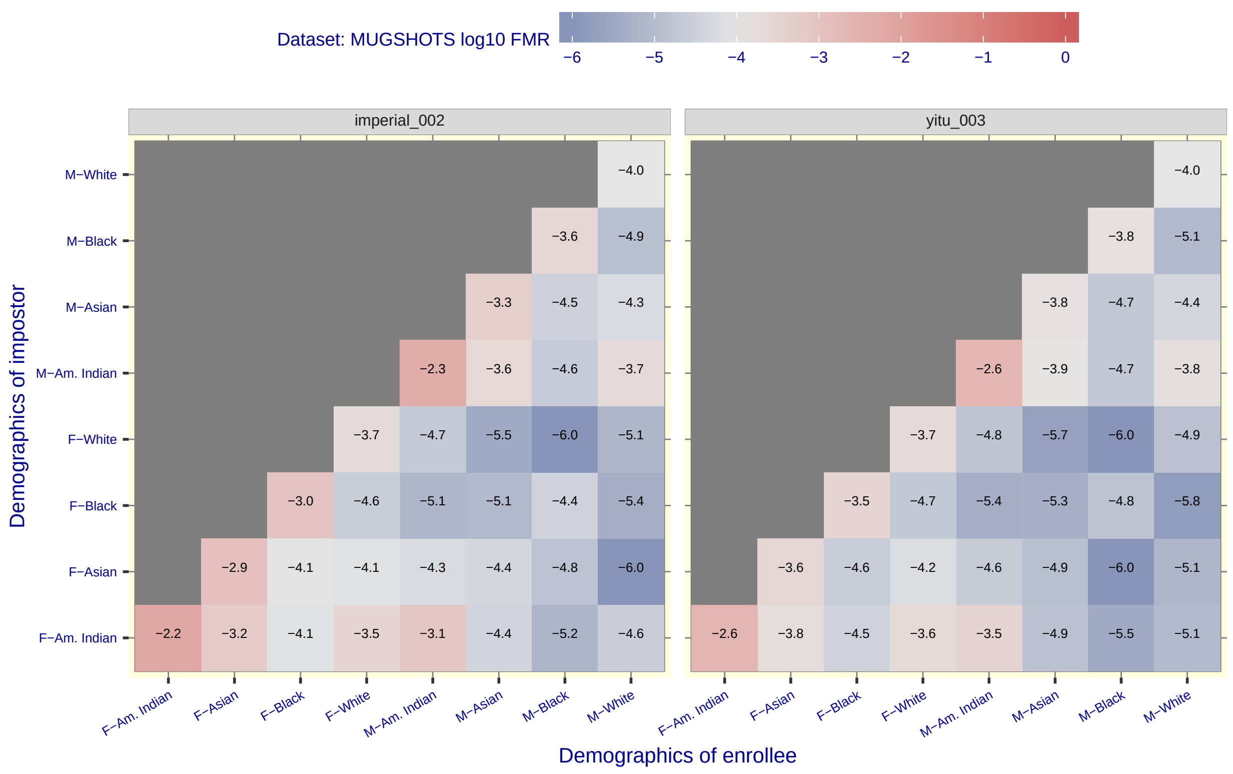

Figure 12: For mugshot photos tagged with one of four race labels and a sex label, the heatmaps show false positive rates for comparison of randomly selected photos from the groups identified in the respective rows and columns. Two algorithms are used, one in each panel, and the threshold for each is set to a fixed value everywhere. The value is the smallest threshold that gives FMR ≤ 0.0001 *on the white male imposters. Each cell depicts FMR on a logarithmic scale. The text value is* $\log_{10}(\mathrm{FMR})$ *with large negative values encoding superior false match rates. Annex 6 contains the corresponding figure for all algorithms.*

4.4 Dependence of FMR on race in United States mugshots

Method: Using high quality mugshot portraits from the mugshot images detailed Annex 1 , we apply each verification algorithm to conduct 3 million comparisons for each of the eight demographics defined by two sexes and four races. The origin and meaning of these labels is described in the Annex. We executed this set of comparisons with 126 verification algorithms submitted to the FRVT Verification track. These are listed in Tables 4-6. We compared scores with a threshold to produce FMR estimates for each demographic pairing. Each threshold was selected as the lowest value that gave FMR at or below a target FMR. The target FMR value was 0.0001. The threshold was computed over the set of 3 000 000 mugshot imposter comparisons made for white males. Thus, by design, the FMR for that demographic is exactly 0.0001.

We excluded photographs for which race or sex was unavailable or unknown. We did not report comparisons by age-group.

Analysis: As with the international set of application photos, we use the heatmap to show cross-demographic false match rates, including cross-sex. Heatmaps for two algorithms are shown in Figure 12. The Figure shows FMR as a heatmap. It uses a logarithmic scale, so that a FMR of 0.0001 is represented by a color and a text value of -4, i.e. log to the base 10. Low FMR values are shown in blue. High FMR values are shown in red. A grey color connotes the target FMR value ($\log_{10} 0.0001 = -4$). High FMR values present a security concern in verification applications. Corresponding figures for all algorithms appear in Annex 6

Figure 13 extracts the within-sex and within-race diagonal elements of those figures and summarizes the results for all algorithms, ordering the result by worst-case FMR elevation.

Discussion: From the figure, and those in the annex, we make a number of observations.

- ▷ Higher FMR in women: As with application photos, most algorithms give systematically higher false match rates in women than in men. The magnitude of this difference is lower with mugshots than with application photos.

- ▷ Highest FMR in American Indians: First, the highest FMR occurs in images of American Indians[11]. For the Imperial-002 algorithm featured in Figure 12 the FMR for American Indian women is 0.0068, i.e. a 68 fold increase over the FMR of 0.0001 in white males. In men, the multiple is 47. Why such large increases occur is not known. One component of the increase may stem from database identity labelling errors[12]. We discount this possibility because the database has otherwise excellent ground-truth integrity, supported by fingerprint enrollments.

- ▷ Higher FMR in Asian and Black women: There are order-of-magnitude increases in FMR in mugshots of Asian and Black women. Some algorithms developed in China reduce this differential, for example Yitu-003 in the right panel of Figure 12.

[11] The data supplied to NIST tags this group with letter "I" per the EBTS standard which describes this group as "American Indian, Eskimo, Alaskan native, or a person having origins in any of the 48 contiguous states of the United States or Alaska who maintains cultural identification through tribal affiliation or community recognition". In the figures we replace the letter "I" with "American Indian" to distinguish from subjects from India in the international datasets.

[12] Specifically instances of "one person under two IDs" can cause apparent false positives, that are actually true positives.

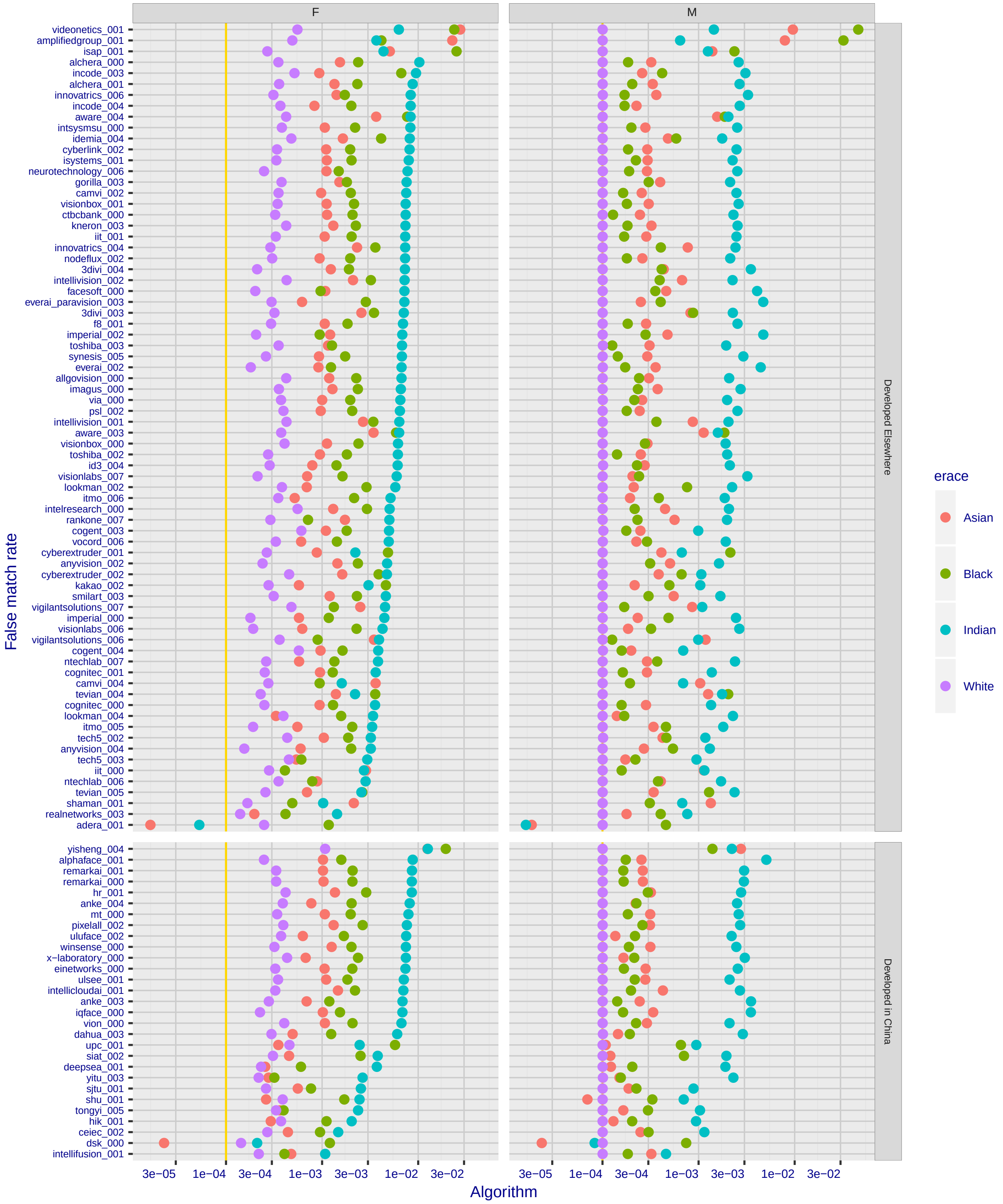

Figure 13: For each verification algorithm, the dots give the false match rates for same-sex and same-race imposter comparisons. The threshold is set for each algorithm to give FMR = 0.0001 on white males (the purple dots in the right hand panel). The algorithms are sorted in order of worst case FMR, usually for American Indian women. Algorithms developed in China appear in the lower panel.

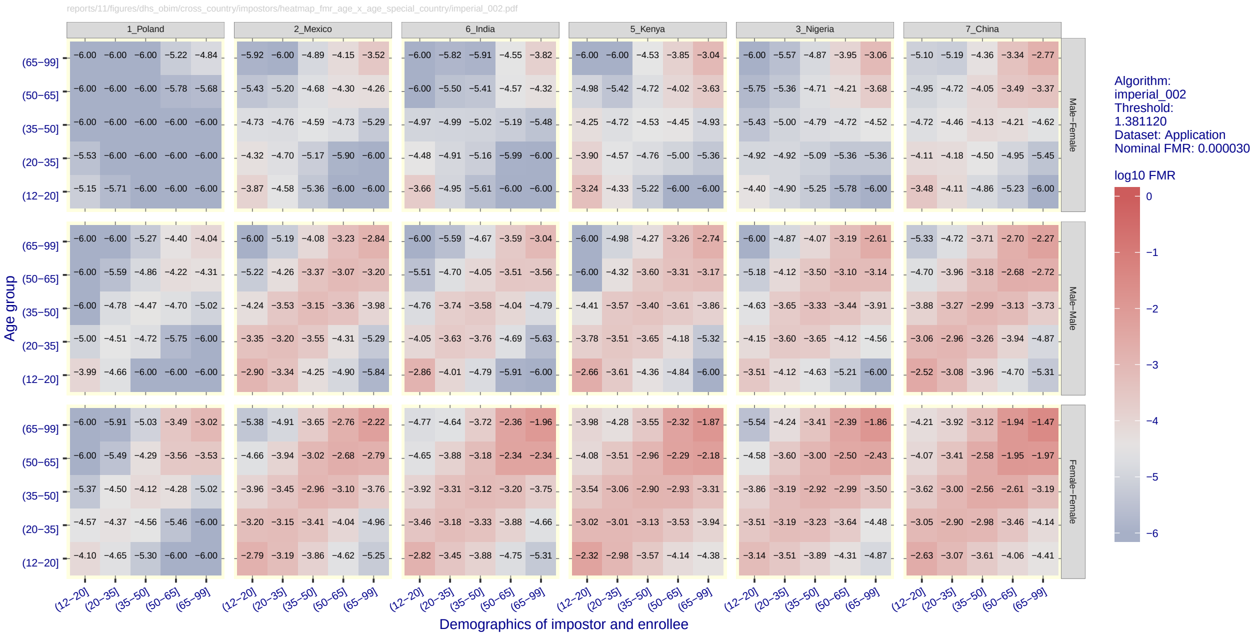

Figure 14: For six countries selected for the high number of images in the dataset and from distinct regions the heatmaps show cross-age false match rates for imposters of the same sex from the age groups given on the respective axes. Each cell depicts FMR on a logarithmic scale. The text value is $\log_{10}(\text{FMR})$ *with large negative values encoding superior false match rates. Annex 9 contains the corresponding figure for all algorithms.*

4.5 Do some or all algorithms yield more false positives on certain age groups

Method: Using high quality application portraits drawn from the corpus described in Annex 2 , we compared 442 019 images from 24 countries with 441 517 images of different individuals within and across age groups $(00-20]$, $(20-35]$, $(35-50]$, $(50-65]$, and $(65-99]$.

We executed this set of comparisons with 126 verification algorithms submitted to the FRVT Verification track. These are listed in Tables 4-6. Each comparison yield a score. When many scores are compared with a fixed threshold, we obtain an estimate of the false match rate. The threshold was computed over a set of 93 070 400 imposter comparisons made using a different set of images, namely the mugshots detailed in Annex 1 . The threshold is the smallest value that for which the FMR is less than or equal to 0.00003. This was repeated for other thresholds giving FMR $\{0.000001, 0.000003, 0.00001, 0.00003, 0.0001, 0.0003, 0.001, 0.003, 0.01, 0.03\}$.

Each comparison is accompanied by sex, country of birth and age group metadata for the two individuals represented in the photographs. We excluded small numbers of photographs for which age information was unavailable or for which sex was not listed as male or female.

Given many comparisons with the same demographic pairing, we can produce a measurement of FMR when comparing individuals from two age groups, for example Polish men over the age of 65 with Polish men under 20.

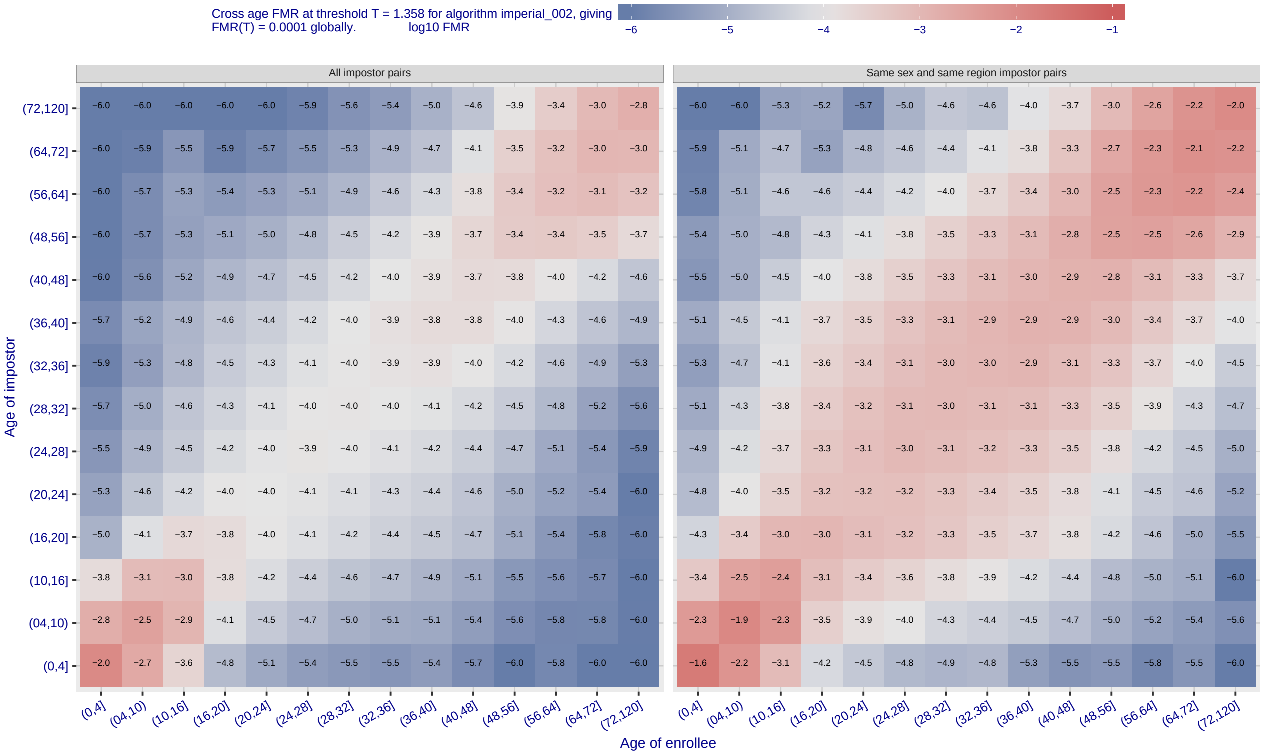

Figure 15: For visa photos from all countries, the heatmap shows for one algorithm cross-age false match rates for imposters of the same sex. Each cell depicts FMR on a logarithmic scale. The text value is $\log_{10}(\text{FMR})$ with large negative values encoding superior false match rates. The threshold is fixed to the value that gives a FMR of 0.0001 over all zero-effort imposter pairs. Annex 10 contains the corresponding figure for all algorithms.

Analysis: To address the issue of age we produced figures depicting cross-age false match rates. We do this within-country only, as cross-country effects have been covered in section 4.3. We include male-male, female-female, and also male-female comparisons (although they are of less interest operationally). Figure 14 is an example, showing results for one of the more accurate algorithms. The Figure includes results for six countries, one per region. We dropped one region (the Caribbean) and 18 of the 24 countries because the effects are similar everywhere.

Figure 14 shows cross-age group FMR for one of the more accurate algorithms. Annex 9 contains corresponding Figures for all algorithms, and therefore extends to more than 130 pages.

Discussion: From Figure 14 and those in the annex, we make these observations.

▷ Lower FMR for persons in different groups: In almost all cases - for all algorithms, countries of origin and both sexes, comparison of images of persons in different age groups yields lower (better) false match rates than for persons in the same age group. This, obviously, is an aggregate result; it will generally be possible to find some individuals from different age groups who produce high imposter scores but this will be increasingly difficult as the age difference increases.

▷ Highest FMR in the oldest age group: For women from all most countries, comparison of images of individuals in the 65-and-over age group produce the highest false match rates. For men this is often true also.

▷ High FMR in the youngest age group: For both sexes, but men in particular, comparison of images of persons in the $12-20$ age group produce high false match rates. The dataset does not include any subjects below 12. Below that age we consider a smaller dataset of visa photographs (see Annex 3) that includes individuals in age groups $(0, 4]$ and $(4, 10]$. The results are included in the heatmap of Figure 15. Note that each FMR estimate is formed from comparisons from all countries, not just one, so they hide the geographic idiosyncrasies of the algorithms.

These results are similar to those reported by Michalski et al. [28] for false positives in children using one commercial algorithm. The report also shows false negative ageing effects broken out by age at enrolment, and time lapse.

▷ Lower FMR across sex: Comparison of images of persons of different sex usually produces very low FMR. However, within the youngest and oldest age groups, FMR is again higher and substantially above the nominal FMR.

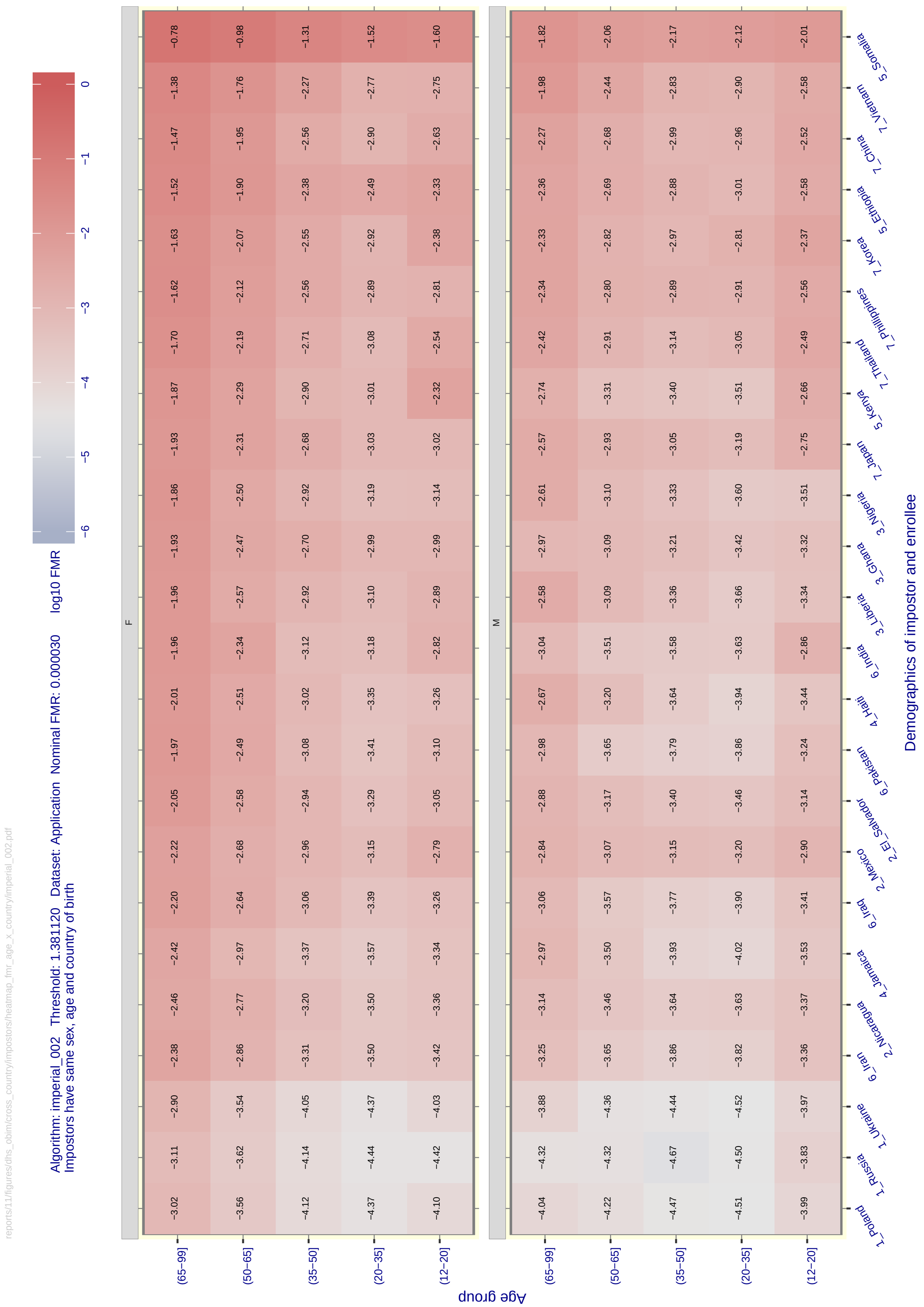

Figure 16: For application photos, the The heatmap shows one-to-one false match rates for same-sex, same-age and same-country of birth imposters, broken out by age and country. The text value is $\log_{10}$(FMR) with large negative values encoding superior false match rates. Each cell depicts FMR on a logarithmic scale. The text value is $\log_{10}$(FMR) with large negative values encoding superior false match rates. Annex 11 contains the corresponding figure for all algorithms.

5 False negative differentials in verification

5.1 Introduction

False negatives occur in biometric systems when samples from one individual yield a comparison score below a threshold. This will occur when the features extracted from two input photographs are insufficiently similar. Recall that face recognition is implemented as a differential operator: two samples are analyzed and compared. So a false negative occurs when two from the same face appear different to the algorithm.

5.2 Tests

This section gives empirical quantification of the variation in false negative rates across demographics. We base this on recognition results from three one-to-one verification tests:

- ▷ **Mugshot - Mugshot**: In the first test we look for demographic effects in the groups defined by the sex and race labels provided with these United States images - see Annex 1 .
- ▷ **Application - Application photo:** We consider also a high quality dataset collected from subjects hailing from twenty four countries in seven global regions.
- ▷ **Application - Border crossing photo:** As discussed in Annex 4 , the border crossing photos are collected under time constraints, in high volume immigration environments. The photos there present classic pose and illumination challenges to algorithms.

5.3 Metrics

The metrics appropriate to verification have been detailed in section 3.1. These are related to particular applications in Figure 2. The dicussion in subsequent sections centers on false non-match rates at particular thresholds, i.e. FNMR(T).

5.4 Results

Figure 17 summarizes the false non-match rates for the 52 most accurate algorithms comparing mugshot photos. It does this for each of four race categories and two sexes[13]. Figure 18 takes the same approach but for 20 countries of birth and two age groups (over/under 45). It summarizes comparison of high quality immigration

[13] See Annex 1 for descriptions of the images and metadata.

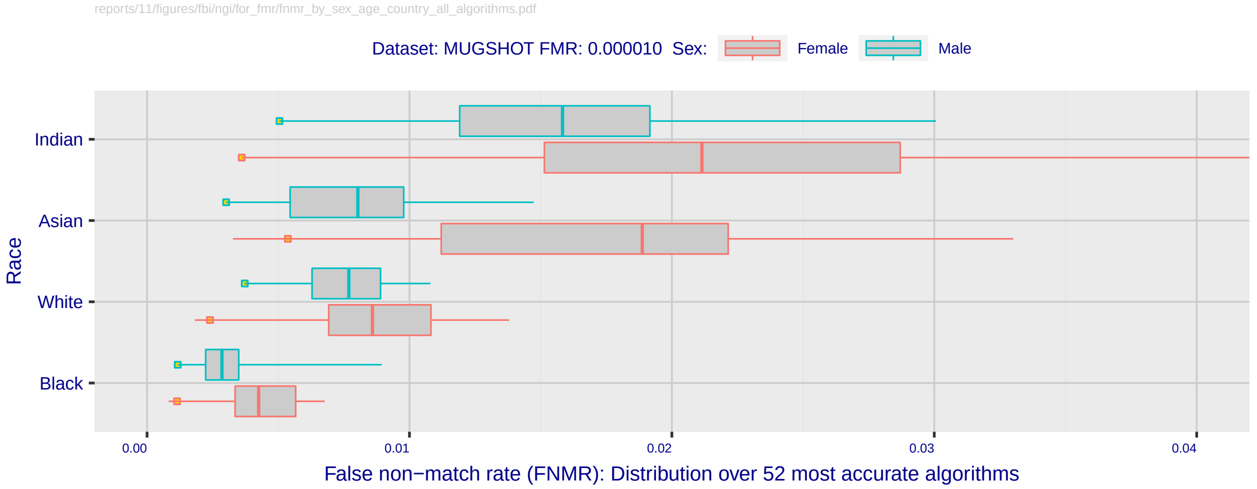

Figure 17: For mugshot comparisons, the figure shows the distribution of FNMR values over the 52 most accurate verification algorithms, by sex and race. The threshold was set for each algorithm to achieve FMR = 0.00001 over all imposter comparisons. The line within each box is the median over those algorithms; the box itself spans the interquartile range (26 algorithms) and the lines here extend to minimum and maximum values. The small box on the left side indicates the accuracy for best algorithm overall, on this dataset alphaface-001.

application photos with lower quality border crossing photos. These are described in Annex 2 and Annex 4 respectively.

We make the following observations.

- ▷ FNMR is absolutely low: In one-to-one verification of mugshots, the best algorithms give FNMR below 0.5% at the reasonably stringent FMR criterion of 0.00001. FNMR is generally below 1% with exceptions discussed below. For the more difficult application-border crossing comparisons, the best algorithm almost always gives FNMR below 1%. These error rates are far better than the gender-classification error rates that spawned widespread coverage of bias in face recognition. In that study [5], two algorithms assigned the wrong gender to black females almost 35% of the time. The recognition error rates here, even from middling algorithms, are an order of magnitude lower. Thus, to the extent there are demographic differentials, they are much smaller than those that (correctly) motivated criticisms of the 2017-era gender classification algorithms.

- ▷ FNMR in African and African American subjects: In domestic mugshots, the lowest FNMR in images of subjects whose race is listed as black. However, when comparing high-quality appliction photos with border-crossing images, FNMR is often highest in African born subjects. We don't formally measure contrast or brightness in order to determine why this occurs, but inspection of the border quality images shows underexposure of dark skinned individuals often due to bright background lighting in the border crossing environment. In mugshots this does not occur. In neither case is the camera at fault.

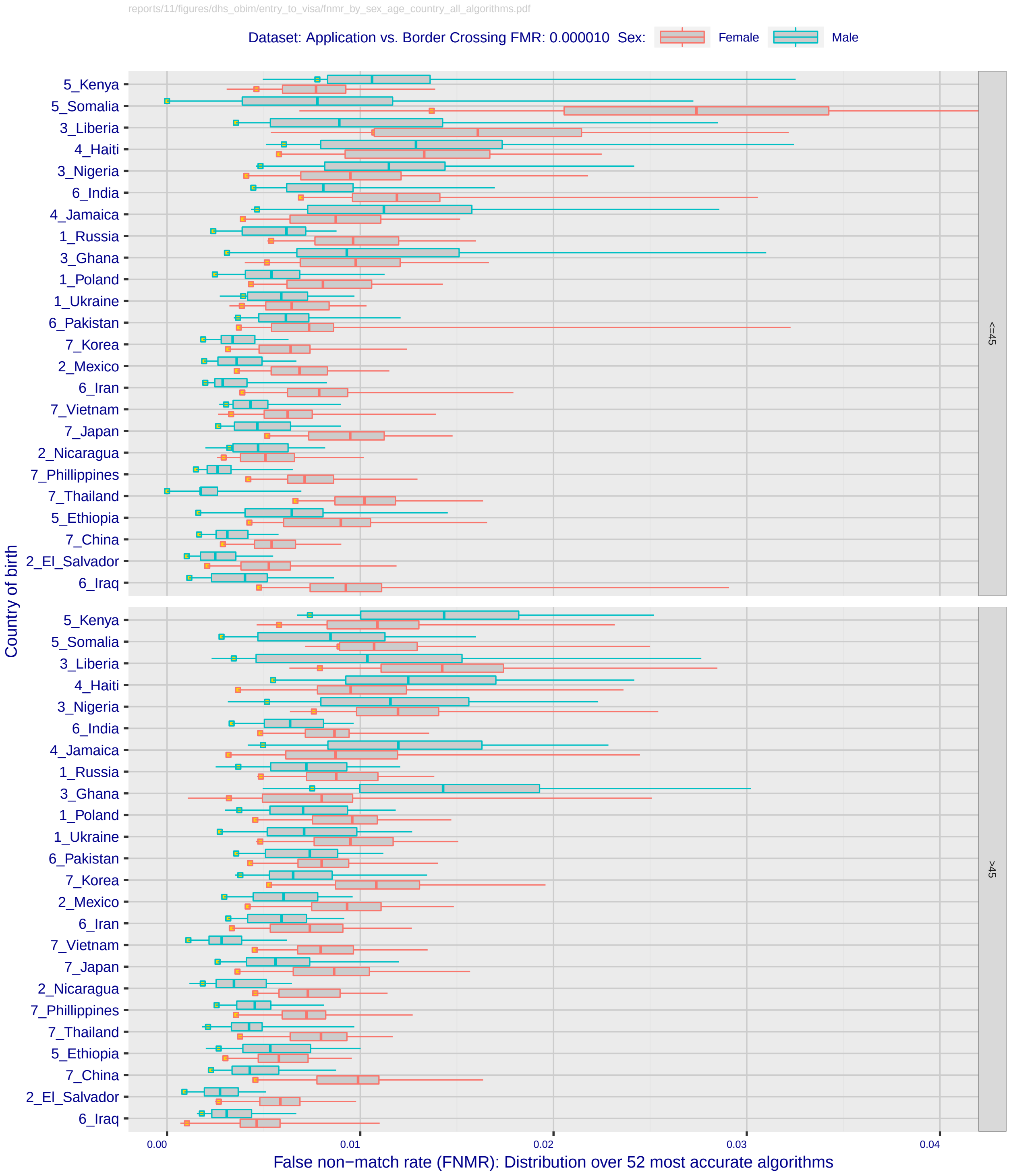

Figure 18: For the application - border crossing photo comparisons, the boxplots show the distribution of FNMR values over the 52 most accurate algorithms, by sex, country of birth, and age group. The threshold was set for each algorithm to achieve FMR = 0.00001 over all imposter comparisons. The line within each box is the median over those algorithms; the box itself spans the interquartile range (26 algorithms) and the lines here extend to minimum and maximum values. The small box on the left side indicates the accuracy for best algorithm overall, on this dataset visionlabs-007.

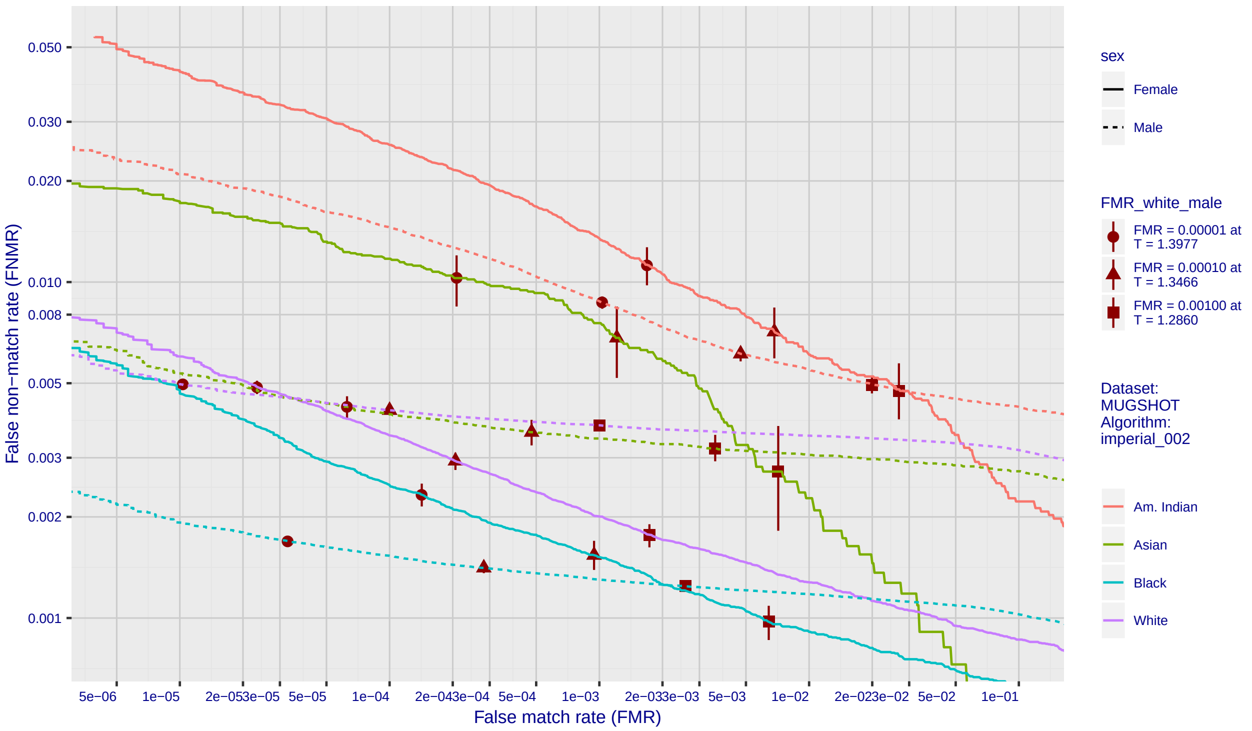

Figure 19: For one algorithm verifying mugshot images, the error tradeoff characteristics show false non-match vs. false match rates. The FMR estimates are computed for same-sex and same-race imposter comparisons. Each symbol (circle, triangle, square) corresponds to a fixed threshold - their vertical and horizontal displacements reveal, respectively, differences in FNMR and FMR between demographic groups. The vertical line through each symbol indicates uncertainty related to sample size - it spans 95% of bootstrap samples of the genuine scores. Annex 12 contains the corresponding figure for all algorithms.

- Women give higher FNMR: In most cases, algorithms give higher false non-match rates in women than men. Note that this is a marginal effect - perhaps 98% of women are still correctly verified - so the effect is confined to fewer than 2% of comparisons where algorithms fail to verify. It is possible that the error differences are due to relative prevalence some unknown covariate. There are some exceptions, however: In Kenya, Nigeria, Jamaica men give higher FNMR. This applies in Haiti and Ghana also but only for people aged 45 or over.

These aggregations of results over a large number of algorithms is intended to expose coarse differences between demographic groups. In so doing it hides that certain algorithms may differ from the trends evident in the Figure. Full error tradeoff characteristics appear in Annex 12 .

The false negative results for law enforcement images apply to high quality mugshots, collected with deliberate consideration of standards. When image quality degrades, false negatives are expected to increase. We next consider results for the comparison of high quality Annex 2 application reference photos with Annex 4 border crossing images collected in a less controlled environment under some (implicit) time constraint. We report

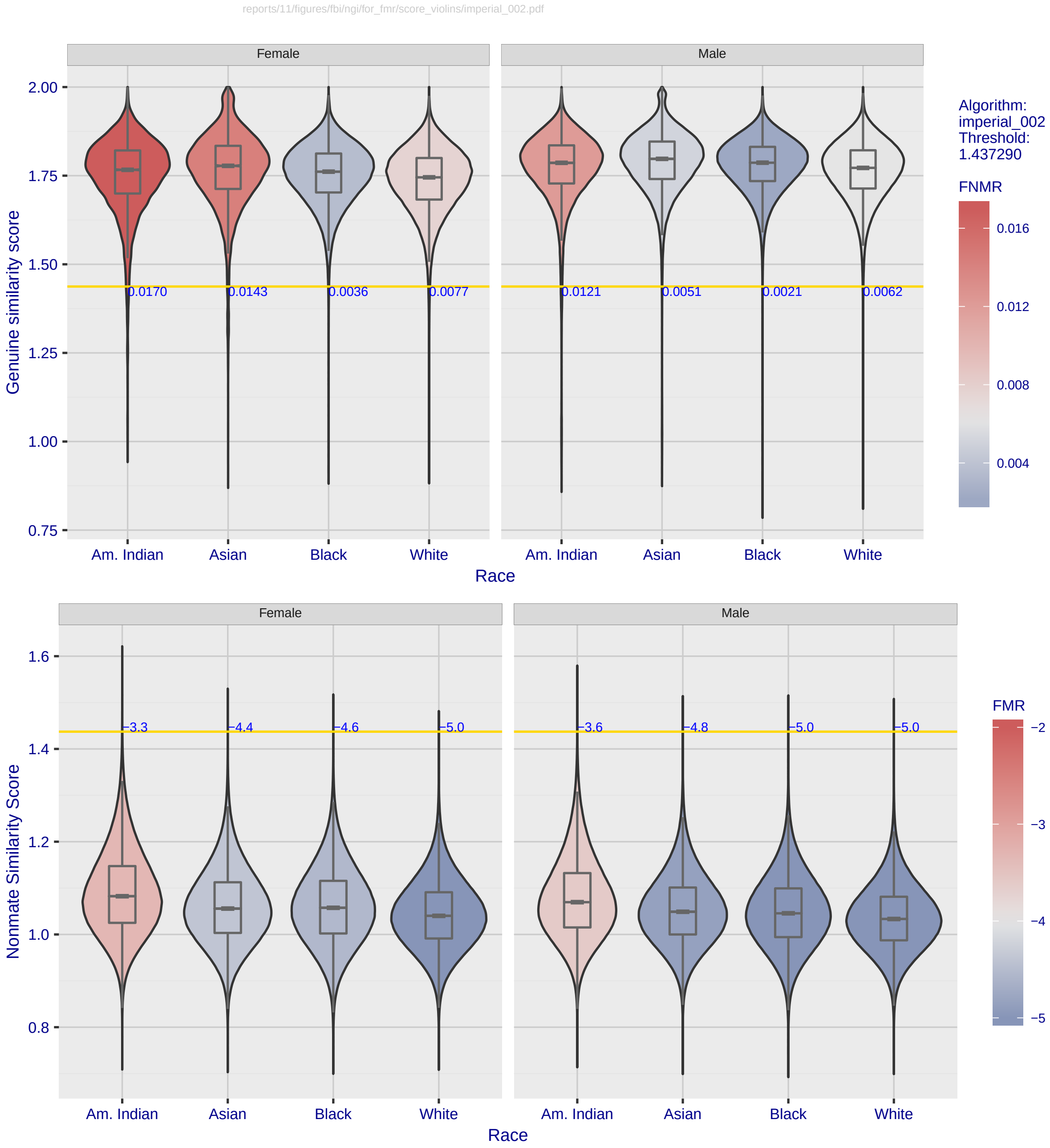

Figure 20: For one algorithm verifying mugshots, the violin plots show native similarity score distributions. The horizontal line shows the threshold that gives FMR = 0.0001 over all the imposter pairs. The imposters have the same sex and race. The upper figure shows genuine scores and the color indicates FNMR at the given threshold on a linear scale. The lower figure shows imposter scores with color indicating FMR on a logarithmic scale. FMR values below 10^{-5} are pinned to that value. Annex 15 contains the corresponding figure for all algorithms.

results in two ways:

▷ Per algorithm: Annex 14 shows FNMR by country of birth for two sexes and two age groups (above and below age 45).

▷ As Figure 22 heatmap showing results for all algorithms and all countries of birth. Each FNMR is the arithmetic mean of the four FNMR estimates for male and female and age over and under 45. The rows of the figure are sorted in order of mean FNMR, the mean being taken over all twenty four countries. The columns of the figure are sorted in order of mean FNMR from the 50 most accurate algorithms - this statistic was chosen so that high FNMR estimates from poor algorithms did not skew the results.

From these figure we note the following:

- **Wide variation across algorithms:** False non-match rates range from near 0.1% up to above 10%. This two-orders-of-magnitude range shows that some algorithms are intolerant of the quality problems inherent in the image the border crossing images. These problems are: low contrast, non-centered and cropped faces, non-frontal pose, and poor resolution, in part due to poor compression.

- **The most accurate algorithms give low FNMR:** The most accurate algorithms given FNMR below 1% for almost all countries and demographic groups. For example, the Visionlabs-007 algorithm has outliers only for Liberian and Somali women under the age of 45, for whom FNMR is below 1.4%.

- **Lower variation across countries:** For the more accurate algorithms, false non-match rates generally range by a factor of two or three from the left side of Figure 22 to the right i.e. FNMR in El Salvador is almost always lower than that in Somalia.

- **No clear patterns by age and sex:** By considering the Figures of Annex 14 , the differences between the over- and under-45s is often small, varies by country and by algorithm. However, broad statements do not mean that certain algorithms do not exhibit demographic differentials.

- **Higher FNMR in subjects from Africa and the Caribbean:** The heatmap is constructed with countries appearing in order of the mean FNMR over the fifty most accurate algorithms. This reveals higher FNMR in Africa and the Caribbean. After those two regions, the next highest FNMR is in the Eastern Europe countries.

The low error rates stem from efforts over the last decade to train algorithms that are invariant to nuisance variables such as non-frontal pose and poor contrast. The absolute magnitude of FNMR drives inconvenience. In many applications, any subject experiencing a false rejection could make a second attempt at recognition.

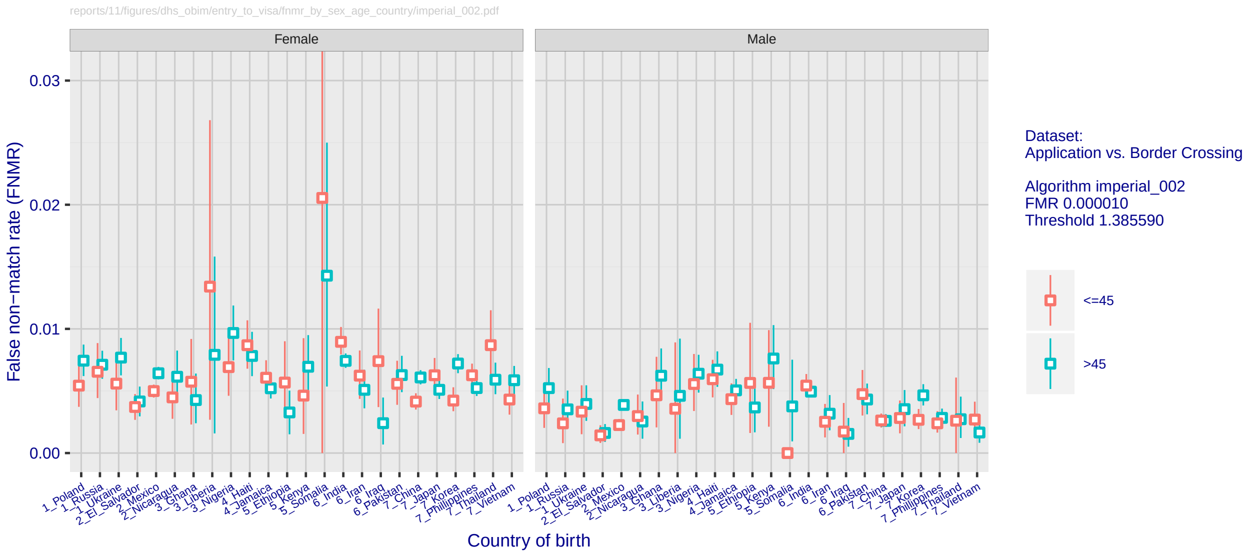

Figure 21: For 24 countries the figure shows false negative rates when the reference algorithm is used to compare two photos of subjects from the countries identified in the respective columns. The square box gives the median false non-match rate computed over 2000 bootstrap resamples of the genuine scores. The ends of the line span 95% of those re-samples, thereby giving a measure of uncertainty in the FNMR estimate. The threshold is set to a fixed value everywhere; it is the lowest value that gives FMR ≤ 0.00001. *Annex 14 contains the corresponding figure for all algorithms.*

Why these effects occur would require some multivariate analysis of image- and subject-specific properties. We suggest that analysis might start with measurement of image related quantities from the digital images to include such as contrast, intensity, areas of over and under exposure, presence of cropping, and head orientation. For tools, mixed-effects regression models could be an initial starting point [4] but such work would need to address correlation between quantities such race and contrast. We have not yet initiated such work and it is possible that such analysis would be incomplete due to influential but unknown covariates. In particular, given the border crossing images were collected with cameras mounted at fixed height and are steered by the immigration officer toward the face it is possible that subject height influences genuine matching scores. For example very tall subjects might be subject be underexposed because strong ceiling lights in the background might cause underexposure. Inspection of failure cases invariably leads to insight in such cases. We have not yet conducted that work.

reports/11/figures/dhs_obim/entry_to_visa/fnmr_by_sex_age_country_all_algorithms_heatamp.pdf

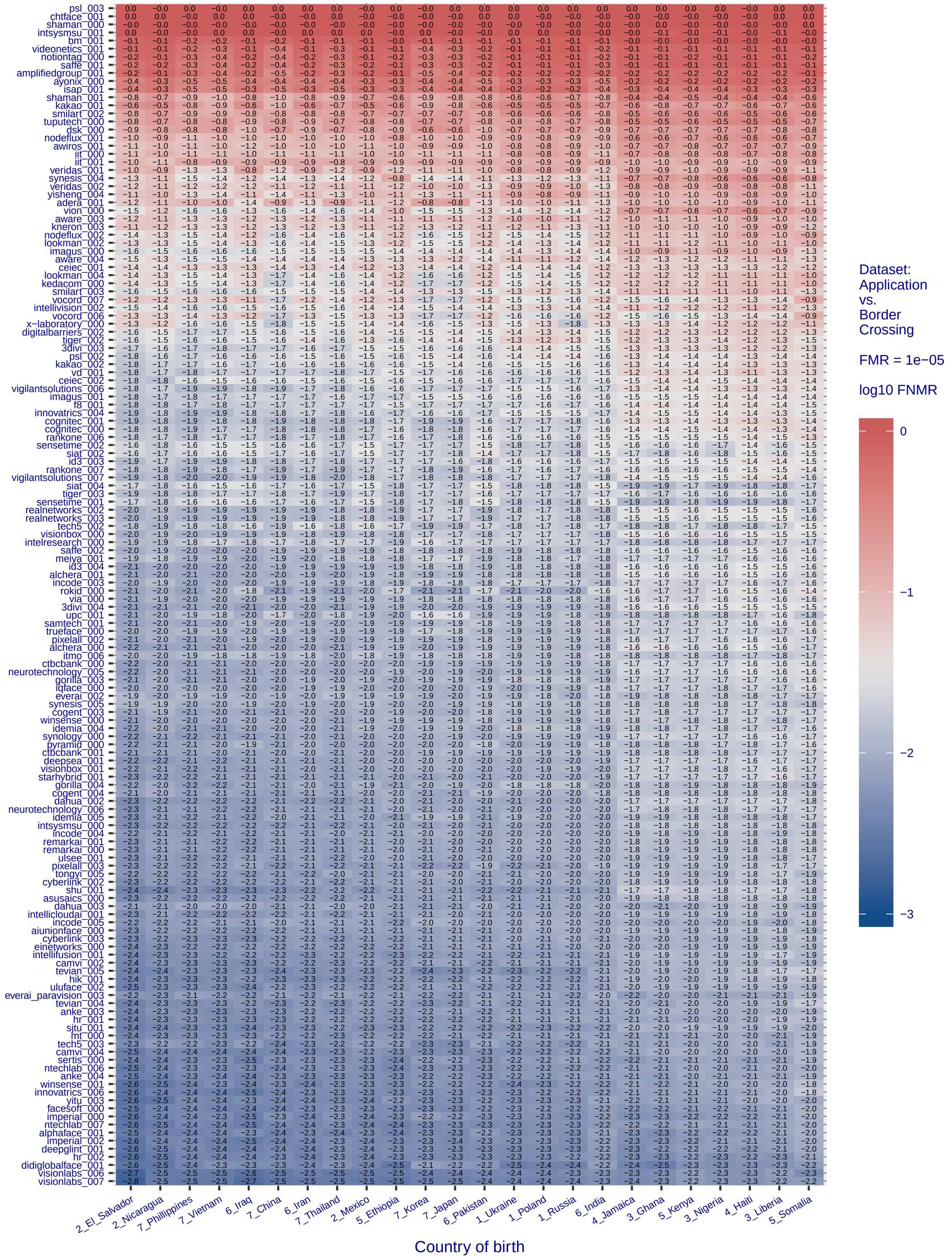

Figure 22: For 24 countries in seven regions the figure shows verification false non-match rates when the reference algorithm is used to compare two photos of subjects from the countries identified in the respective columns. The FNMR value is the mean over men/women and over/under age 45, so represents FNMR in situations where those four populations were balanced. The threshold is set to a fixed value everywhere; is is the lowest value that gives FMR ≤ 0.00001. Each cell depicts FNMR on a logarithmic scale. The text value is $\log_{10}(FNMR)$ with large negative values encoding superior false match rates.

6 False negative differentials in identification

The three identification trials all use just mugshot photographs. They were conceived of to isolate specific demographic factors as follows.

- ▷ **Sex**: We construct a gallery containing 800 000 white men, and 800 000 white women, aged 20 - 40. We search that with mated probes taken in a different calendar year to the enrolled photo but no longer than 5 years after. We search with balanced sets of non-mate probes, also aged 20-40.
- ▷ **Sex**: We construct a gallery containing 500 000 black men, and 500 000 black women, aged 20 - 40. We search that with mated probes taken in a different calendar year to the enrolled photo but no longer than 5 years after. We search with balanced sets of non-mate probes, also aged 20-40.
- ▷ **Race**: We construct a gallery containing 800 000 black men, and 800 000 white men, aged 20 - 40. We search that with mated probes taken in a different calendar year to the enrolled photo but no longer than 5 years after. We search with balanced sets of non-mate probes, also aged 20-40.

More detail appears in Annex 16 . In each case the mated probes are used to measure false negative identification rate, and the nonmated probes are used to measure false positive identification rate. These tests all employ domestic mugshots, and only younger adults. Further work will extend analysis to a global population with more range in age.

6.1 Metrics

The metrics appropriate to identification have been detailed in section 3.2. These are related to particular applications in Figure 23 reflecting two modes of operation. The general metric FNIR(N, R, T) covers both as follows:

- ▷ **Investigation:** For investigators willing to traverse long candidate lists in pursuit of a lead, the metric FNIR$(N, R, 0)$ is the proportion of missed mates when searching an N-enrollee gallery and considering the R most similar candidates without applying a threshold (T = 0). The utility of longer lists is shown by plotting FNIR vs. R.
- ▷ **Identification:** For those applications where a non-zero threshold is used to only return results when a search has a likely enrolled mate, the metric is FNMR(N, R, T). The use of thresholds $T > 0$ will suppress many false positives, but will also elevate false negatives, the tradeoff being shown as a plot of FNIR(T) vs. FPIR(T).

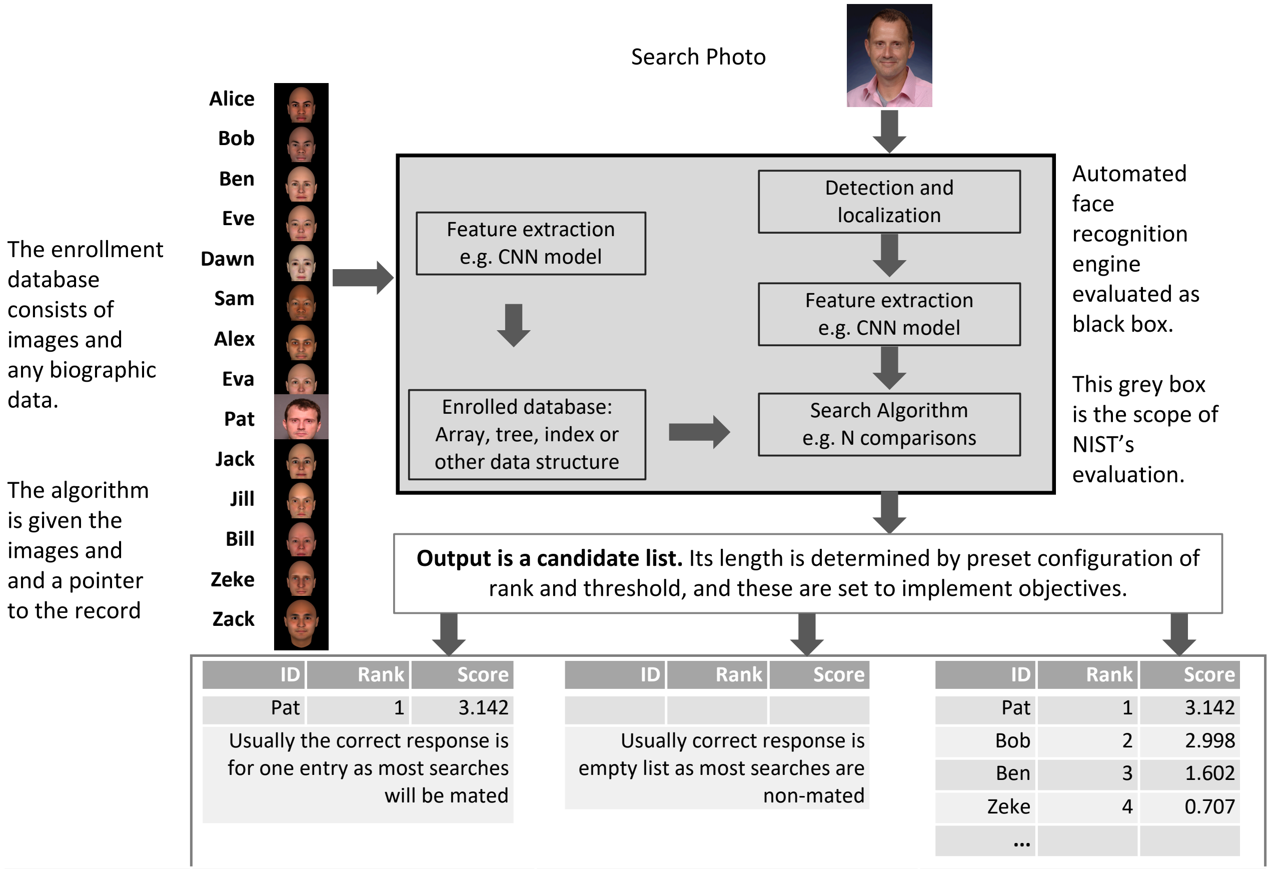
Search Photo
Alice
Bob
Ben
Eve
Dawn
Sam
Alex
Eva
Pat
Jack
Jill
Bill
Zeke
Zack
Detection and localization
Feature extraction e.g. CNN model
Feature extraction e.g. CNN model
Enrolled database: Array, tree, index or other data structure
Search Algorithm e.g. N comparisons

The enrollment database consists of images and any biographic data.

The algorithm is given the images and and a pointer to the record

Automated face recognition engine evaluated as black box.

This grey box is the scope of NIST's evaluation.

Output is a candidate list. Its length is determined by preset configuration of rank and threshold, and these are set to implement objectives.

ID	Rank	Score
Pat	1	3.142

Usually the correct response is for one entry as most searches will be mated

ID	Rank	Score

Usually correct response is empty list as most searches are non-mated

ID	Rank	Score
Pat	1	3.142
Bob	2	2.998
Ben	3	1.602
Zeke	4	0.707
...		

	Positive identification	Negative identification	Post-event investigation
Example	Access to a gym or cruise ship	Watchlist e.g. Detection of deportee or duplicate drivers license applications	Crime scene photos, or of detainee without ID documents.
Claim of identity	Implicit claim to be enrolled	Implicit claim to not be enrolled	No claim: Inquiry
Threshold	High, to implement security objective	High, to limit false positives	Zero
Num. candidates	1	0	L, set by request to algorithm
Human role	Review candidate to assist user in resolution of false negatives, or to detect impostor	Review candidate to determine false positive or correct hit	Review multiple candidates, refer possible hits to examiners see [26]
Intended human involvement frequency	Rare – approx. the false negative identification rate plus prior probability of impostor	Rare – approx. the false positive identification rate plus prior probability of an actual mate	Always
Performance metric of interest	**FNIR at low FPIR. See sec. 3.1, 3.2 and Tables 10, 19**	**FNIR at low FPIR. See sec. 3.1, 3.2 and Tables 10, 19**	**FNIR at ranks 1... 50, say. FPIR = 1. See sec. 3.2 and Table 12, 14, 16**

Figure 23: Identification applications and relevant metrics.

6.2 Results

Figures 24 and 25 show identification error rates for two algorithms. Plots for all algorithms are included in Annex 16 . In each case, the upper panels show FNIR vs R. The lower panels show FNIR vs. FPIR. We make the following observations

▷ Differentials by race in men: From the left-side panels, black men invariably give lower false negative identification rates than white men. This applies in the investigate and identification modes, and particularly for the more accurate algorithms. The differentials are often small, well below a factor of two. The are some exceptions including algorithms from 3DiVi, Aware, Eyedea, Idemia, Kedacom, Tevian and Vocord.

▷ Differentials between the sexes: Women invariably give higher false negative rates than men. This applies within both racial groups. There are exceptions, notably that searches of white women are more likely to produce the correct result in the top ranks than are search of men. This is less true for black women. A possible mechanism for this is available from section 4 verification results, namely that black women tend to produce high one-to-one false match rates. High non-mate scores may be displacing the correct black women from rank 1 position.

▷ Low FPIR is not attainable: The error tradeoff characteristics show a rapid increase FNIR as the threshold is increased to reduce FPIR. For example, in FNIR Figure 24, FNIR reaches 50% when FPIR is reduced to 0.0001. This is due to the presence of high scoring non-mates in the imposter searches. They can occur for several reasons. First, ground truth identity labeling errors in which photos of a person are in the database under multiple IDs. These cause apparent false positives. We discount this because the mugshot ground truth integrity is excellent, and underpinned by ten-print fingerprint matching. A second reason is the presence of twins in the population. Given the population represented by the dataset, we estimate a few percent of the United States adult population is present in the dataset. Given well documented twinning rates[14] [27], we expect twins to be in the data, both identical and, more commonly, fraternal. Siblings will be expected to give elevated similarities along the same lines.

▷ Higher false positive identification rates in black women: The lines connecting points of fixed threshold are often long and slanted in the error tradeoff plots in the center column of the bottom row - see Figure 24, for example. This is a common occurence revealing an order-of-magnitude increase in FPIR, with magnitudes varying by algorithm. Notably some algorithms do not exhibit this excursion. For example, the algorithm featured in Figure 25 gives much smaller excursions in FPIR.

[14] See the CDC's National Vital Statistics Report for 2017: https://www.cdc.gov/nchs/data/nvsr/nvsr67/nvsr67_08-508.pdf

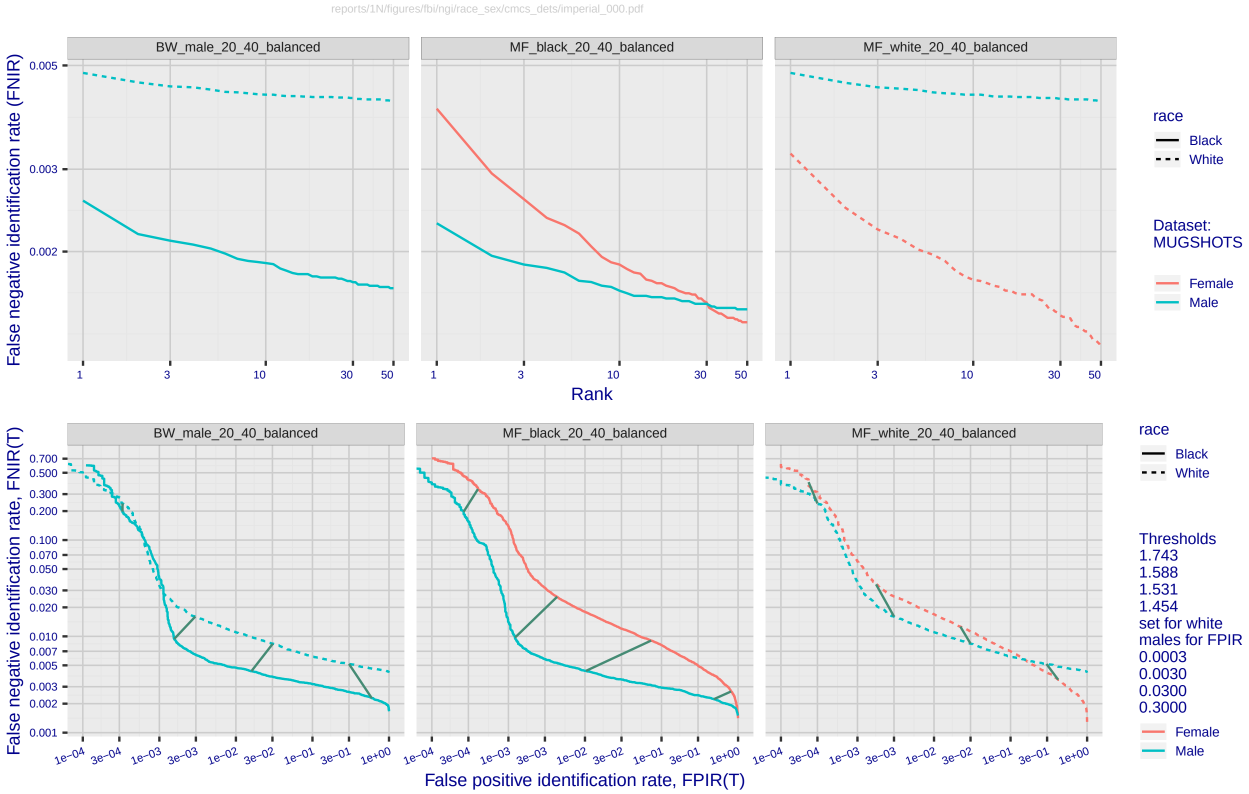

Figure 24: For mugshot identification, the top row shows false negative identification "miss" rates as a function of rank, a metric appropriate to investigators traversing candidate lists for lead generation. The bottom row shows miss rates as a function of false positive identification rate, where a threshold is swept from a low value on the right to high values on the left. This metric is appropriate to organizations for which the volume of searches is high enough that they cannot afford labor to review results from every search. The left panels show the effect of race in young men. The center and right panels show difference between men and women, in black then white subjects respectively. The grey lines join points of equal threshold. The four thresholds are chosen to give FPIR of $\{0.0003, 0.003, 0.03, 0.3\}$ *respectively for one baseline demographic, here white males. The figure applies to one algorithm, provided to NIST in August 2019. The corresponding figures for all identification algorithms appear in Annex 16 .*

reports/1N/figures/fbi/ngi/race_sex/cmcs_dets/idemia_4.pdf

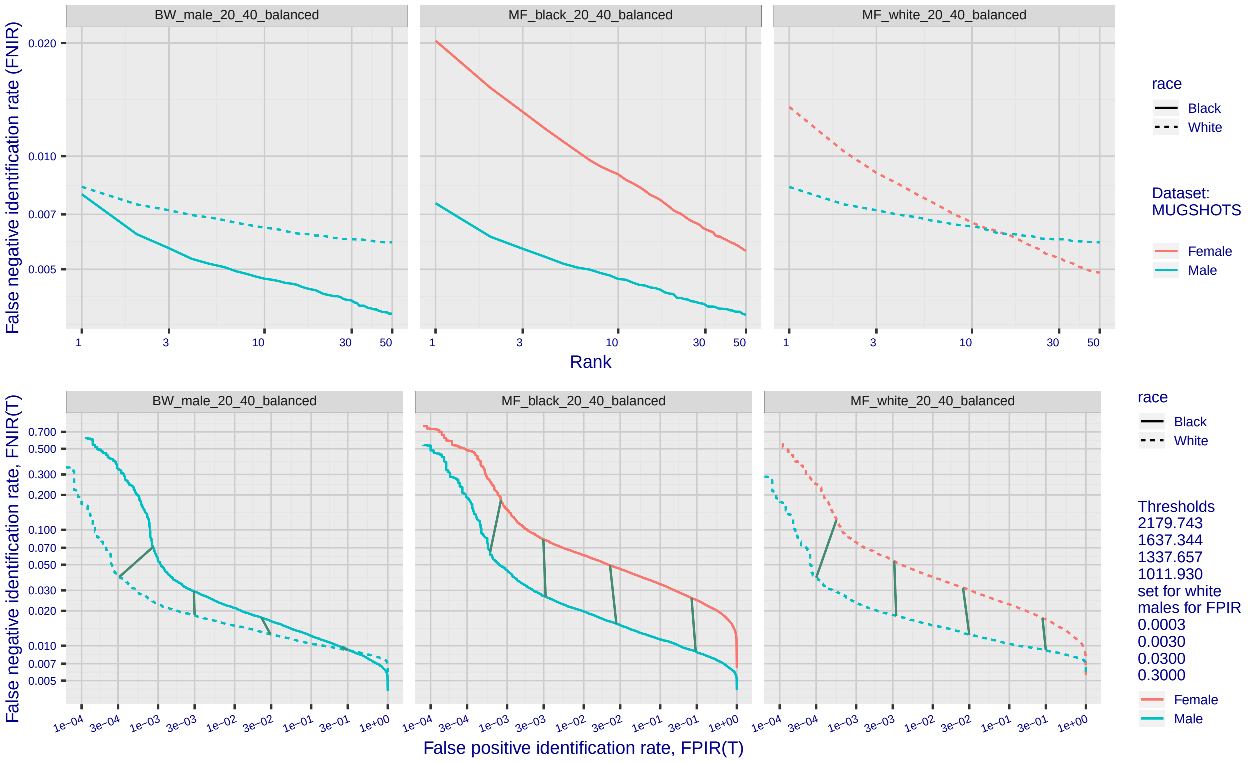

Figure 25: For mugshot identification, the top row shows false negative identification "miss" rates as a function of rank, a metric appropriate to investigators traversing candidate lists for lead generation. The bottom row shows miss rates as a function of false positive identification rate, where a threshold is swept from a low value on the right to high values on the left. This metric is appropriate to organizations for which the volume of searches is high enough that they cannot afford labor to review results from every search. The left panels show the effect of race in young men. The center and right panels show difference between men and women, in black then white subjects respectively. The grey lines join points of equal threshold. The four thresholds are chosen to give FPIR of $\{0.0003, 0.003, 0.03, 0.3\}$ *respectively for one baseline demographic, here white males. The figure applies to one algorithm, provided to NIST in June 2018. The corresponding figures for all identification algorithms appear in Annex 16 .*

7 False positive differentials in identification

The section addresses whether identification algorithms exhibit similar false positive differentials to verification algorithms. We first note that large-scale one-to-many identification deployments typically operate at false match rates much lower than those targeted in verification applications. It is typical in verification access control to target false match rates (FMR) between 0.00001 and 0.001, i.e. between one per hundred thousand and one per thousand. Identification applications, howveer, often enroll very large numbers of individuals numbering into the 10s or 100s of millions. If such systems are configured with thresholds aimed at producing false positive outcomes say one in 100 times, i.e. FPIR = 0.01, then the implied likelihood that a comparison will yield a false match is given by this formula

$$\text{FMR} = \frac{FPIR}{N} \tag{10}$$

where N is the size of the enrolled population. With FPIR= 0.01, and N= $10^6 s$ this formula implies FMR= 10^{-8}. The formula gives a first order equivalence of identification with verification: the former needs low false positive rates in large galleries. Metrics are discussed in section 3.

Some one-to-many search algorithms implement a 1:N search of a probe image as N 1:1 comparisons of the probe with the N enrolled items. This is followed by a sort operation which yields N candidates sorted in decreasing order of similarity. The result of that is returned in either of two ways: The system will return an operator-specified number of candidates, or it will return however many candidates are above an operator-specified threshold[15]. In the case where a threshold is used, the number of candidates returned will be a random-variable that is dependent on the image data itself.

Other algorithms do not implement 1:N search as N 1:1 comparisons. Instead they might employ a set of fast-search algorithms aimed at expediting search [2, 19, 21, 26]. These include various techniques to partition the enrollment data so that far fewer than N comparisons are actually executed. However, this does not mean that false positive occurences will be reduced because the algorithms are still tasked with finding the most similar enrollments.

For the three experiments listed in section 6, Figure 26 shows median scores returned by one identification algorithm when non-mated searches are conducted. It is clear that if a threshold is applied there will be demographic differences in the number of candidates returned, and in the score values. Such behavior applies to many algorithms - see Annex 17 .

This effect disappears in the algorithm featured in Figure 27. This is an important result because it implies much more equitable likelihoods of false positives. This is especially important result in negative identification

[15] The “operator-specified” parameters might sometimes be set by-policy, or by the manufacturer of the system.

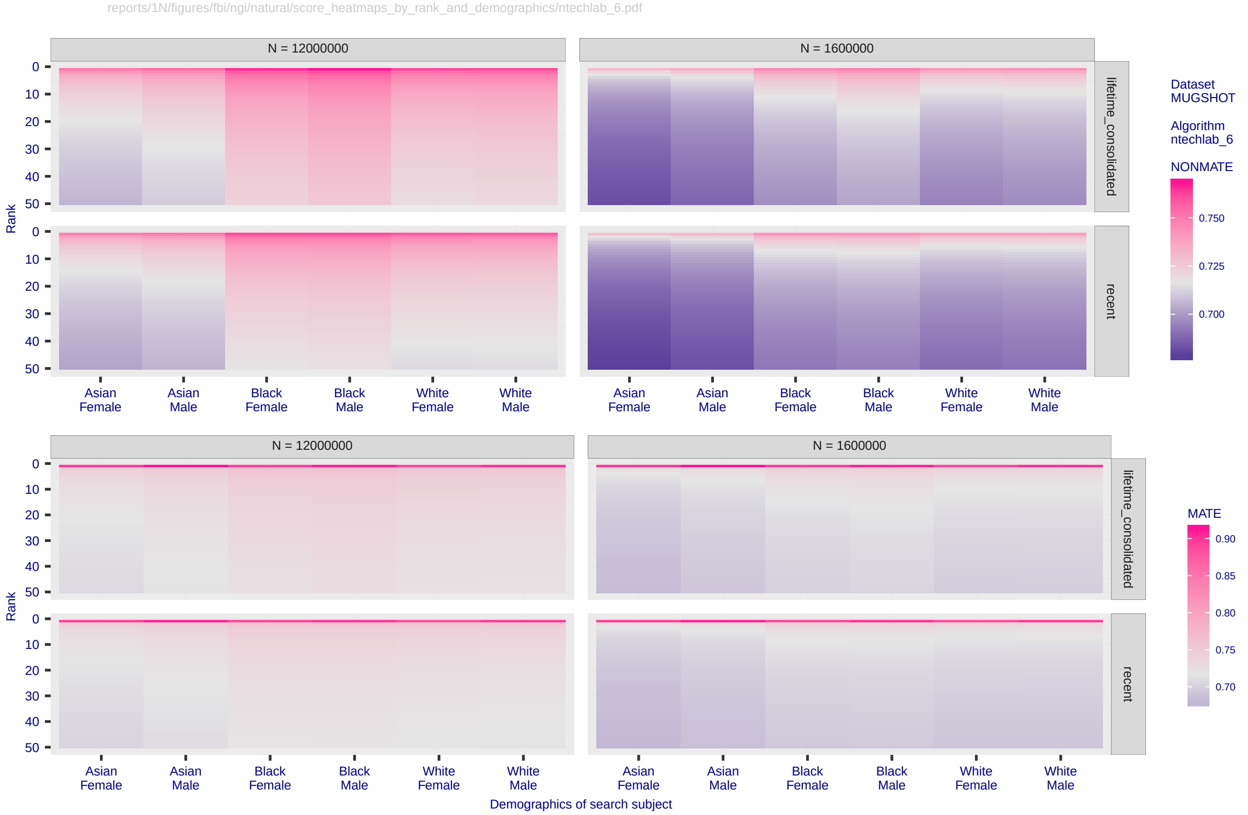

Figure 26: For searches of Asian, black, white men and women's faces into mixed galleries of mugshot photos the heatmaps show median similarity scores for candidates placed at rank 1 to 50. The upper four panels are produced in nonmated searches; the lower four from mated searches. The left-side panels are produced from searches into galleries with 12 000 000 people enrolled. The right-side uses galleries with N = 1 600 000 enrolled. The "lifetime consolidated" and "recent" labels refer to inclusion of multiple images per person, or just one - see [17].
Contrast the behavior here with that in Figure 27 and the corresponding figures for developers Aware, Idemia, NEC, Tevian, and Toshiba that are included in Annex 17 .

applications where the prior probability of a searched person actually being is in the database is low, e.g. card-sharp surveillance in a casino, or soccer hooligans at a sports game[16]. The lack of an effect on false positive identification rates is evident in Figure 25 where the grey lines join points of equal threshold. From left-to-right, the FPIR values for black and white males, black men and women, and white men and women are closely similar. The more normal behavior (see Figure 24 and Annex 16) is for larger shifts in false positive rates.

We now consider the implications for **investigative "lead generation" applications**. In such cases, algorithms return a fixed number of candidates and human reviewers compare the probe photo alongside each candidate gallery photo to determine if the photos are a match. In mugshot-mugshot searches the reviewer will very often look no further than rank 1 per the very high accuracy results documented in NIST Interagency Report

[16] For example, a recent news article noted the use of automated face recognition to search around 21 000 spectators at soccer games against a watch-list of about 50 people.

reports/1N/figures/fbi/ngi/natural/score_heatmaps_by_rank_and_demographics/idemia_5.pdf

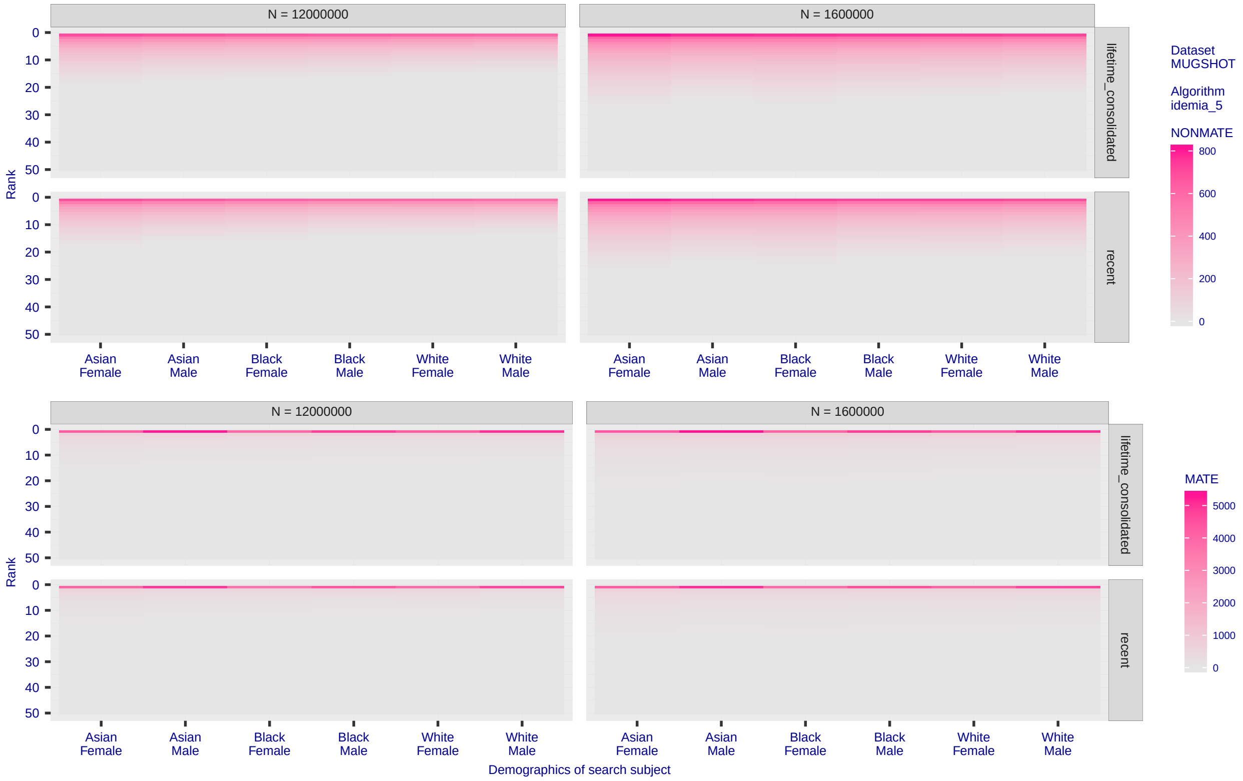

Figure 27: For searches of Asian, black, white men and women's faces into mixed galleries of mugshot photos the heatmaps show median similarity scores for candidates placed at rank 1 to 50. The upper four panels are produced in nonmated searches; the lower four from mated searches. The left-side panels are produced from searches into galleries with 12 000 000 people enrolled. The right-side uses galleries with N = 1 600 000 enrolled. The "lifetime consolidated" and "recent" labels refer to inclusion of multiple images per person, or just one - see [17]. The uniformity of the scores across demographic groups is in contrast to that evident in Figure 26 and many others in the Annex 17 compendium.

8271. That report also includes a workload measure summarizing the expected number of candidates that will have to be reviewed before a mate is located. A very important parameter in such applications, however, is the prior probability that a mate is actually present. In boarding a cruise ship for example, almost everyone attempting to board would be present in the gallery. In a casino application aimed at detecting "high rollers" the likelihood a patron of the casino is in that set is much lower. In such cases a human reviewer, if so employed, would in most searches review all say 50 candidates on the list. That's laborious and may not be tenable from an operations research perspective due to fatigue and reward factors in humans.

But in whatever circumstances human reviewers are tasked with reviewing candidate lists, how are demographic differentials such as those in Figure 26 expected to influence the human? The human will see fifty candidates regardless. However, if those candidates are accompanied by scores, presented as text in a GUI for example, the reviewer will see higher scores in the black female population and potentially elsewhere. Over time this may influence the human, though one earlier study [12] looked at cognitive bias issues in the human review of fingerprint search results, without demographic effects, and found scant evidence that scores influence the reviewer. That study did, however, find that just the order in which candidates are presented to reviewers affects both false positives and false negatives. For example, reviewers are more likely to miss (i.e. a false negative) a mated candidate that appears far down the candidate list. The issues involved in human review are beyond the scope of this document, but full consideration of *systems* comprised of automated face search algorithms and human reviewers is an experimental psychology, human factors and operations research issue.

8 Research toward mitigation of false negatives

False negative error rates, and demographic differentials therein, are reduced in standards-compliant images. This motivates the following two research and development possibilities.

▷ **Improved standards compliance:** The ISO/IEC 19794-5 standard includes requirements regulating geometry and exposure. Recent research [24] noted that higher quality images, as determined by an automated quality assessment algorithm, yields a reduced false negative differential. While commercial packages exist for the automated assessment of quality, and NIST has an ongoing assessment of the underlying algorithms, rejection of single images on quality grounds can itself have demographic problems [1]. The ISO/IEC SC 37 biometrics subcommittee has recently initiated work on quality (ISO/IEC 29794-5 and 24357).

▷ **Face-aware cameras:** The same ISO/IEC committee has recently initiated work on specifications for capture subsystems that may require real-time face detection, pose estimation, and exposure measurement. Analogous "auto-capture" quality control mechanisms exist in iris and fingerprint scanners. That standard, ISO/IEC 24358, will be developed through 2020 with completion expected in 2021. Participation is open via national standardization groups.

Along similar lines further research into automated image quality assessment, and particularly specifications for closed-loop face-aware capture would prove valuable in averting low-contrast and over- and under-exposed images. Many enrollment operations still rely on documentary photography standards with cameras that are not detecting and metering off faces.

This work would be supported by research into two further topics:

Analysis: There is a need for improved models of demographic effects, particularly to how subject-specific properties including phenotypes, imaging artefacts and algorithms interact. Such models would extend work [9] in separating the relative contributions of at least, sex, age, race and height. Efforts to automatically estimate phenotypic information from images will involve algorithms that may themselves exhibit demographic differentials. Such work will need to address this possibility.

Information theoretic analysis: Given the potential for poorly illuminated photographs to produce false negatives, via under- or over-exposure of dark or light skin, an information theoretic approach to characterize algorithmic response to poor lighting would be useful for future standardization. In particular, the ISO/IEC 19794-5 standard has, since 2004, required portrait photos to have at least 7 bits of content in each color channel. Such work should quantify both false negative and false positive dependence.

9 Research toward mitigation of false positives

9.1 Summary

The threshold manipulation strategies described above would be irrelevant if the algorithm developer provided software with homogeneous false match rates. That will prove impossible as there will always be some distribution around a mean - the goal should be much more homogeneous false match rates than is currently the case.

9.2 Algorithm training

A longer-term mitigation is prompted by our observation that many algorithms developed in China do not give the elevated false positive rates on Chinese faces that algorithms developed elsewhere do. This affirms a prior finding of an "other-race effect" for algorithms [33] though that paper did not separate false positive from false negative shifts. This suggests that training data, or perhaps some other factor intrinsic to the development, can be effective at reducing particular false positive differentials. Thus, the longer-term mitigation would be for developers to investigate the utility of more diverse, globally derived, training data. Absent such data, developers might consider whether their cost functions can be altered to reduce differentials. One developer advanced such a concept in November 2018 [15].

9.3 Greater discriminative power

Face recognition algorithms measure similarity between face images. Facial appearance is partially determined by genes, the phenotypic expression of which determines skin tone and a large set of characteristics related to shape of the face. In NIST recognition tests [17], identical twins invariably cause false positives at all practical operational thresholds. Twins are characterized by very similar features given identical genes. Similarities in faces in fraternal twins [17] are expected to extend also to siblings (which also share half of the genes), and then to more distant relatives. In 2004, an algorithm was patented that can correctly distinguish twins [US Patent: US7369685B2]; it operates by extracting features from skin texture (adjacent to the nose, and above the eyebrows). This algorithm requires high resolution and, moreover, knowledge that any given image has that resolution. However, contemporary deployments of face recognition are very often based on processing of images at or below VGA spatial sampling rates (i.e., 480 x 640 pixel images), and this is often insufficient for skin texture to be viable. The human reviewer community has long specified much higher resolution for forensic purposes (see ANSI/NIST Face Acquisition Profiles).

9.4 Collection and use of face and iris

The texture of the human iris is known to have a structure that when imaged and processed by published feature extraction algorithms [11, 29] will correctly discriminate between identical twins [40] - something that contemporary marketplace face algorithms do not [17]. The reason for this appears to be that the iris features detected by automated algorithms are not genetically determined. However genetics research [25] does show iris textures have some genetic linkage, so a better characterisation of the tails of the impostor distribution is needed, at least for large scale one-to-many identification. Nevertheless, a 2019 DHS Science and Technology study noted that false positives are no higher within individuals of the same sex, age and race as they are across those groups [39]. As shown in Figure 4 and Annex 8 that is not the case for face recognition. NIST has near-term plans to investigate the impostor distribution in twins more fully.

Given the marketplace presence of multiple cameras that collect face and iris essentially simultaneously, one approach to consider for mitigation of false positive differentials in face recognition would be for face records to include adjunct iris images. The standards infrastructure is in place for this (ANSI/NIST Type 17, ISO/IEC 39794-6, and ICAO 9303 Data Group 4). This would afford very low false positive rates.

The apparent lack of genetic influence, and demonstrated low false match likelihoods, has been the primary property in establishing the use of the iris for the identification of individuals in large populations - most notably in the Indian National ID program Aadhaar. The iris recognition industry has multiple camera developers, multiple algorithm suppliers, and image interchange and quality standards that support interoperable recognition across cameras.

These aspects afford solutions to higher and heterogeneous false positive rates in face recognition. The first is simply to replace face with iris. There would be advantages and disadvantages to this - detailing and weighing those is beyond our scope here. However a second solution would be to augment face with iris, to produce a compound biometric "face-and-iris"[17]. This is made possible by the marketplace availability for at least a decade now of cameras that collect iris and face images essentially simultaneously. Recognition of the combined biometric would involve a particular kind of biometric fusion that in which both the face and iris must match (against respective thresholds) so as to limit false positives. This differs from some convenience-driven implementations that authenticate a person with either face or iris alone.

Use of iris in some applications, for example surveillance, is limited by the difficulty and expense of imaging the iris at long distances.

We don't mention fingerprints in this context because even though genetic influence is considered to be absent

[17] Such a compound biometric would conventionally still require collection of two images: First an iris image with near infrared illumination and the face image either entirely in ambient light, or ambient light with a near infrared component. The recognition of irises in purely visible-light images is highly problematic in brown-eyed people as melanin in the iris absorbs incident light at visible wavelengths.

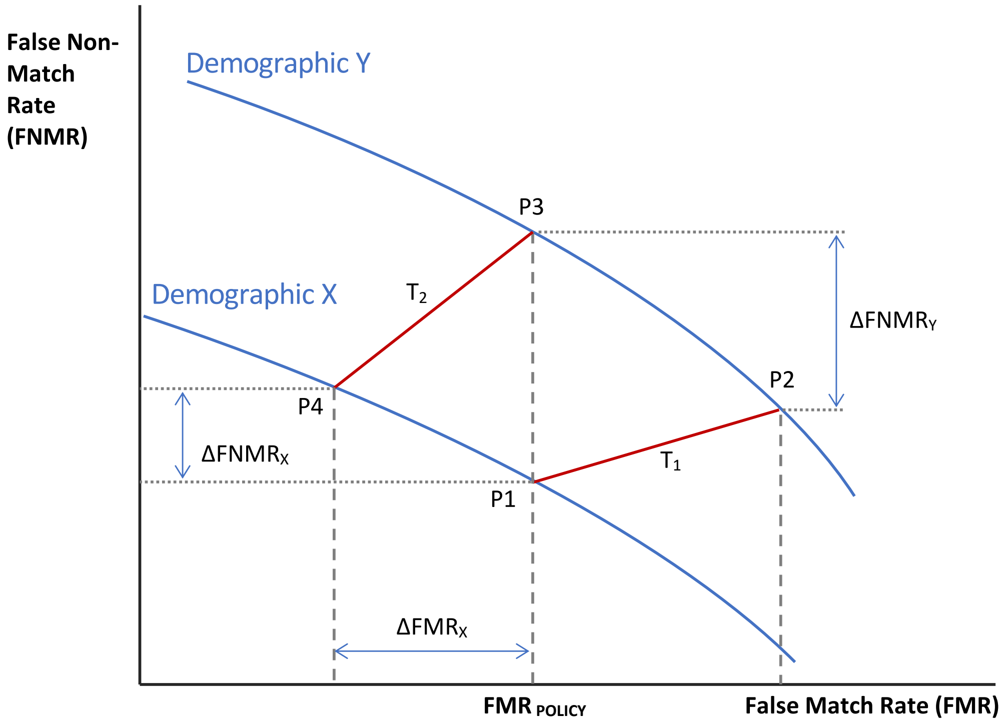

Figure 28: The figure shows the increases in FNMR implied by increasing the operating threshold to achieve the target FMR on the high-FMR demographic, Y.

or minimal, the collection of both fingerprint and face is not simultaneous.

9.5 Threshold elevation

We detail one mitigation of heterogeneous variable false match rates, and its consequences, as follows. The explanation uses a graphical construct based on the error tradeoff characteristics shown in Figure 28.

- ▷ We start with a target false match rate FMR_{POLICY} that has been set to implement some security objective. This value, in a verification application might reasonably be set to say 1 in 5000 (i.e. 0.0002). This is implemented by setting a threshold T_1. Suppose that this threshold was perfectly calibrated for Demographic X i.e. $FMR(T_1) = FMR_{POLICY}$. This corresponds to the point P1.
- ▷ Now suppose that we later discover, perhaps as a result of some biometric performance test or audit that, for some new group Demographic Y, that the observed false match rate at the fixed threshold T_1 is much higher, a factor of five say (0.001). This point P2 therefore represents therefore a failure to meet the original security objective for that group.
- ▷ To bring the overall system into policy compliance, the system owner consults the error tradeoff charac-

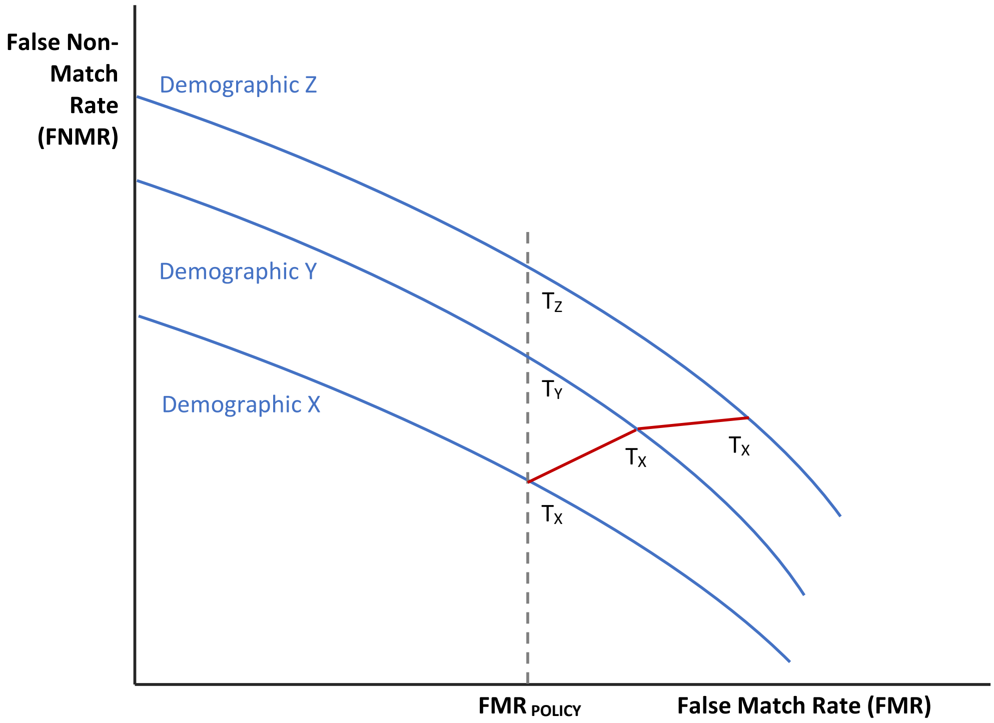

Figure 29: The figure shows the effect of setting thresholds to achieve the target FMR on demographics X and Y.

teristic for Demographic Y and notes that by elevating the threshold to T_2, the false match rate would be returned to policy compliance, at point P3.

▷ The effect of this however is that FNMR is necessarily elevated both demographic groups. This is because the new threshold T_2 is higher than T_1, and applies to all transactions from all demographics. These increases are shown as ΔFNMR_X and ΔFNMR_Y would have a magnitude that depends on the gradients of the error-tradeoff characteristics (which may differ). The only gain is a reduction in FMR for Demographic X, to a value which beats the original target policy.

Using this kind of construct, we see the benefit in having a biometric algorithm for which false match rates are homogenous i.e. do not vary (much) over any demographics.

The above argument assumes that the original high $\text{FMR}_Y(T_1)$ is indeed problematic. It may be tolerable in cases where individuals in that Demographic are rare, e.g. elderly persons entering a gym or nightclub. Any decision to not elevate the threshold to T_2 should be deliberated in the security context defined by threat, risk and cost.

9.6 Explicit thresholds for each demographic

In this section we discuss the suggestion [23] to address heterogeneous false match rates by assigning a threshold to each demographic. The proposal is for a verification system to set the threshold each time a subject executes a verification transaction tailoring it on the basis of who is using the system. Referencing Figure 29, this would correspond to adopting thresholds T_1 and T_2 (i.e. points P1 and P3) on-the-fly. How to do this presents a problem. Naively one could encode in an identity document (e.g. a passport) some indication of the demographic group (e.g. female, middle aged, south Asian) and the system would read this information, consult a lookup table, and set T accordingly. This would be effective for genuine legitimate users of the system. The security consequences of this are, however, more complicated. Consider what an imposter would do given knowledge that thresholds are variable.

- ▷ If the imposter were from a demographic for which the threshold is low, he would procure / steal a credential from somebody of the same age, sex and ethnicity. This would be typical behavior for any imposter. However, if particular countries passports were known to be used with low-thresholds, we'd expect genesis of a black-market for stolen credentials in those places.
- ▷ If the imposter were from a demographic for which the threshold is high he might procure / steal a credential from somebody in one of the low-threshold demographics, matching age and sex minimally the same sex. To better induce a false match the imposter would still need to have the same age, sex and ethnicity. This would be typical behavior anyway.

  Note that societal construction will often naturally afford opportunities for imposters to have access to identity credentials from other persons who, naturally, have the same ethnicity, sex and age group.

Another aspect to this approach is that it shifts responsibility for threshold management to the system owner rather than the developer. That may sound fully appropriate but imposes two responsibilities on the operator: First, figuring out what the thresholds should be via some appropriate testing, and secondly to implement the strategy with capture of demographic information and use of that in software.

References

[1] December 2016. https://www.telegraph.co.uk/technology/2016/12/07/robot-passport-checker-rejects-asian-mans-photo-having-eyes/.

[2] Artem Babenko and Victor Lempitsky. Efficient indexing of billion-scale datasets of deep descriptors. In *The IEEE Conference on Computer Vision and Pattern Recognition (CVPR)*, June 2016.

[3] L. Best-Rowden and A. K. Jain. Longitudinal study of automatic face recognition. *IEEE Transactions on Pattern Analysis and Machine Intelligence*, 40(1):148–162, Jan 2018.

[4] J. Ross Beveridge, Geof H. Givens, P. Jonathon Phillips, and Bruce A. Draper. Factors that influence algorithm performance in the face recognition grand challenge. *Computer Vision and Image Understanding*, 113(6):750–762, 2009.

[5] Joy Buolamwini. Gender shades: Intersectional phenotypic and demographic evaluation of face datasets and gender classifiers. Technical report, MIT Media Lab, 01 2017.

[6] J. Campbell and M. Savastano. Iso/iec 22116 identifying and mitigating the differential impact of demographic factors in biometric systems. Technical report, ISO/IEC JTC 1, SC 37, Working Group 6, http://iso.org/standard/72604.html, 11 2018.

[7] Jacqueline G. Cavazos, Eilidh Noyes, and Alice J. O'Toole. Learning context and the other-race effect: Strategies for improving face recognition. *Vision Research*, 157:169 – 183, 2019. Face perception: Experience, models and neural mechanisms.

[8] Jacqueline G. Cavazos, P. Jonathon Phillips, Carlos D. Castillo, and Alice J. O'Toole. Accuracy comparison across face recognition algorithms: Where are we on measuring race bias? In *https://arxiv.org/abs/1912.07398*, 12 2019.

[9] Cynthia Cook, John Howard, Yevgeniy Sirotin, Jerry Tipton, and Arun Vemury. Demographic effects in facial recognition and their dependence on image acquisition: An evaluation of eleven commercial systems. *IEEE Transactions on Biometrics, Behavior, and Identity Science*, PP:1–1, 02 2019.

[10] White D., Kemp R. I., Jenkins R., Matheson M, and Burton A. M. Passport officers errors in face matching. *PLoS ONE*, 9(8), 2014. e103510. doi:10.1371/journal. pone.0103510.

[11] J. Daugman. How iris recognition works. *IEEE Transactions on Circuits and Systems for Video Technology*, 14(1):21–30, Jan 2004.

[12] Itiel Dror and Kasey Wertheim. Quantified assessment of afis contextual information on accuracy and reliability of subsequent examiner conclusions. Technical Report 235288, National Institute of Justice, July 2011.

[13] H El Khiyari and Wechsler H. Face verification subject to varying (age, ethnicity, and gender) demographics using deep learning. *Journal of Biometrics and Biostatistics*, 7:323, 11 2016. doi:10.4172/2155-6180.1000323.

[14] C. Garvie, A. Bedoya, and J. Frankle. The perpetual line-up: Unregulated police face recognition in america. Technical report, Georgetown University Law School, Washington, DC, 10 2018.

[15] Stéphane Gentric. Face recognition evaluation @ idemia. In *Proc. International Face Performance Conference, National Institute of Standards and Technology NIST, Gaithersburg, MD*, November 2018.

[16] Patrick Grother, Mei Ngan, and Kayee Hanaoka. Face recognition vendor test (frvt) part 1: Verification. Interagency Report DRAFT, National Institute of Standards and Technology, October 2019. https://nist.gov/programs-projects/frvt-11-verification.

[17] Patrick Grother, Mei Ngan, and Kayee Hanaoka. Face recognition vendor test (frvt) part 2: Identification. Interagency Report 8271, National Institute of Standards and Technology, September 2019. https://doi.org/10.6028/NIST.IR.8271.

[18] Patrick Grother, George W. Quinn, and Mei Ngan. Face recognition vendor test - still face image and video concept, evaluation plan and api. Technical report, National Institute of Standards and Technology, 7 2013. http://biometrics.nist.gov/cs_links/face/frvt/frvt2012/NIST_FRVT2012_api_Aug15.pdf.

[19] Feng Hao, John Daugman, and Piotr Zielinski. A fast search algorithm for a large fuzzy database. *IEEE Transactions on Information Forensics and Security*, 3(2):203–212, 2008.

[20] John J. Howard, Yevgeniy Sirotin, and Arun Vermury. The effect of broad and specific demographic homogeneity on the imposter distributions and false match rates in face recognition algorithm performance. In *Proc. 10-th IEEE International Conference on Biometrics Theory, Applications and Systems, BTAS 2019, Tampa Florida,USA*, September 2019.

[21] Masato Ishii, Hitoshi Imaoka, and Atsushi Sato. Fast k-nearest neighbor search for face identification using bounds of residual score. In *2017 12th IEEE International Conference on Automatic Face & Gesture Recognition (FG 2017)*, pages 194–199, Los Alamitos, CA, USA, May 2017. IEEE Computer Society.

[22] B. F. Klare, Burge M. J., Klontz J. C., Vorder Bruegge R. W., and Jain A. K. Face recognition performance: Role of demographic information. *IEEE Trans. on Information Forensics and Security*, 7(6):1789–1801, 9 2012.

[23] K. S. Krishnapriya, Kushal Vangara, Michael C. King, Vitor Albiero, and Kevin Bowyer. Characterizing the variability in face recognition accuracy relative to race. *CoRR*, abs/1904.07325, 2019. http://arxiv.org/abs/1904.07325.

[24] K. S. Krishnapriya, Kushal Vangara, Michael C. King, Vitor Albiero, and Kevin Bowyer. Us study: better image quality could cut face system bias. *Biometric Technology Today*, 2019(5):11 – 12, 2019.

[25] Mats Larsson, David L. Duffy, Gu Zhu, Jimmy Z. Liu, Stuart Macgregor, Allan F. McRae, Margaret J. Wright, Richard A. Sturm, David A. Mackey, Grant W. Montgomery, Nicholas G. Martin, and Sarah E. Medland. GWAS findings for human iris patterns: Associations with variants in genes that influence normal neuronal pattern development. *American Journal of Human Genetics*, 89(2):334–343, August 2011.

[26] Yury A. Malkov and D. A. Yashunin. Efficient and robust approximate nearest neighbor search using hierarchical navigable small world graphs. *CoRR*, abs/1603.09320, 2016.

[27] Joyce A. Martin, Brady E. Hamilton, Michelle J.K. Osterman, Anne K. Driscoll, , and Patrick Drake. National vital statistics reports. Technical Report 8, Centers for Disease Control and Prevention, National Center for Health Statistics, National Vital Statistics System, Division of Vital Statistics, November 2018.

[28] Dana Michalski, Sau Yee Yiu, and Chris Malec. The impact of age and threshold variation on facial recognition algorithm performance using images of children. In *International Conference on Biometrics*, February 2018.

[29] D. M. Monro, S. Rakshit, and D. Zhang. Dct-based iris recognition. *IEEE Transactions on Pattern Analysis and Machine Intelligence*, 29(4):586–595, April 2007.

[30] Vidya Muthukumar. Color-theoretic experiments to understand unequal gender classification accuracy from face images. In *The IEEE Conference on Computer Vision and Pattern Recognition (CVPR)*, June 2019.

[31] Vidya Muthukumar, Tejaswini Pedapati, Nalini Ratha, Prasanna Sattigeri, Chai-Wah Wu, Brian Kingsbury, Abhishek Kumar, Samuel Thomas, Aleksandra Mojsilovic, and Kush R. Varshney. Understanding unequal gender classification accuracy from face images. *CoRR*, abs/1812.00099, November 2018.

[32] P. Jonathon Phillips, J. Beveridge, Bruce Draper, Geof Givens, Alice O'Toole, David Bolme, Joseph Dunlop, Yui Lui, Hassan Sahibzada, and Samuel Weimer. The good, the bad, and the ugly face challenge problem. *Image and Vision Computing*, 30:177185, 03 2012.

[33] P. Jonathon Phillips, Fang Jiang, Abhijit Narvekar, Julianne Ayyad, and Alice J. O'Toole. An other-race effect for face recognition algorithms. *ACM Trans. Appl. Percept.*, 8(2):14:1–14:11, February 2011.

[34] P. Jonathon Phillips, Amy N. Yates, Ying Hu, Carina A. Hahn, Eilidh Noyes, Kelsey Jackson, Jacqueline G. Cavazos, Géraldine Jeckeln, Rajeev Ranjan, Swami Sankaranarayanan, Jun-Cheng Chen, Carlos D. Castillo, Rama Chellappa, David White, and Alice J. O'Toole. Face recognition accuracy of forensic examiners, superrecognizers, and face recognition algorithms. *Proceedings of the National Academy of Sciences*, 115(24):6171–6176, 2018.

[35] P.J. Phillips, P. Grother, R. J. Micheals, D. M. Blackburn, E. Tabassi, and M. Bone. Face recognition vendor test 2002. Evaluation Report IR 6965, National Institute of Standards and Technology, www.itl.nist.gov/iad/894.03/face/face.html or www.frvt.org, March 2003.

[36] Inioluwa Raji and Joy Buolamwini. Actionable auditing: Investigating the impact of publicly naming biased performance results of commercial AI products. In *Conference on AI, Ethics and Society*, pages 429–435, 01 2019.

[37] K. Ricanek and T. Tesafaye. Morph: a longitudinal image database of normal adult age-progression. In *7th International Conference on Automatic Face and Gesture Recognition (FGR06)*, pages 341–345, April 2006.

[38] K. Simonyan and A. Zisserman. Very deep convolutional networks for large-scale image recognition. In *Proc. International Conference on Learning Representations*, volume https://arxiv.org/abs/1409.1556v6, 2015.

[39] Yevgeniy Sirotin. A comparison of demographic effects in face and iris recognition. Technical report, Iris Experts Group, Gaithersburg, MD, 6 2019.

[40] Zhenan Sun, Alessandra Paulino, Jianjiang Feng, Zhenhua Chai, Tieniu Tan, and Anil Jain. A study of multibiometric traits in identical twins. *Proc. of the International Society of Optical Engineering*, 7667, 04 2010.

[41] Darrell M. West. 10 actions that will protect people from facial recognition software. Technical report, Brookings Institution, Artificial Intelligence and Emerging Technology Initiative, Washington, DC, 10 2019.

[42] David White, James D. Dunn, Alexandra C. Schmid, and Richard I. Kemp. Error rates in users of automatic face recognition software. *PLoS ONE*, October 2015.